Ivo Miguel Ferreira da Paixão Reis

Degree in Cell and Molecular Biology

Unveiling human Cardiac Stem Cells role in myocardial ischemia-reperfusion injury

Dissertation to obtain a Master's degree in Biotechnology

Supervisor: Patrícia Gomes Alves, PhD, Senior scientist, IBET/ITQB-NOVA

Jury:

President: Prof. Dr. Isabel Maria Godinho de Sá Nogueira
Arguer: Dr. Ana Fernandes-Platzgummer
Supervisor: Dr. Patrícia Gomes Alves

FACULDADE DE CIÊNCIAS E TECNOLOGIA
UNIVERSIDADE NOVA DE LISBOA

September 2018

Ivo Miguel Ferreira da Paixão Reis

Degree in Cell and Molecular Biology

Unveiling human Cardiac Stem Cells role in myocardial ischemia-reperfusion injury

Dissertation to obtain a Master's degree in Biotechnology,
by Universidade Nova de Lisboa, Faculdade de Ciências e Tecnologia

Supervisor: Patrícia Gomes-Alves, PhD, Senior scientist, IBET/ITQB-NOVA

Jury:

President: Prof. Dr. Isabel Maria Godinho de Sá Nogueira
Arguer: Dr. Ana Fernandes-Platzgummer
Supervisor: Dr. Patrícia Gomes Alves

September
2018

Copyright

Unveiling human Cardiac Stem Cells role in myocardial ischemia-reperfusion injury

Ivo Miguel Ferreira da Paixão Reis, Faculdade de Ciências e Tecnologias, Universidade Nova de Lisboa

Acknowledgments

“Science is far from a perfect instrument of knowledge. It's just the best we have.”

Carl Sagan

I would like to acknowledge all the people directly or indirectly involved in this thesis.

To Prof. Dr. Paula Alves, for giving me the opportunity to do my master thesis at Animal Cell Technology Unit at ITQB/IBET, for the good working conditions offered and for being a strong example of leadership.

To my supervisor Dr. Patricia Gomes-Alves and to Dr. Margarida Serra, for all the encouragement, motivation and precious support, thank you for the scientific discussions and advices. Thank you!

I would (particularly) like to thank to Dr. Maria João for her encouragement and never-ending support and guidance throughout this year. For always being there to help whenever I needed, for her confidence and friendship.

To all the Animal Cell Technology Unit colleagues, for the good working environment and help throughout this year, specially to Maria João, Marta Silva, Bernardo Abecasis, Henrique Almeida and Marta Paiva for all the good moments and support during this year. To my desk neighbour Pedro for the constant good mood and help. To Marcos Sousa for the availability to assist during the bioreactor runs. To Ricardo Gomes from UniMS for all the help regarding proteomic data.

Em especial, à Rita por todo o carinho, paciência e motivação e pelo apoio incondicional.

À minha família, principalmente aos meus Pais, ao meu Irmão e Irmã, pelo apoio constante e por me terem proporcionado todas as condições para que fosse possível concluir esta etapa.

Obrigado.

Preface

The following work was developed at the Animal Cell Technology Unit of IBET and ITQB-UNL within the scope of the funded projects CardioStem (ref. MITP-TB/ECE/0013/2013), NETDIAMOND (SAICTPAC/0047/2015) and iNOVA4Health (UID/Multi/04462/2013. Part of the work was developed in close collaboration with TiGenix (https://tigenix.com/).

Part of this work has been included in poster communications, a conference proceeding, and a manuscript is being prepared for publication:

Poster Presentations:

- Sebastião, M. J., Reis, I., Sousa, M., Palacios, I., Serra, M., Gomes-Alves, P., Alves, P. *Applying proteomic tools to disclose human cardiac stem cells regenerative potential in ischemia/ reperfusion injury.* 20-22/04/2018: Frontiers in Cardiovascular Biology, Vienna, Austria;
- Sebastião, M. J., Reis, I., Sousa, M., Palacios, I., Serra, M., Gomes-Alves, P., Alves, P. *Decoding the role of human cardiac stem cells in acute myocardial infarction using proteomic tools.* 28/02-02/03/2018: Proteomics in Cell Biology and Disease Mechanisms, Cambridge, UK;

Conference proceedings:

- Sebastião, M. J., Paiva, M., Reis, I., Palacios, I., Serra, M., Gomes-Alves P., & Alves, P. *"P494 – Applying proteomic tools to disclose human cardiac stem cells regenerative potential in ischemia/ reperfusion injury."* Cardiovascular Research 114, S120, 2018. doi: 10.1093/cvr/cvy060.351

Manuscript in preparation:

- Sebastião, M.J., Reis I., Palacios, I., Serra, M., Gomes-Alves, P., Alves, P.M. *Merging bioreactor technology with 3D culture: a novel myocardial I/R in vitro model.*

Abstract

Acute myocardial infarction (AMI) is one of the leading causes of death worldwide. During AMI, Ischemia/Reperfusion (I/R) injury occurs: Ischemia, triggered by the complete artery blockage causes death to cardiomyocytes (CMs) while reperfusion, although mandatory for patient survival, further exacerbates the damage in the heart. Cell-based approaches are widely used in disease models, including myocardial I/R injury. However, most *in vitro* models rely on two-dimensional (2D) culture strategies and use murine cells, thus failing on the recapitulation of human AMI pathophysiology. To better mimic the physiology of the human myocardium regarding cell to cell contact as well as nutrient and gas gradients, a novel human *in vitro* model of CMs aggregates derived from human induced pluripotent stem cells (hiPSC-CMs) was developed in stirred-tank bioreactors (STBR). This strategy allowed the recapitulation of important features of AMI, including CMs death, mitochondria and sarcomere ultrastructural damage and increased release of pro-angiogenic, pro-migratory and pro-inflammatory cytokines.

Cell therapies using human Cardiac Stem/Progenitor Cells (hCSCs) in AMI context are now being explored. These heart-resident cells are usually quiescent and become activated after AMI, leading to improved cardiac function mainly due to paracrine signalling. Although CSCs have regenerative properties, their mechanisms of action are still not fully resolved. To further unveil the mechanism of action of hCSCs in AMI context, hCSCs were incubated with conditioned media of hiPSC-CMs subjected to the previously described I/R setup. Quantitative proteomics showed an activation of pathways and functions related to proliferation, migration, paracrine signalling and stress response in hCSCs exposed to I/R hiPSC-CMs conditioned media vs CTL conditioned media, which are features already described to be hallmarks of hCSC activation in AMI context. This work provides a novel human-based I/R injury model as well as new insights regarding hCSCs response to AMI.

Key words: I/R, hiPSC-CMs, hCSC, quantitative proteomics, bioreactor

Resumo

O enfarte agudo do miocárdio (EAM) é uma das principais causas de morte. Durante o EAM, segue-se uma lesão designada por Isquemia/Reperfusão (I/R): A isquemia, provocada pelo bloqueio de uma artéria, provoca a morte dos cardiomiócitos (CMs), enquanto que a reperfusão, embora obrigatória para a sobrevivência, aumenta os danos no coração. Os ensaios *in vitro* são amplamente utilizados como modelos de doenças, incluindo na lesão do miocárdio causada por I/R. No entanto, a sua maioria baseia-se em cultura celular planar com células de ratinho, falhando assim na recapitulação da fisiopatologia humana. Para simular melhor a fisiologia do miocárdio humano em termos do contato célula-célula, bem como dos gradientes de nutrientes e gases, desenvolveu-se um novo modelo *in vitro* utilizando agregados de CMs derivados de células estaminais pluripotentes humanas induzidas (hiPSC-CMs) em biorreactores de tanque agitado. Nesta estratégia recapitularam-se aspectos do EAM, incluindo morte dos CMs, danos ultraestruturais nas mitocôndrias e sarcómeros e aumento da secreção de citocinas pró-angiogénicas, pró-migratórias e pró-inflamatórias.

As terapias celulares baseadas em células humanas estaminais cardíacas (hCSCs) são actualmente muito exploradas no contexto do EAM. Estas células residem no coração e encontram-se quiescentes. Ao serem activadas após o EAM, melhoram a função cardíaca, principalmente devido à comunicação parácrina. Embora as hCSCs tenham propriedades regenerativas, os mecanismos de acção ainda não são totalmente conhecidos. Para conhecer melhor o mecanismo de acção das hCSCs no contexto do EAM, incubaram-se hCSCs com os meios condicionados de hiPSC-CMs submetidos ao ensaio de I/R. Através de proteómica quantitativa, demonstrou-se que esta incubação activa nas hCSCs vias relacionadas com proliferação, migração, sinalização parácrina e resposta ao stress. Neste trabalho desenvolveu-se um novo modelo I/R com células humanas, que foi explorado para se compreender melhor os mecanismos de resposta das hCSC ao EAM.

Palavras-chave: I/R, hiPSC-CMs, hCSC, análise proteómica quantitativa, biorreactor

*Este Resumo não foi escrito ao abrigo do Acordo Ortográfico.

List of Contents

List of Figures

List of Tables

Abbreviations

2D	Two-dimensional
3D	Three-dimensional
AMI	Acute Myocardial Infarction
BMSCs	Bone marrow mesenchymal stem cells
CDCs	Cardiosphere-derived CSCs
CMs	Cardiomyocytes
CSCs	Cardiac Stem Cells
CTL	Control
CVD	Cardiovascular diseases
DIA	Data-independent acquisition
DMEM	Dulbecco modified Eagle medium
DNA	Deoxyribonucleic acid
DPBS	Dulbecco's phosphate-buffered saline
ECGs	Electrocardiogram
ECM	Extracellular matrix
ECGM2	Endothelial Cell Growth medium 2
ELISA	Enzyme-linked immunosorbent assay
FBS	Fetal bovine serum
FDA	Fluorescein diacetate
FDR	False discovery rate
FSG	Fish skin gelatin
hCPC	Human Cardiac Progenitor cells
hCSCs	Human Cardiac Stem cells
hESC	Human Embryonic Stem Cell
HF	Heart failure
HGF	Hepatocyte growth factor
HIF-1	Hypoxia-inducible factor 1
hiPSC-CMs	Human induced pluripotent stem cell derived cardiomyocytes
HSP90	Heat shock protein 90
HUVECs	Human umbilical vein endothelial cell
iPSCs	Induced pluripotent stem cells
I/R	Ischemia/Reperfusion

IDA	Information-dependent acquisition
IGF	Insulin-like growth factor
IHD	Ischemic Heart Disease
IMS	Ischemic mimetic solution
IPA	Ingenuity Pathway Analysis
LC-MS/MS	Liquid chromatography-tandem mass spectrometry
miR	microRNA
mPTP	Mitochondrial permeability transition pore
MS	Mass Spectrometry
NSTEMI	non-ST segment elevation myocardial infarction
PCA	Principal component analysis
PCI	Percutaneous coronary intervention
PI	Propidium iodide
PSC	Pluripotent stem cells
ROS	Reactive oxygen species
SP CSCs	Side population cardiac stem cells
STBR	Stirred-tank bioreactor
STEMI	ST-segment elevation myocardial infarction
SWATH-MS	Sequential Window Acquisition of All Theoretical Mass Spectrometry
Sca1	Stem cell antigen-1
TEM	Transmission electron microscopy
TOF	Time-of-flight

1. Introduction

1.1. Acute Myocardial Infarction

Cardiovascular diseases (CVD), a group of disorders of the heart and blood vessels, are currently the main cause of death worldwide, accounting for 17.3 million deaths per year (Figure 1.1) [1]. By the year 2030, this number is estimated to grow to more than 23.6 million deaths [1]. Within CVD, ischemic heart disease (IHD) is the largest contributor of mortality and includes diseases such as stable and unstable angina, sudden cardiac death and acute myocardial infarction (AMI) [2].

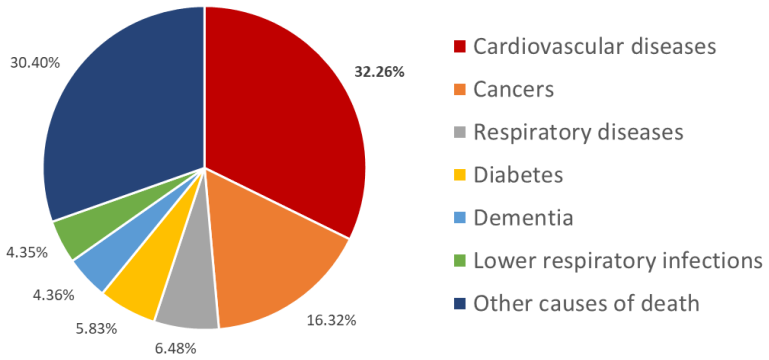

Figure 1.1 Share of deaths by cause in 2016. (adapted from Institute for Health Metrics and Evaluation, Global Burden of Disease, https://ourworldindata.org/causes-of-death, accessed on July 05th 2018)

AMI, commonly known as a heart attack, consists in the sudden decrease or cessation of blood flow to a part of the heart muscle, causing local ischemia. The most common cause of AMI is the complete blockage of a coronary artery triggered by the rupture of an atherosclerotic plaque (i.e. buildups of fatty deposits) with the formation of a vascular blood clot (i.e. a thrombus) [3]. This leads to changes in the balance between oxygen and nutrient supply of the affected myocardium causing death to the heart muscle cells - the cardiomyocytes (CMs) - and consequently myocardial tissue damage [4].

In order to help diagnose AMI correctly, a different number of tests can be performed, including coronary angiography to identify intra-coronary thrombus, blood tests to track specific markers in the serum such as cardiac troponins and/or creatine kinase MB and electrocardiograms (ECGs) [5]. Regarding the heart's electrical activity visualized by ECG, an AMI can be generally classified in two different types [6]: a ST elevation Myocardial Infarction (STEMI) usually caused by a fully blocked artery and a non-ST segment elevation myocardial infarction (NSTEMI) which normally results from a partially clogged one [7].

After an AMI, rapid transportation to the hospital followed by initial assessment and treatment are crucial since the increasing extension of cell death (e.g. necrosis) and prehospital cardiac arrest play major roles in the patient's prognostics. The initial management of acute cardiac

disorders comprises bed rest, patient's monitoring by ECG and early administration of antithrombotic agents [8].

1.1.1. Ischemia/Reperfusion Injury

During AMI, the deficient blood flow is responsible for the ischemic condition. Therefore, the treatment of choice (later discussed in section 1.1.2.) is the restoration of coronary blood flow through reperfusion. However, reperfusion strategies, although needed, exacerbate the damage even further, thus the overall damage is usually referred as Ischemia/Reperfusion (I/R) injury.

Myocardial I/R injury was first observed in 1960 by *Jennings et al*. in canine hearts after observing that reperfusion enhanced the degree of necrosis [9]. The consequences of an I/R injury evolve in a time-dependent manner, starting with exacerbated oxidative stress, overload of intracellular Ca^{2+}, inflammation and then quickly reaching to irreversible cell death by mechanisms such as necrosis and apoptosis [10, 11].

1.1.1.1. The Ischemic phase

Ischemia is a condition that is characterized by the decrease or restriction of the blood flow (and therefore of oxygen) in the tissues. Regarding cardiac ischemia, the deficiency in oxygen causes irreversible cell death (e.g. in CMs) within minutes of the ischemic event [12].

The deprivation of nutrients and oxygen supply leads to severe changes in terms of CMs metabolism and biochemical pathways within the myocardial tissue. Since no oxygen is available, CMs metabolism shifts from oxidative phosphorylation to anaerobic glycolysis, leading to energy depletion by the reduction of ATP (via degradation and defective synthesis), to the depolarization of the mitochondrial membrane and the inhibition of myocardial contractile function. The prevalence of anaerobic metabolism is also responsible for the reduction of intracellular pH caused by the production and accumulation of lactate, NAD^+ and protons [12, 13]. The subsequently decrease in ATP deranges the activity and function of ion transporters (Na^+-H^+ and $2Na^+$-Ca^{2+} exchangers) within the cell, that overall result in an overload of intracellular Ca^{2+} which can contribute to cell death following I/R (Figure 1.2) [14].

1.1.1.2. The Reperfusion phase

Current reperfusion strategies, although crucial to improve the AMI patients' health condition, are considered a "mixed blessing" [15]. Even though the reperfusion intervention restores the nutrients and oxygen required for the generation of ATP through aerobic metabolism and also normalizes the extracellular pH by washing out the accumulated protons, it comes with severe consequences [13]. During this phase, several mediators contribute to cell death, including oxidative stress, the overload of intracellular Ca^{2+}, the opening of the mitochondrial permeability transition pore (mPTP) and inflammation [12] (Figure 1.2).

Oxidative stress, i.e. the imbalance of antioxidant and oxidant species, is caused by the burst production of reactive oxygen species (ROS) mainly by the CMs' mitochondria with the activation of the electron transport chain [12] and the decrease in the ability of ROS scavenging leading to cellular damage in CMs [16]. This oxidative stress (either caused by ROS or reactive nitrogen species) leads to damage in DNA, lipids and proteins [17]. These compounds can also increase proteolysis of proteins involved in the cardiac excitation-contraction coupling [10, 17]. Oxidative stress during reperfusion can also decrease the bioavailability of nitric oxide, an intracellular signalling molecule, that has an important role in ROS inactivation (e.g. superoxide radicals) and in the improvement of coronary blood flow [18].

The intracellular Ca^{2+} accumulation that was initiated during the ischemic period is aggravated after reperfusion due to mitochondrial reenergization, plasma membrane disruption and oxidative stress damage induced to the sarcoplasmic reticulum [12]. The consequential Ca^{2+} accumulation in the mitochondrion's matrix, together with the sudden return to the physiological pH and the generated ROS, leads to the opening of the mPTP, a nonselective channel localized in the inner mitochondrial membrane [19, 20]. While the mPTP remains closed during ischemia due to acidic conditions (pH<7) [21], during reperfusion, its opening causes the depolarization of the mitochondrial membrane, CM's hypercontracture [22] and the uncoupling of oxidative phosphorylation inhibits the production of ATP, ultimately leading to cell death [23, 24]. The pore opening also leads to the entry of water and solutes which contribute to the swelling of the mitochondrial matrix. Even though the inner mitochondrial membrane can outstand the increase of volume, the outer membrane is ruptured and all the content inside the intramembranous space, including apoptogenic signals (e.g. apoptosis-inducing factor and cytochrome c) are released into the cytosol where apoptosis is initiated by the activation of specific apoptogenic proteases (e.g. caspases) [19]. Overall, the mitochondria can act as "fate decider" within the cell: if the damage is severe, the cell may undergo necrosis due to failure in energy production; if the damage is moderate, the cell may die by apoptosis; and if the damage is minimal the cell may recover [25].

Inflammation also plays a role in myocardial I/R injury and, since it is induced in the absence of microorganism invasion, it is usually referred to as sterile inflammation. Besides promoting apoptotic cell death, ROS also increase the expression of adhesion molecules, activating the complement system (a biochemical cascade of the innate immune system) and acting as a chemoattractant for neutrophils [26]. Neutrophils are also activated through the release of endogenous molecules from necrotic and injured cells within the myocardium, including CMs and endothelial cells [27]. The inflammatory environment created by the activity of these immune system mediators contributes to further cell death and myocardial injury by prolonging the pro-inflammatory response [28].

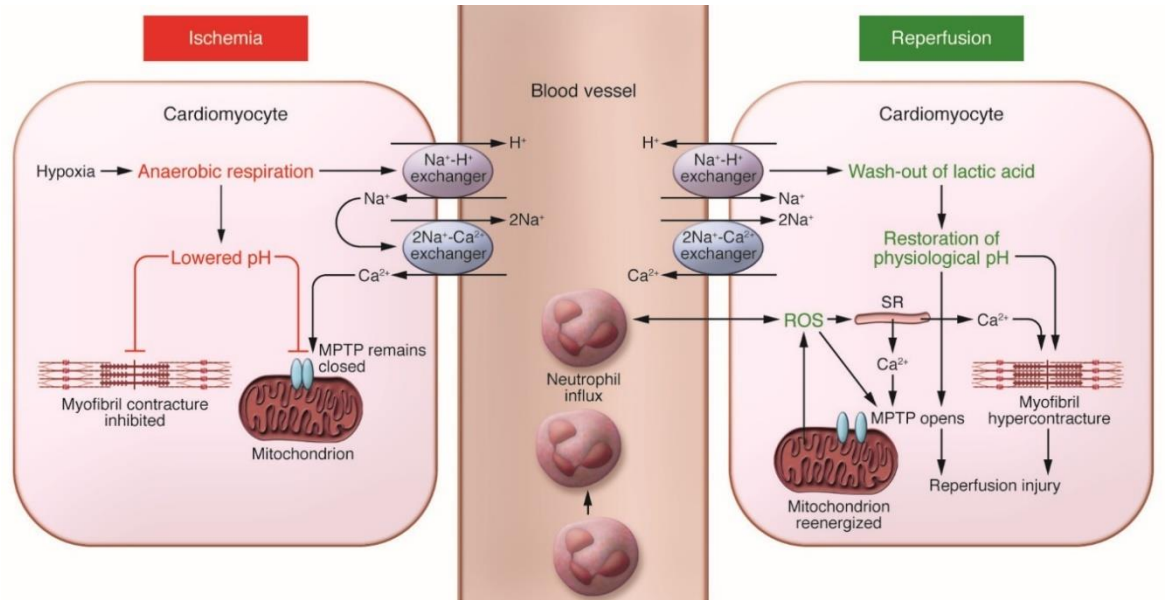

Figure 1.2 Overall key mediators responsible for myocardial ischemia/reperfusion (I/R) injury. Key mediators include oxidative stress, Ca^{2+} overload, opening of the mitochondrial permeability transition pore (mPTP) and inflammation. Briefly, the anaerobic respiration caused by the ischemic event leads to an acidic intracellular pH. This contributes to the derangement of ion transporters function leading to Ca^{2+} overload. The mPTP remains closed and cardiomyocyte contracture is inhibited due to the decrease in pH. Reperfusion allows the mitochondrion reenergization, creating reactive oxygen species (ROS) that induce oxidative stress and act as chemoattractant for neutrophils. During reperfusion, the pH is also re-established, inducing the opening of the mPTP and cardiomyocyte hypercontracture (reproduced from [12]).

The inflammatory response also takes part in the wound healing and scar formation process. For the healing of the damaged myocardial tissue and scar formation upon AMI, a three-phased cellular response occurs: (1) an inflammatory phase with a quick influx of immune cells to help remove damaged tissue; (2) a reparative phase where myofibroblasts start proliferating and secreting collagen to replace dead tissue; (3) and a maturation phase marked by the apoptosis of immune cells, crosslinking of collagen fibers and scar maturation (reviewed in [29]).

During the reparative phase of inflammation, the process of fibrosis occurs. This process consists in the excess formation and deposition of extracellular matrix (ECM) components (e.g. collagen) that promote tissue hardening and scarring [30]. It can be divided in two types: i) replacement fibrosis and ii) reactive fibrosis, both mediated by myofibroblasts. Replacement fibrosis is the mechanism that replaces necrotic CMs by fibrotic tissue. On the other hand, reactive fibrosis is characterized by the abnormal deposition of ECM in the heart's interstitium in areas remote to the infarction, induced by paracrine and hormonal mediators together with the mechanical stress caused by the AMI. While replacement fibrosis is essential to prevent cardiac rupture, an exaggerated fibrotic response and reactive fibrosis in the adjacent zone of the injured areas contribute to impairment of the heart function [31]. The newly formed fibrotic scar tissue increases the stiffness of the heart, impairs the oxygen diffusion and its lesser conductive nature leads to electrophysiological remodelling. These factors also contribute to the diminishing of ventricular function, the increase of CMs' workload and arrhythmias [32] leading to chronic Heart Failure (HF) [33]. Regarding chronic HF patients, heart transplantation is the only viable treatment

to restore function which comes with logistic, economic and biological limitations derived from its high costs, the need for constant immunosuppressive agents and the shortage of organ donors [34].

1.1.2. Strategies in AMI treatment

1.1.2.1. Current therapeutic strategies

For patients with a clinical diagnose of a STEMI, restoration of coronary blood flow and myocardial reperfusion should be done as soon as possible. This reperfusion is either done mechanically by percutaneous coronary intervention (PCI) or pharmacologically by intravenous fibrinolytic therapy. Primary PCI (angioplasty and stenting), an urgent catheter intervention PCI without previous administration of fibrinolytic agents, is the chosen strategy for reperfusion in patients with STEMI [8, 35]. If the patient is medically suggested as unsuitable for PCI, a Coronary Artery Bypass Grafting surgery may be indicated [35]. In this procedure, a healthy vein or artery is used to bypass the blocked portion of the coronary artery.

Regarding the NSTEMI diagnoses where residual perfusion still exists, the patients can either follow the same invasive treatment strategies that are used in STEMI or undergo an ischemia-guided strategy. The latter approach seeks to avoid the routinely early use of coronary angiography and revascularization by the possible stabilization of the patient's condition. However, if the patient's condition fails to stabilize and severe ischemia is detected they are promptly redirected to undergo the mentioned invasive treatments [36].

1.1.2.2. Emerging strategies

Reperfusion treatments are continuously being improved with the advances in PCI technology, with earlier reperfusion and the use of more efficient antithrombotic and antiplatelet drugs. Emerging strategies on preventing I/R injury outcome are being tested in randomized clinical trials as well as in proof of concept studies (reviewed in [12]).

Ischemic postconditioning, in contrast to uninterrupted reperfusion, has been reported to attenuate the reperfusion injury and to reduce the infarction size by 40% to 50% [37]. This technique is a modified form of reperfusion created in the 1980s that has been demonstrated to be a beneficial form of gradual reperfusion [38, 39].

Preconditioning, i.e. repetitive angioplasty balloon inflations and deflations, although with known effectiveness, is not favourable for clinical translation since this therapy must be done prior to the known ischemic event [40].

Primary PCI and ischemic postconditioning are both invasive interventions that are directly applied to the heart. An alternative strategy called remote ischemic conditioning, consists on brief and transient cycles of ischemia and reperfusion to another organ or location (e.g. upper arm), protecting the heart from distance against an I/R injury [41, 42].

The practice of hypothermia (low temperature) [43] and hyperoxemia (increased arterial O_2 partial pressure) [44] as therapeutic interventions have also shown beneficial effects on reducing reperfusion injury in animal studies [12].

Several pharmacological drugs are also being investigated against I/R injury. Such agents include atorvastatin, atrial natriuretic peptide, erythropoietin or glucagon-like peptide 1 and act by activating the RISK (Reperfusion Injury Salvage Kinase) pathway (reviewed in [45])). This pathway comprises a group of pro-survival protein kinases that are activated during myocardial reperfusion and confer cardiac protection [46].

Unfortunately, these novel cardioprotective therapeutics that target the individual I/R injury key players (e.g. calcium overload, pH correction, inflammation and oxidative stress) have resulted in disappointing clinical translation [47]. Nowadays, advanced strategies of treatment based in regenerating myocardial tissue, such as cell therapy, are being studied. Stem cell therapy can provide new treatment alternatives focused not only in the replacement of affected cells but also on the release of autocrine and paracrine factors that ultimately lead to cell survival, tissue remodelling and angiogenesis [48].

1.2. Stem Cells

Stem cells are undifferentiated and unspecialized cells that play a crucial role in both tissue homeostasis and regeneration. They are able to self-renew into identical daughter cells (clonogenic) by undergoing cell division and are also capable of differentiating into more mature specialized cell types [49]. These cells can be divided into different categories depending on their ability to differentiate (i.e. potency). For instance, totipotent stem cells that are able to develop a complete organism (e.g. zygote and early stages of blastomere), pluripotent stem cells including Embryonic Stem Cells (ESCs) or induced Pluripotent Stem cells (iPSCs) that are capable of forming any cell type from the three primary cell germ layers (ectoderm, mesoderm, and endoderm) and lastly, multipotent stem cells which are only capable of differentiating into cell types from a specific cell lineage [50].

Due to their inherent paracrine properties and differentiation potential, a lot of research has been developed in the possible transplantation of different types of stem cells and its derivatives into AMI patients. Cell populations including skeletal myoblasts, the “first generation” of stem cells such as bone marrow mesenchymal stem cells (BMSCs) and the “second generation” of stem cells including derivatives of ESCs and iPSCs (e.g CMs) and Cardiac Progenitor/Stem Cells (CSCs) are currently being explored [51].

Skeletal myoblasts, although not a type of stem cell, were the first cell type to be used for the treatment of damaged myocardium. However, even though studies performed in animal models such as the rabbit [52] or small sized studies in humans [53] showed promising results, the potential use of these cells for cardiac repair is diminished given the associated risk of cardiac arrhythmias [54].

BMSCs are currently the most used cell type in clinical trials. The early data obtained from clinical trials showed beneficial results, however, the long-term results remain inconclusive. For instance, REPAIR-AMI trial (NCT00279175) showed an improvement in myocardial function following the intracoronary delivery of autologous BMSCs while on the other hand, BOOST trial (NCT00224536) showed little effect in the long run [54].

Regarding pluripotent stem cell derivatives, *in vivo* studies have been performed in rat models using ESCs-derived progenitor cells embedded in a fibrin scaffold that resulted in improved cardiac function [55]. There is also a clinical trial ongoing, ESCORT trial (NCT02057900), that aims to use hESCs-derived cardiac progenitors in severe HF. While similar studies for CVD using iPSCs-derivates are not being performed, they should be expected anytime soon since differentiation protocols are effective in both type of cells. However, iPSCs-based studies in humans should be performed with further caution due to the additional mutation risk inherent to cell reprogramming [56].

1.2.1. Cardiac Stem Cells

The mammalian heart was previously thought to be a terminally differentiated post-mitotic organ without any regenerative potential. In 2003, Beltrami and his colleagues first isolated and expanded CSCs in the adult rat heart, which were able to differentiate into the myogenic cell lineage (CMs, vascular smooth muscle cells and endothelial cells) both *in vitro* and *in vivo* and improve cardiac dysfunction in the infarcted heart [57]. In the following year, Messina and his group successfully identified a type of clonogenic cell in cardiospheres in both human and murine heart which shared similar properties of adult CSCs and expressed stem cell antigens [58]. Cardiospheres (later defined in section 1.2.1.2.) are a multicellular cluster that contain not only CSCs, but also supporting cells and partially differentiated progenitor cells [59].

The discovery of this multipotent cell population in the human heart with regenerative potential led to a paradigm shift in cardiovascular biology. Since the myocardium harbours CSCs that can be isolated and expanded *in vitro*, new therapies that exploit such endogenous regenerative potential could emerge with the goal of recovering or replacing damaged cardiac muscle [60].

1.2.1.1. Cardiac Stem Cells in transplantation

Given the characteristics of CSCs, researchers have undertaken much effort in the past years to evaluate their potential in cardiac repair and regeneration and also its effectiveness, safety and feasibility in cell transplantation therapies. For instance, *Dawn et al.* reported a decrease of 29% in myocardial infarction size after the transplantation of CSCs into a rat model after reperfusion, concluding that these cells could both limit infarct size and induce myocardial regeneration [61]. Other studies in larger animal models, such as the pig (with greater similarity in terms of tissue physiology and organ size to the human), reported similar results. Johnston and

his colleagues revealed that treatment using cardiosphere-derived CSCs (CDCs) by intracoronary infusion in infarcted pigs also limited infarct size, reduced adverse cardiac remodelling, formed new myocardial tissue and improved the hemodynamics [62].

Since these studies have shown that CSCs transplantation could enhance cardiac regeneration, the next logical step was to perform clinical trials using allogenic (i.e. donor derived) and autologous (i.e. self-derived) CSCs. These trials include SCIPIO (NCT00474461) using autologous c-kit$^+$ CSCs, CADUCEUS (NCT00893360)) with autologous CDCs, ALCADIA (NCT00981006) also using autologous CDCs together with the controlled release of basic fibroblast growth factor (bFGF), ALLSTAR (NCT01458405) using allogenic CDCs' therapy and more recently CAREMI trial testing allogenic c-kit$^+$ CSCs (NCT02439398).

Although these clinical trials promoted growing evidence that the use of CSCs exert some effects in improving myocardial function on infarcted patients, the transplantation of these cells showed somewhat disappointing results. Only a few percentage of the transplanted CSCs could be successfully engrafted in the affected myocardium. This low retention rate is mainly due the harsh microenvironment created by the infarction itself where the necrotic myocardium together with the inflammatory response, restrict the growth, survival and homing of the infused cells, thus affecting their capability of regenerating the heart [63].

To overcome this limitation, research has been focused on strategies to enhance the survival and/or improve of the engraftment rate of CSCs upon transplantation, including the use of biomaterials (e.g. cell sheets), hydrogels and porous scaffolds [64]. Alternative cell-free approaches bring advantages over transplantation therapies: (1) it would be more affordable regarding manufacturing costs, (2) it would be easier to apply and implement in the clinics like the widespread use of PCI and (3) its therapeutic agents would be "off the shelf" available, thus reducing treatment initiation time [65].

1.2.1.2. Endogenous Cardiac Stem Cells Populations

CSCs are located in hypoxic areas within the myocardium [66], usually clustered in niches with other types of early differentiated heart cells and adult CMs. It's estimated that the adult mammalian heart harbours around one CSC per 8000 to 20000 CMs [67]. By comprising only 0.005 to 2% of the adult cardiac cells, these cells are considered rare *in vivo*, making challenging to study and understand their physiological roles [68].

Several CSCs populations have been identified and characterized according to their phenotypic properties and surface molecular markers (Table 1.1). These different subpopulations include c-kit$^+$ CSCs, CDCs, Sca-1$^+$ CSCs, side population CSCs (SP CSCs) and Islet-1$^+$ CSCs [60].

C-kit$^+$ CSCs:

These cells were the first to be described as CSCs [57]. C-kit$^+$ CSCs appear in small clusters within the interstitium of the ventricular and atrial myocardium with highest density in the atria and the ventricular apex [69]. C-kit$^+$ CSCs are negative for blood lineage markers and are characterized by the absence of CD45 and CD34 and expression of the stemness marker c-kit. Additionally, they express transcription factors associated with early cardiac development such as GATA-4, MEF2C and Nkx2.5 [68].

Sca-1$^+$ CSCs:

This type of CSC is characterized by the expression of the endothelial marker stem cell antigen-1 (Sca1) and the absence of c-kit and blood lineage markers. These cells express cardiac transcription factors such as GATA4, MEF2c and TEF1 but lack other cardiac lineage markers like NkX2.5, hematopoietic markers CD45 and CD34, and mature endothelial markers such as CD31 [70].

Islet-1$^+$ CSCs:

CSCs within this subpopulation are characterized by the expression of cardiac transcription factors GATA4 and Nkx2.5 but do not express c-kit, CD31 and Sca1 markers [71]. This subpopulation can only be found in neonatal and fetal tissues, existing in low or non-existing amounts in the adult mature hearts, which limits their potential use in clinical applications [70].

Cardiosphere-derived CSCs:

Cardiospheres are self-assembling multicellular spheroids originated from the cellular outgrowth (i.e. cells in culture growing out of an explant) from cardiac tissue explants cultured in suspension [72]. The core of this spheroids contains proliferating cells, including c-kit$^+$ cells whilst the outer layer is composed of mesenchymal cells and differentiating cells that express cardiac, stromal and endothelial cell markers [69, 72].

Side Population CSCs:

SP CSCs have an immature phenotype representing around 1% of all cells in the human heart. They are identified using flow cytometry based on their ability to efflux DNA binding dyes (e.g. hoechst dye) through an ATP-binding cassette transporter [68]. This population overlaps with Sca-1$^+$, sharing the expression of the cardiac transcription factors like GATA4 and Nkx2.5 with no myofilament or hemopoietic markers expression [68]. Consequently, SP CSCs can be subdivided into two different populations according to their phenotype, namely, CD31$^-$/Sca-1$^+$SP CSCs and CD31$^+$/Sca-1$^+$ SP CSCs. However, only CD31$^-$/Sca-1$^+$SP CSCs show considerable cardiomyogenic potential [60].

CSCs can also be obtained using other strategies, for instance, by the differentiation of ESCs [73] and iPSCs [74].

Table 1.1 CSCs subtypes, molecular markers and transcription factors. *(reviewed in* [75]*).*

CSCs subtype	**Molecular markers and Transcription factors:**
c-kit^{+}	c-kit^{+}, CD34^{-}, CD45^{-}, Sca-1^{+}, Abcg2^{+}, CD105^{+}, CD166^{+}, GATA4^{+}, Nkx2.5^{low}, MEF2C^{+}
Sca-1^{+}	Sca1^{+}, CD34^{-}, CD45^{-}, FLK1^{-}, c-kit^{low}, GATA4^{+}, Nkx2.5^{low}, MEF2C^{+}
SP	CD34^{+}, CD45^{+}, Abcg2^{+}, Sca1^{+}, c-kit^{+}, Nkx2.5^{-}, GATA4^{-}
CDCs	CD105^{+}, CD34^{+}, CD45^{+}, Abcg2^{+}, Sca1^{+}, c-kit^{low}
Islet^{+}	Islet^{+}, CD31^{-}, Sca1^{-}, c-kit^{-}, GATA4^{+}, Nkx2.5^{+}

1.2.1.3. Endogenous Cardiac Stem Cells in cardiac regeneration

Normally, the endogenous CSCs residing in the adult heart are in a quiescent state and only a few are active to maintain tissue homeostasis by replacing cardiac cells such as CMs and vascular cells damaged by wear and tear. However, a fraction of endogenous CSCs can quickly become activated upon environmental stimuli (e.g. ischemic injury [76], stress, hypoxia, exercise and work overload) thus contributing to cardiac regeneration by paracrine action and by proliferating and differentiating towards new cardiac muscle and coronary vessels [77-79]. Regarding whether CSCs actually differentiate or not into new cardiac cells remains controversial.

The controversy started when *Orlic et al.* [80] reported back in 2001 that c-Kit^{+} cells (in this case, bone marrow-derived cells) had the capability of regenerating infarcted myocardium. Three years later, *Murry et al.* reported otherwise using the same cell type [81]. The heat of the controversy seemed to have settled down with the narrower definition of CSCs, being it only c-kit^{+} cells that resided in the heart (excluding the circulating c-kit^{+} cells). However, in 2012, Jesty and his colleagues [82] reported that c-kit+ CSCs did not contribute to new CMs and a year later *Ellison et al.* [83] demonstrated that CSCs could differentiate into different cardiac cells and were the main source of regeneration in both human and mouse hearts, thus, reigniting the controversy (reviewed in [84]). More recently, using genetic lineage tracing, it has been demonstrated that c-kit^{+} CSCs minimally contribute to new CMs formation either in post-injury regeneration or in normal conditions [85].

1.2.1.3.1. Mechanisms of action of Cardiac Stem Cells

Cardiac differentiation was thought to be the key event in the success of an eventual therapy based on CSCs. Today, it's widely accepted that the production and secretion of paracrine modulators (e.g. cytokines, growth factors and exosomes) induced by paracrine cross-talk are the main factors responsible for the reported beneficial effects of CSCs' transplantation studies [86]. In fact, as mentioned above, while it's still controversial whether CSCs can differentiate and generate new CMs upon injury [85], the potential towards cardiac regeneration via paracrine communication was already well recognized in many animal and *in vitro* studies. For example, *Park et al.* reported that mouse Sca-1^{+}/CD31^{-} CSCs secreted factors such as MCP-1, EGF, TGF-β1, IGF-1 (Insulin-like growth factor I), IGF-2, HGF-R and IL-6 that protected CMs from hypoxia after incubating them with conditioned media [87]. More recently, *Sebastião et al*. reported in an

in vitro human myocardial I/R injury model, an increased secretion of the angiogenic chemokine CXCL6 [88] by CSCs. In this study, a co-culture of human cardiac stem cells (hCSCs) and CMs derived from human induced pluripotent stem cells (hiPSCS-CMs) was used to show CXCL6 relevance in the CSCs paracrine-mediated cardioprotection [*Sebastião et al*. submitted].

By taking advantage of paracrine communication between endogenous CSCs and injured cardiac cells, novel cell-free therapies that stimulate the heart's endogenous regeneration mechanisms based on the use of paracrine modulators have been explored. *Ellison et al.* tested a cocktail of growth factors, combining IGF-1 and hepatocyte growth factor (HGF) injected intracoronarily during reperfusion in pig models of AMI. The authors reported a regenerative response from c-kit^{+} CSCs leading to the regeneration of the damaged myocardial tissue, reduction of fibrosis and increased CMs survival rate. Both HGF and IGF-1 activated the endogenous CSCs, contributing to their proliferation, migration and differentiation into CMs, smooth muscle cells and endothelial cells [89]. In fact, IGF-1 had been previously reported to be released by CMs in stress (e.g. infarction) [90]. Similar improved cardiac function was reported by Koudstaal and his colleagues using the same molecules administered trans-endocardial in a hydrogel carrier [91].

Exosomes (membrane vesicles ranging from 40 to 100 nm in size), are also vehicles of paracrine signals produced by CSCs. CDCs were reported to produce exosomes that may induce angiogenesis and also proliferation of CMs and apoptosis inhibition. These vesicles can hold micro RNAs (miR), such as miR-146a, that have been shown to induce some cardioprotective effects in murine myocardial models of AMI [92]. Other examples of miRs that boost cardiac repair are miR-17 and miR-19a that belong to the miR-17-92 cluster. The overexpression of this cluster has been shown to reduce the injury of a myocardial infarction in adult CMs. The joint use of miR-590 and miR-199a (in lipid formulations) reduced infarct size and improved overall cardiac function in mouse after myocardial infarctions (reviewed in [93]). More recently, *Gallet et al.* reported a decrease in scarring and in adverse cardiac remodelling in pigs after intramyocardial injection of human CDCs exosomes after reperfusion [94], making exosomes another conceptual attractive cell-free therapeutic agent.

To further understand the mechanism of action of CSCs upon AMI, there is a clear need for the development of relevant and predictable I/R models and robust analytical tools for detailed cell characterization.

1.3. I/R models

The development of disease models plays a critical role in biomedical research. Disease models aim to understand the molecular basis of human diseases in order to improve and develop new forms of diagnosis and novel therapeutics. The currently available myocardial I/R injury models include *in vivo* (animal models), *ex vivo* (e.g. Langendorff model) and *in vitro* (e.g. cell-based assays) approaches.

Over the past century, myocardial injury has been studied by the development of numerous animal models [95]. Large animal models include the pig and dog, whereas small animal models include rabbits and rats [96]. However, animal experimentation comes with high costs, ethical issues and, although in animal models biochemical interactions and mechanisms are present, they often differ from the human disease phenotype [97]. This inability to completely mimic human disease, is likely the reason why many drugs fail to translate the efficacy and safety when advancing from animal studies to human clinical trials [98]. Thus, the magnitude of the studies are beginning to rely on the use of cultured human cells, including primary cells, cell lines and derivatives of PSCs [99]. However, while primary human CMs would be the ideal cell source for an *in vitro* model, their short availability, low to no proliferation capacity and poor consistency limit their use. Given this, other cell types, including CMs derived from ESC and iPSCs are more prevalent *in vitro* models [100, 101].

I/R *in vitro* models induce artificial conditions to simulate the environmental features of both ischemia and reperfusion phases by exposing cells to hypoxia and reoxygenation. Strategies used in I/R models include the culturing of cells in hypoxic sealed chambers (to simulate ischemia) or incubators (to mimic both ischemia and reperfusion depending on the oxygen content). For instance, *Li et al.* performed this strategy using neonatal rat CMs, applying a three-hour period of both ischemia (5% CO_2 and 95% N_2) and reperfusion (5% CO_2 and 95% O_2) [102]. *Kang et al.* also followed the same strategy using adult rat primary CMs, applying a six-hour period of ischemia followed by reoxygenation [103]. For further oxygen scavenging, hypoxic chambers can also contain deoxygenation reagents that lead to the O_2 consumption and production of CO_2 (e.g. Pack-Anaero) [104] and culture media can feature enzymatic oxygen scavengers (e.g. EC-Oxyrase®) which act by reducing molecular oxygen to water [105]. Other I/R *in vitro* strategies include the removal of media components (e.g. nutrients) and the removal of oxygen from the culture media through bubbling with nitrogen. *Xu et al.* followed this approach using H9c2 (a rat heart myoblast cell line) cell line by removing both glucose and fetal bovine serum (FBS) from the media during ischemia and then culturing cells under normoxic conditions in nutrient rich media during reperfusion phase [106] while *Li et al.* followed the same setup with the addition of a serum deprivation step prior to the I/R experiments [107]. Other approaches include the culturing of cells in ischemic mimetic solutions (IMS) which induce acidosis, lactate accumulation, glucose deficiency and hyperosmosis, thus better mimicking the pathophysiological state of ischemia. *Zhao et al.* used IMS to simulate ischemia in H9c2 cell line [108] and more recently, *Sebastião et al*. applied the same formulation in an heterotypic cell-based human model of hiPSC-CMS and hCSCs [*Sebastião et al*. submitted]. Other human cell types have also been subjected to I/R, including CMs derived from ESCs [109].

However, despite the attempt to correctly mimic *in vivo* features of AMI, most I/R models are 2D (planar) disease models which fail to recapitulate the complexity of tissue architecture, that is of major importance in disease pathophysiology, and are mostly based on a single cell type. Therefore, there is a need to create and improve more relevant human cell-based experimental *in vitro* settings that better recapitulate tissue physiology.

1.4. Bioreactor technology and 3D cell culture

1.4.1. 3D cell culture strategies

To produce a robust *in vitro* disease model, the combination of physiological relevant cell source together with a culture system that allows the recapitulation of *in vivo* architecture is needed.

Most of cell-based assays and screenings are performed in two-dimensional (2D) systems. 2D cell cultures rely on the cultivation of a monolayer of cells adherent to a flat and rigid surface (e.g. glass petri dish, polystyrene plates) [110]. However, in 2D cell culture, only a portion of cells are interacting with their neighbour cells and the ECM, which can lead to incorrect cell polarization affecting phenotypic cell fate and pathway signalling (reviewed in [111]).

On the other hand, 3D cell culture systems are able to establish the physiological cell-cell and cell-ECM interactions [112] which mimic the 3D communication network that is responsible for the homeostasis and specificity of the *in vivo* tissues [113]. Furthermore, 3D cultures recapitulate more closely the tissue microenvironment by influencing intracellular signalling that contributes to phenotypic cell fate by changing both gene and protein expression [114].

There are many methods to culture anchorage-dependent cells in 3D suspensions, including cell adhesion on microcarriers, cell encapsulation in hydrogels and self-aggregated spheroids. Microcarriers are small spherical particles that allow the growth of adherent cells while cell encapsulation comprises the entrapment of cells in a semi-permeable membrane. Lastly, self-aggregated spheroids are a scaffold-free strategy that induce cell-cell interaction by promoting cell self-organization into 3D structures, known as spheroids or aggregates (reviewed in [115]). Some examples are already reported for 3D cardiac *in vitro* cell models. For instance, using the hanging-drop method, where self-aggregation is induced by gravity, cardiac models were developed using a triculture of CMs, endothelial cells and fibroblasts to study the heart microenvironment [116] and cardiac fibrosis [117]. In terms of myocardial I/R 3D models, a 3D paper-based culture system was developed using primary CMs and fibroblasts cultured in stacked layers of paper to study fibroblasts' migratory response caused by CMs under ischemic stress [118]. Other example, was the development of engineered heart tissue where CMs were cultured in a ring-shaped scaffold to study cardiac function under hypoxic conditions [119].

In order to move from 2D culture systems to 3D, a change from static culture conditions to a dynamic system is needed. Dynamic culture systems include shaking erlenmeyer's and bioreactors, where the latter, allows the managing of cell culture environment that is required for the development of disease models. In this context, bioreactors have emerged as the optimal setting for reproducible and scalable 3D cell culture, having already been reported to improve cell survival, differentiation efficiency and proliferation rates over 2D systems [120, 121].

1.4.2. Bioreactors for culture of advanced cell models

Bioreactors are defined as devices that enable the tight control and monitoring of environmental parameters required for cell culture (e.g., pH, oxygen, pressure, temperature, nutrient supply and metabolite removal) [122]. There are several types of bioreactors, including rotating wall vessels, stirred-tank bioreactors (STBR), airlift bioreactors, hollow fiber bioreactors and wave bioreactors [123, 124] (Figure 1.3).

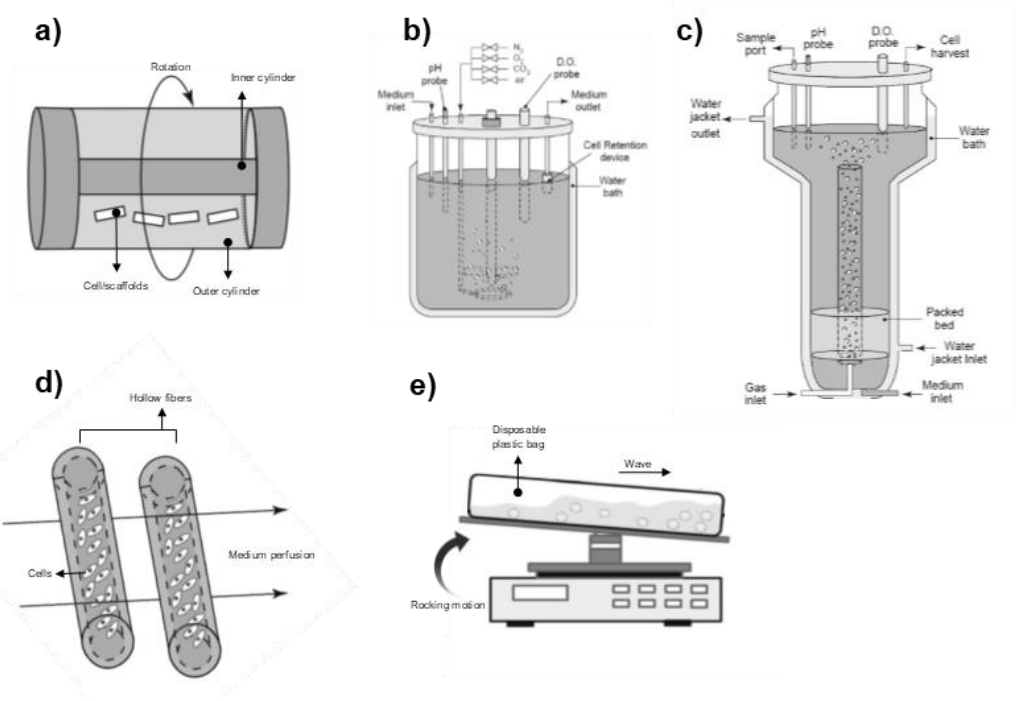

Figure 1.3 Examples of different bioreactor systems used in cell culture: a) rotating wall vessel; b) stirred-tank bioreactor (STBR); c) airflow bioreactor (adapted from [125]); d) hollow fiber bioreactor (adapted from [122]) and e) wave bioreactor (adapted from [126]).

Rotating wall vessels are a rotatory cell culture system providing a low shear stress culture with high rates of mass transfer. By having two cartridges, one outer cartridge that's fixed and an inner one that rotates around the central axis, the cultures are suspended by the creation of the microgravity environment of space. STBR feature a vessel, valves, pipes and a motor. The stirring of the culture is provided by an impeller powered by the motor and in the top of the vessel, several sensors and probes can be attached (e.g. temperature sensors, pH and dissolved oxygen probes, metabolite measuring devices). Airlift bioreactors are a type of culture system that produce lower shear stress when comparing to stirred-tank bioreactors since both the oxygenation and culture mixing is performed by a stream of air. The hollow fiber bioreactors are made of semi-permeable membranes arranged in parallel arrays allowing diffusion of nutrients and oxygen between the intra-capillary space within the hollow fibers and the extra-capillary space. The wave bioreactor comprises a disposable plastic bag and a platform responsible for a wave-like motion that promotes the mixing in the culture medium (reviewed in [115, 123]).

Even though there is a lack of reported myocardial I/R modelling based on bioreactors, the feasibility of their use on disease models has already been proven using cells from other tissues. For instance, *Allen et al.* developed a perfusion bioreactor system that allowed the study of the effect of oxygen gradients in primary rat hepatocytes [127] while *Santos et al.* exposed a brain model of 3D neural aggregates to hypoxia in STBR [128]. Hypoxia has also been combined with STBR and wave bioreactors by *Correia et al.* but in this case, for the yield improvement in the differentiation of murine iPSC into CMs [129].

Another main advantage of some bioreactor types (e.g. STBR) is the ability of withdrawing samples in a non-destructive way [115]. With this, several assays can be performed including metabolite analysis, live/dead assays, estimation of cell concentration and -omics analysis of cell phenotype and conditioned medium, such as proteomic profiling methods.

1.5. Proteomics

Since its known that cardiac regeneration can be mediated via paracrine signalling (discussed above on section 1.2.1.3.), the use of proteomic tools (both whole proteomics and secretome, i.e proteins secreted by cells) is crucial to understand the molecular basis regarding stem cell response to disease [130], including AMI.

Proteomics can be defined as the study of proteins [131], including protein-protein interaction, protein modifications, function and localization. Since proteins are the main effectors of a given cell phenotype, the proteome (i.e. the set of proteins expressed under specific conditions at a given time) reflects a response to the environment, allowing the elucidation of mechanisms of disease, protein signalling and both identification and characterization of therapeutic targets and biomarkers [132]. There are many methods to study proteomes, including 2-dimensional separation followed by protein staining, binding of fluorescently-labelled antibodies (e.g. ELISAs) or high-throughput techniques, such as microarrays or mass spectrometry (MS) [133].

Protein microarrays allow the isolation and subsequent study of proteins, being considered one of the most powerful proteomic tools. A typical protein microarray consists in a support (e.g. piece of glass or plastic) coated with capture agents (e.g. antibodies) that recognize specific proteins [134].

On the other hand, MS-based proteomics take advantage of the availability of the annotated genomes and protein sequence databases. Combined with the technological advances, MS has become the approach of choice in the field of proteomics. MS consists in the ionization and gasification of molecules by an ion source, which are then separated according to their mass-to-charge (m/z) ratio by a mass analyser. Then a detector registers the number of ions at each m/z value, resulting in a spectrum of m/z and intensity pairs [135].

There are two main approaches for the identification of proteins using MS. Top-down proteomics which analyses intact proteins without the need of proteolytic digestion of the sample, while its counterpart, bottom-up proteomics, requires protein cleavage into short peptides prior to MS analysis. One of the most applied methods for the identification and quantification of proteomes is Liquid chromatography coupled to tandem mass spectrometry (LC-MS/MS) [136] (Figure 1.4).

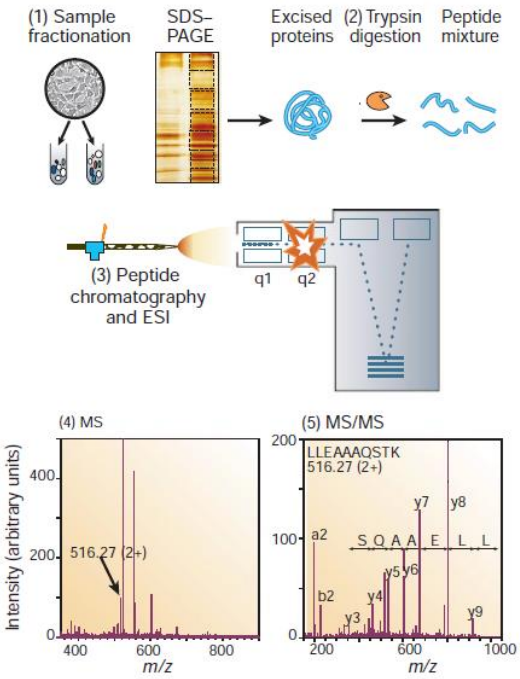

Figure 1.4 Generic workflow schematization of a mass spectrometry (MS) proteomics experiment: (1) Sample fractioning, starting with isolation of proteins to be analysed from cell lysates and a final step of sodium dodecyl sulfate-polyacrylamide gel electrophoresis (SDS-PAGE) for further separation of proteins of interest; (2) proteolytic digestion (e.g. trypsin digestion); (3) Peptide separation (e.g. high pressure liquid chromatography-HPLC) and ionization using ion sources such as electrospray ionization (ESI) or matrix-assisted laser desorption/ionization (MALDI); (4) Acquisition of mass spectra; (5) Additional round of MS (i.e. tandem MS) [123].

Following bottom-up proteomics, LC-MS/MS starts with the proteolytic cleavage of the sample into short peptides which are then separated by liquid chromatography (Figure 1.4). LC-MS/MS can be operated using two different strategies: discovery/shotgun proteomics and targeted proteomics. In discovery proteomics, the MS is performed in information-dependent acquisition mode (IDA), where a subset of precursor ions (commonly the more abundant) formed at a first stage of MS (MS1) are selected and fragmented by collision resulting in fragment ions (MS2). The resulting MS/MS spectra are then analysed by sequence database search. Targeted proteomics is operated in selected reaction monitoring (SRM) where a limited number of predetermined ions of a specific mass are selected in the first stage of the MS1 and are fragmented in a second MS for detection. To overcome the limitations of IDA and SRM, such as low sensitivity to less abundant proteins and the limited number of target proteins per run, respectively, a data-independent acquisition (DIA) strategy has been emerging in this field (reviewed in [137]). In the DIA strategy, every ion (and not just a subset) in the chosen m/z range

is fragmented and analysed in the second MS stage. An example of DIA method is Sequential Windowed Acquisition of All Theoretical Fragment Ion Mass Spectra (SWATH-MS) which is a recent developed MS-based proteomic tool to identify and quantify proteins [138].

1.5.1. SWATH-MS

There are several MS-based methods used in the quantification of proteomes, including chemical tagging methods such as isobaric tags for relative and absolute quantification (iTRAQ), isobaric labelling with tandem mass tags (TMT) and isotope-coded affinity tags (ICAT) and metabolic labelling, namely stable isotope labelling with amino acids (SILAC) (reviewed in [139]).

In contrast, SWATH-MS is a novel approach of MS-based quantification of peptide ions in a sample that doesn't require labelling [140]. First introduced by *Gillet et. al*., SWATH-MS appeared to combine the high throughput advantages of shotgun proteomics with the consistency and reproducibility of SRM. Its high-resolution MS data is obtained using a mass analyzer combination of a quadrupole and TOF (time-of-flight) instruments (Q-TOF) through repeated analysis of sequential windows (called swaths) throughout the chromatographic elution range [138]. The procedures of the tagging methods usually contribute to loss of protein which is avoided in SWATH-MS [141]. Being label-free, also removes the errors in quantification caused by incomplete labelling [142].

Proteomic tools have already been applied in studies regarding stem cells, including CSCs. For example, in the unveiling of hCSCs' receptome [143] (i.e. plasma membrane receptors) or in the phenotypic characterization upon scale-up production and expansion of hCSCs [144]. More recently, using label-free quantitative proteomic tools (in this case, MaxLFQ), the human heart proteome has been mapped for the first time, making it easier to identify differences between diseased and healthy hearts in the future [145].

2. Aim of the thesis

This thesis was divided in two major parts. The first goal was to develop and characterize a novel human cell-based myocardial *in vitro* I/R injury model by combining both 3D culture of hiPSC-CMs and stirred tank bioreactor technology. This approach aimed at filling the gap between *in vitro* and *in vivo* research tools by better mimicking human CM AMI pathophysiology.

The second aim of the thesis was to investigate the mechanism of action of hCSCs upon contact with paracrine factors from hiPSC-CMs subjected to I/R injury. Since it is known that paracrine cross-talk plays a key role on the activation of these cells, it is important to understand how hCSCs respond to the secretome of CMs in AMI context, aiding in the development of novel therapies based on the activation of the endogenous heart regeneration capacity.

The rational of the thesis is demonstrated in the figure below (Figure 2.1):

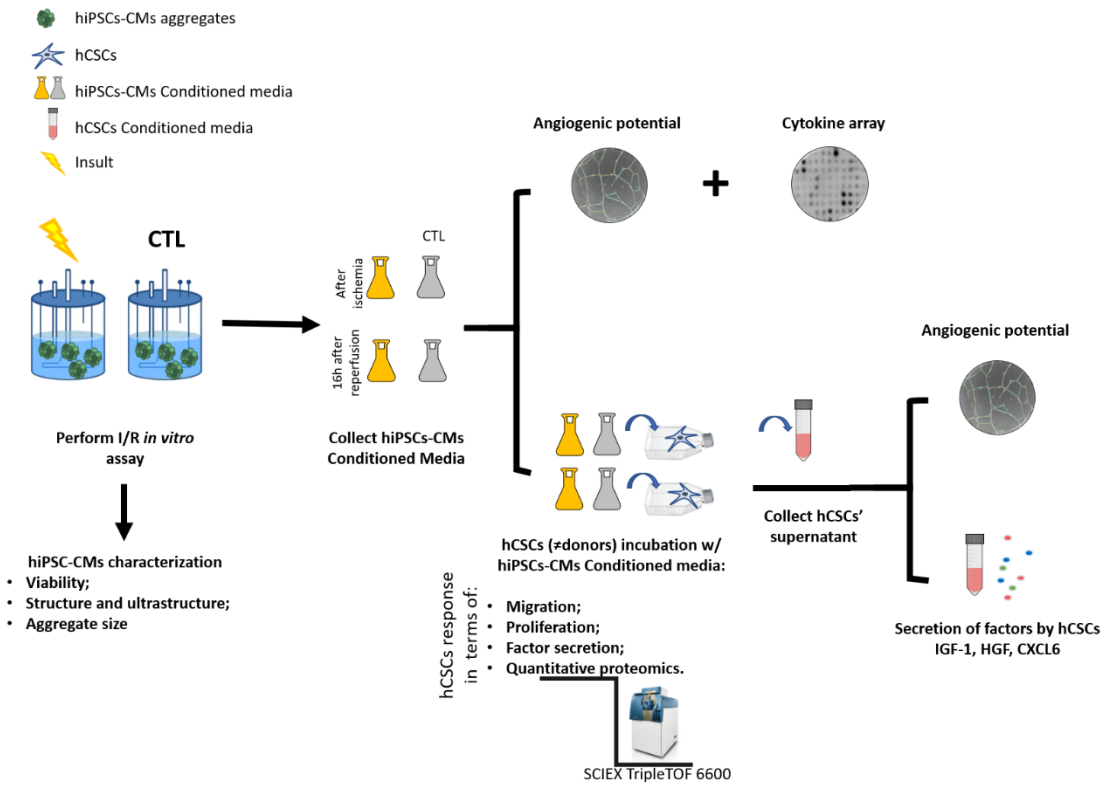

Figure 2.1 Thesis rational. Outlined strategy and major readouts**.** hiPSCs-CMs: human induced pluripotent stem cell derived cardiomyocytes; hCSCs: human cardiac stem cells.

3. Materials and Methods

3.1. hiPSCs culture

3.1.1. hiPSCs cell source and maintenance

hiPSCs (DF19-9-11T.H, WiCell) were cultured in Matrigel® (Corning) coated plates in mTESR1 medium (STEMCELL Technologies) at 37°C in humidified incubators (5% CO_2, 21% O_2) and subcultured when about 80-90% confluent using Versene (Gibco) for 7 min at 37°C.

3.1.2. Differentiation, aggregation and maturation of hiPSCs-CMs

Differentiation into CMs was initiated when cell culture confluence reached about 90%, as described elsewhere [146]. At day 7 (when a high proportion of beating zones was observed), cells were dissociated by incubation with TrypLE Select (ThermoFisher Scientific) for 5 min at 37ºC and replated in AggreWell™400Ex plates (Stem cell technologies) at a density of 1500 cell/microwell, as previously described for aggregation of hPSC-CMs [147]: cells were centrifuged at 100 xg during 3 min, and cultured in RPMI Medium supplemented with B27 (without insulin) at 37°C in humidified incubators (5% CO_2, 21% O_2). After 48 h, hiPSCS-CM aggregates were transferred to erlenmeyers and were kept in suspension in orbital shakers at an agitation rate of 70 rpm. Medium (RPMI supplemented with B27 without insulin) was replaced every two days until day 15 of differentiation, where aggregates composed of >90% of cTnT positive cells (confirmed by flow cytometry) were obtained [148]. To further improve the maturation state of this cell population, hiPSC-CMs were cultured for additional 10 days in a commercial triiodothyronine (T3) hormone rich medium (Pluricyte Medium, NCardia) in humidified incubators (5% CO_2, 21% O_2) at 37ºC, as described in elsewhere [149]. Medium was exchanged every two days.

3.2. I/R setup in bioreactors

After day 10 of hiPSCs-CM maturation, aggregates were harvested and inoculated at a concentration of $1.3x10^5$ CMs/mL (200 aggregates/mL) in computer-controlled stirred tank bioreactors (DASGIP® cellferm-pre bioreactor system Eppendorf AG), equipped with trapezoidal-shaped impellers (working volume of 230 ml). hiPSCs-CMs aggregates were kept for at least 15 h in culture prior the I/R experiments in CM001-R media composed by DMEM:F12: Neurobasal medium (1:1), supplemented with 1% penicillin streptomycin, 3% fetal bovine serum (FBS) embryonic stem cell-qualified, N2 supplement (1X), B27 supplement (1X), 0.9 mM l-glutamine, 50 µM β-mercaptoethanol (Sigma) (all percentages in v/v). Data acquisition and process control were performed using DASGIP® Control Software 4.0 (Eppendorf AG). Dissolved oxygen (pO_2), pH and temperature were monitored with pH and oxygen electrodes (Mettler-Toledo) and a temperature sensor, respectively. Electrodes and temperature sensor were calibrated as described by the manufacturer. Cells were cultivated under defined and controlled culture conditions: 37°C, surface aeration rate of 0.1 volume of air per volume of medium per minute

(vvm), pO_2 of 15% in air saturation (that corresponds to pO_2 of 3% in O_2), corresponding to myocardial physiologic normoxia [150]. Stirring rate was set to 70 rpm.

I/R injury experimental setup (an insult) is depicted in figure 3.1. Ischemia was mimicked by replacing CM001-R medium with Ischemic Mimetic Solution (IMS; in mM: NaCl, 135; KCl, 8; MgCl2, 0.5; NaH_2PO_4, 0.33; HEPES, 5.0; $CaCl_2$, 1.8; Na^+-lactate, 20; pH 6.8) [108], and by decreasing pO_2 to values below 0.4% in O_2. After 5 h of ischemia, reperfusion was induced by re-establishing control culture conditions (CM001-R without FBS at a pO_2 of 3% in oxygen) for an additional 16 h. A bioreactor was maintained in parallel, following the same medium exchange intervals (hereafter designated as CTL bioreactor).

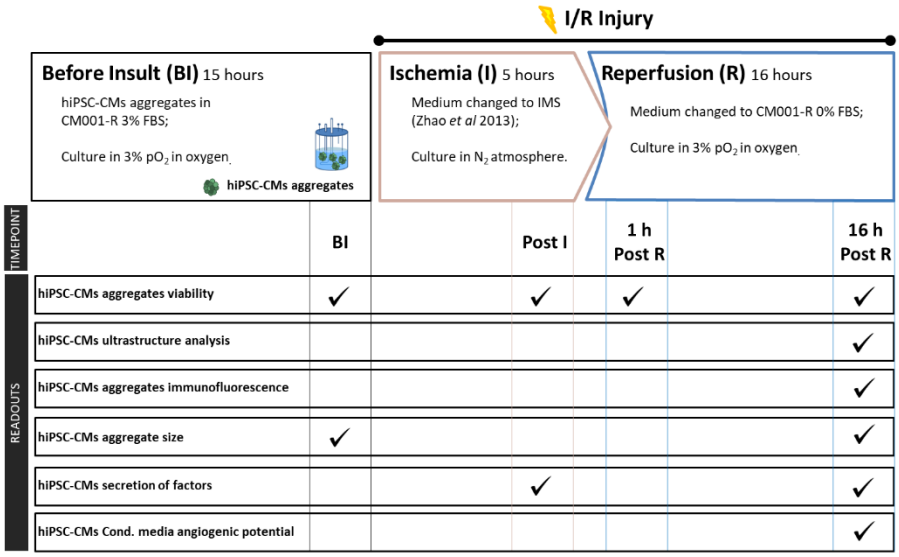

Figure 3.1 Schematic representation of Ischemia/Reperfusion injury (I/R) bioreactor-based experimental setup. A two-phased I/R insult was performed on aggregates of hiPSC-CMs using stirred tank bioreactors. During an ischemic phase of 5 hours, CM001-R medium with 3% FBS was replaced with an Ischemic Mimetic Solution (IMS) and cell culture is performed in N2 atmosphere. After ischemia, reperfusion phase was mimicked by re-establishing normoxic culture conditions (16 hours): IMS is changed to CM001-R and oxygen is set back to 3% of pO_2 in oxygen. The impact of the I/R setup was evaluated in terms of hiPSC-CMs viability, hiPSC-CMs structure and ultrastructure, hiPSC-CMs aggregate size, hiPSC-CMs secretory profile and angiogenic potential of conditioned (Cond.) media throughout several timepoints: BI-Before insult; Post I-Post Ischemia; Post R-Post Reperfusion. Control cultures were maintained in parallel in normoxic conditions.

3.2.1. Generation of hiPSC-CM I/R Conditioned Media

Conditioned media of both CTL and insult bioreactors were collected at the end of reperfusion phase (16 h), centrifuged (1,000 xg for 5 min) to remove dead cells and debris, and stored at -20°C until further use.

3.3. hCSCs culture

3.3.1. hCSCs source and maintenance

hCSCs from three different donors were obtained and isolated from the human right atria appendage myocardial tissue, as described elsewhere [151]. hCSC from three donors were used: hCPC1 (57 years old, male), hCPC03 (78 years old, male) and hCPC04 (17 years old, female). Cells were cultured in humidified atmosphere of 5% CO_2 and 3% O_2 at 37ºC in CM001-R medium (with 10% FBS, Insulin Transferrin Selenium (0.5X), 10 ng/mL bFGF, 20 ng/mL EGF-I and 30 ng/mL IGF-II (Prepotech)). A medium exchange of 50% was performed 24 h after thawing and every 3 days afterwards. After reaching a confluency of about 80%, cells were subcultured by trypsinization using Tryple™ Select Enzyme for 5 min at 37ºC. Cells were used between passages 7–8.

3.3.2. Incubation of hCSCs with I/R Conditioned Media

hCSCs were plated at $1.5x10^4$ cells/cm^2 in complete CM001-R medium. After 24 h, medium was exchanged by hiPSC-CMs conditioned media of reperfusion phases of both CTL and insult bioreactors. After 3 days in culture, the impact of hiPSC-CMs conditioned media was evaluated regarding hCSC migration, proliferation, growth factor secretion and whole proteomic profile.

3.4. Cytokine/Chemokine quantification

3.4.1. Cytokine array

Cytokine detection of conditioned media from ischemic and reperfusion phases of both CTL and insult bioreactors was performed according to manufacturer's instructions (Ab133997, Abcam) and included the screening for the following 42 targets: ENA-78, GCSF, GM-CSF, GRO, GRO-α, I-309, IL-1α, IL-1β, IL-2, IL-3, IL-4, IL-5, IL-6, IL-7, IL-8, IL-10, IL-12 p40/p70, IL-13, IL-15, IFN-γ, MCP-1, MCP-2, MCP-3, MCSF, MDC, CXCL9, MIP-1δ, CCL5, SCF, SDF-1, CCL17, TGF-β1, TNF-α, TNF-β, EGF, IGF-I, Angiogenin, Oncostatin M, Thrombopoietin, VEGF-A, PDGF BB and Leptin. The intensity of chemiluminescent signal is proportional to the amount of cytokine bound and was determined using the Image LabTM software version 5.0 (Bio-Rad). Spot densities were normalized according to the manufacturer instructions. Mean signal density of each spot was also subtracted with the mean spot densities of basal medium alone (CM001-R medium). IMS-based conditioned medium dismissed similar normalization, since IMS is a DPBS-based medium, with no protein content as confirmed by Microplate BCA Protein Assay Kit (Thermo Scientific).

3.4.2. Growth factor quantification by ELISA

ELISA kits (Quantikine, R&D Systems) were used according to the manufacturer’s instructions to address the concentration of the following cytokines in hiPSC-CMs and hCSCs

conditioned media: CXCL6, HGF and IGF-1. Absorbance was then measured using a plate fluorescent reader (TECAN Infinite 200 Pro NanoQuant).

3.5. Scratch wound migration assay

hCSCs were cultured to reach full confluency in 24-well plates and starved in serum-free media (CM001-R w/o FBS) for 24 h. Each well containing a monolayer culture of hCSCs was vertically and uniformly scratched using a 200 µl pipette tip. Cells were then incubated in hiPSC-CMs conditioned media obtained from the I/R assays (Section 3.2.1). Phase-contrast photographs were taken using a fluorescence inverted microscope (DMI6000, Leica) immediately after scratching (0 h) and then after 5 and 7 h. The acquired images and the migration rates were accessed using ImageJ software (Rasband, WS, ImageJ, U.S. National Institutes of Health, Bethesda, MD, USA, http://imagej.nih.gov/ij/, 1997–2012).

3.6. HUVECs and tube formation assay

Human umbilical vein endothelial cells (HUVECs) (catalog No. 2517A, Lonza) were cultured in previously coated t-flasks with 0.1 % gelatin in Endothelial Cell Growth medium 2 (ECGM2) (PromoCell) and kept at 37ºC in a humidified atmosphere of 5% CO_2. Medium was exchanged every 3 days. HUVECs subculturing was performed before reaching ~90% confluence and were trypsinized using 0.5 % Trypsin-EDTA (Ethylenediamine tetraacetic acid, Life Technologies) for 7 min at 37ºC.

Tube formation assay was performed according to *Pedroso et al.* [152]. Ice-cold undiluted Matrigel (Growth factor Reduced, BD Biosciences) (1.97 mg/cm^2) was used to coat 96-well plates and incubated for 40 min at 37°C to allow the Matrigel to solidify HUVECs were seeded at a density of 5.5x10^4 cell/cm^2 and incubated with the conditioned media from I/R experiments and from hCSC culture after incubation with hiPSC-CMs conditioned media. ECGM2 and DMEM media were used as positive and negative controls for tube formation, respectively. Only HUVECs' cultures with low passage number (3-4) were used. At least four independent images were acquired per condition after 4 h of incubation and the morphological aspects of the tube network were quantified using the ImageJ angiogenesis analyser, including total master segment length (sum of the length of the detected master segments in the analysed area), total segment length (sum of the length of the segments) total branching length (sum of length of the trees composed from segments and branches), number of nodes and number of junctions [153]. All cell culture reagents were purchased from Gibco, Life Technologies unless stated otherwise.

3.7. Determination of cell viability and concentration

3.7.1. Trypan blue viability assay

Single cell suspensions were diluted in 0.1 % (v/v) trypan blue dye (Invitrogen) in PBS (Life Technologies). Non-viable cells with damaged membranes stain blue by incorporating this

impermeable dye. To determine both cell viability and concentration, cell counting was performed using a Fuchs-Rosenthal haemocytometer (Marienfeld Superior).

3.7.2. Nuclei count

Cell suspensions were incubated in lysis buffer (1% Triton X-100 in 0.1M citric acid) for a minimum period of 48 h at 37ºC. The obtained nuclei were stained using crystal violet dye 0.1 % (v/v) in lysis buffer. A Fuchs-Rosenthal haemocytometer (Marienfeld Superior) was used to address total nuclei.

3.7.3. Fluorescent-based viability assay (FDA/Pi and NucView Staining)

Cell viability of 3D aggregates of hiPSCs-CMs was evaluated by the incubation of two fluorescent probes diluted in DPBS for up to 5 min: Propidium iodide (PI) diluted 1:1000 (10µg/mL) and fluorescein diacetate (FDA) 1:1000 (20µg/mL). Samples were then visualized using fluorescence microscopy (DMI6000, Leica). FDA enters freely within all the cells and its converted to fluorescent fluorescein (green coloured fluorophore) by intracellular esterases in viable cells. Since fluorescein is highly polar, it gets trapped in cells free of membrane damage (otherwise it diffuses out of the cell). PI is a fluorescent polar and intercalating compound that can only access intracellular space of cells lacking membrane integrity, allowing the identification of non-viable cells by colouring them red after DNA intercalation [154].

Cell apoptosis of 3D hiPSC-CM cultures was further assessed using NucView® 488 caspase-3 substrate (Biotium), according to the manufacturer's recommendations. Briefly, live aggregates were incubated for 1 h at 37ºC with culture medium containing NucView® 488 reagent (1:200). Samples were then observed under a fluorescence microscope (DMI6000, Leica) and representative images were taken.

3.7.4. Aggregate size determination

Aggregates were imaged in a fluorescence microscope (DMI6000, Leica) and Ferret diameter was measured using ImageJ software.

3.7.5. Immunofluorescence microscopy

hiPSC-CMs aggregates were washed with DPBS, fixed in 4% (w/v) paraformaldehyde (PFA) and 4% (w/v) sucrose in DPBS for 20 min, and dehydrated in 30% (w/v) sucrose overnight. Samples were then embedded in Tissue-Tek® O.C.T. (Sakura) and frozen at −80°C for cryosectioning. Frozen samples were sliced with a thickness of 10 µm in a cryostat (Cryostat CM 3050 S, Leica). Afterwards, sections were permeabilized for 10 min in 0.1% (v/v) Triton X-100 in DPBS and blocked with 0.2% (v/v) Fish Skin Gelatin (FSG) in DPBS for 30 min, at room temperature (RT, 18-20°C). Sections were then incubated with primary antibodies diluted in

0.125% (v/v) FSG, 0.1% (v/v) Triton X-100 for 2 h at RT. Cells were washed with DPBS and incubated with secondary antibodies diluted in the same solution for 1 h at RT in the dark. The following primary antibodies were used: α-sarcomeric actinin (1:200, Sigma) and troponin T (1:100, Millipore). Alexa Fluor 488 phalloidin was used to stain F-actin (1:100, Invitrogen). Alexa Fluor 594 (1:500, Life Technologies) was used as secondary antibody. Samples were then observed using a fluorescence microscope (DMI6000, Leica).

3.7.6. Transmission electron microscopy

hiPSC-CMs aggregates were washed with DPBS and fixed in 4% (w/v) paraformaldehyde (PFA) and 4% (w/v) sucrose in DPBS for 20 min. Samples were stored in DPBS at 4°C until further processing. Aggregates were fixed in a mixture 2% PFA and 2% glutaraldehyde in 0.1 M Phosphate Buffer for 1 h on ice. Subsequently, samples were washed 3 times with 0.1 M Phosphate Buffer and embedded in 2% low melting point agarose. Agarose was allowed to solidify on ice prior to post-fixation with osmium tetroxide (1% v/v in 0.1 M Phosphate Buffer, 30 min on ice protected from light). After several washes in distilled water, the samples were contrasted in 1% Tannic Acid for 20 min on ice, washed several times in distilled water, dehydrated in a graded series of ethanol and infiltrated in epon resin (epon: ethanol mixtures: 1:3, 1:1, 3:1, 1 h and 30 min each, pure epon overnight) and embedded in flat embedding molds. Ultrathin sections were cut in a Reichert Ultramicrotome using a diamond knife. Samples were visualized in a H-7650 Transmission Electron Microscope (Hitachi) and representative images were taken.

3.8. Mass Spectrometry

3.8.1. Quantitative whole proteome analysis

After 3 days in culture, the effect of hiPSC-CMs conditioned media was evaluated regarding hCSC whole proteome quantitative analysis. The experimental design and quantitative proteomics workflow are illustrated in Figure 3.2.

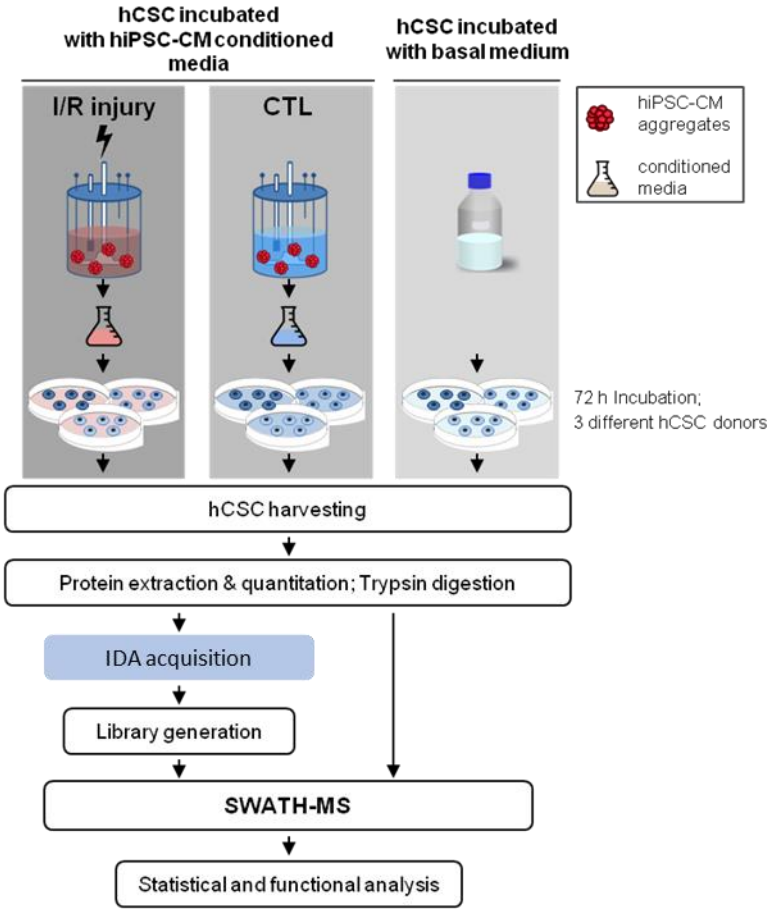

Figure 3.2 Experimental design and proteomic workflow. Conditioned media of Human induced pluripotent stem cell derived cardiomyocytes (hiPSC-CMs) (pool of 2 biological replicates) from Ischemia/Reperfusion (I/R) injury and control (CTL) bioreactor setup were incubated with human cardiac stem cells (hCSCs)

hCSCs were harvested and washed twice with DPBS by centrifugation. Cell pellets were placed at −80°C until further proteomic analysis. Proteins were extracted, quantified and processed from cell pellets as described elsewhere [155]. Briefly, cell pellets were resuspended in lysis buffer [50 mM Tris (pH 7.8); 250 mM Sucrose; 2 mM EDTA] with protease inhibitors and incubated on ice for 10 min. Cells were lysed with 30 passes through the 301/2 Gauge needle at 4 °C. Cell debris and unbroken nuclei were removed by centrifugation at 1,000 x g for 10 min at 4 °C and total protein concentration was quantified using a Microplate BCA Protein Assay Kit (Thermo Scientific). Samples were prepared with 1X NuPAGE LDS sample buffer (Novex) and 1X NuPAGE sample reducing agent (Novex), followed by denaturation at 70ºC for 10 min. Samples were subjected to electrophoresis on pre-casted gels NuPAGE 4-12% Bis-Tris (ThermoFischer Scientific) while using 1X NuPAGE MES Running buffer (Novex). The molecular marker used was SeeBlue®Plus 2 prestained standard (ThermoFischer Scientific). Electrophoresis was performed at 200 V for 5 min. Gels were stained either with Coomassie Blue (InstantBlue, Expedeon) for 1 h under gentle agitation. Proteins were digested in gel as described elsewhere [156]. Briefly, protein gel pieces were distained with 50% (v/V) acetonitrile, reduced with 10 mM DTT, alkylated with iodoacetamide 55 mM, and digested at 37°C with 6.7 µg/mL trypsin.

3.8.1.1. Generation of the spectral reference library

MS analysis was performed at the Mass Spectrometry Facility of iBET/ITQB-NOVA with the assistance of an expert technician. Each sample (2.5 µg) was used for information-dependent acquisition (IDA) analysis by NanoLC-MS using TripleTOF 6600 (ABSciex). A reversed phase nanoLC with a trap and elution configuration, using a Nano cHiPLC Trap column (200 µm × 0.5 mm ChromXP C18-CL 3 µm 120 Å) and nano column (75 µm × 15 cm ChromXP C18-CL 3 µm 120 Å) was performed. Water with 0.1% (v/v) formic acid (solvent A) and acetonitrile with 0.1% (v/v) formic acid (solvent B) were used. Sample was loaded in the trap column at a flow rate of 2 µL/min for 10 min using 100% (v/v) solvent A. Peptide separation was performed in the nano column at a flow rate of 300 µL/min applying a 90 min linear gradient of 5% to 30% (v/v) of solvent B. IDA scanning full spectra (400–2000 m/z) for 250 ms. The top 40 ions were selected for subsequent MS/MS scans (150–1800 m/z for 50 ms each) using a total cycle time of 2.3 s. The selection criteria for parent ions included a charge state between +2 and +5, and counts above a minimum threshold of 125 counts per second. Ions were excluded from further MS/MS analysis for 12 s. Fragmentation was performed using rolling collision energy with a collision energy spread of 5. The spectral library was created by combining all IDA raw files using ProteinPilot™ software (v5.0 ABSciex) with the Paragon algorithm and with the following search parameters: search against Homo sapiens from Uniprot/SwissProt database; trypsin digestion; iodoacetamide cysteine alkylation; through identification efforts. After a false discovery rate (FDR) analysis, only FDR<1% were considered. The output of these searches, in the form of a group file was used as the reference spectral library.

3.8.1.2. SWATH-MS analysis and targeted data extraction

For quantitative analysis, 2.5 µg of each sample were subjected to three SWATH runs. Similar chromatographic conditions to the previously described IDA run were used. The mass spectrometer was operated in a cyclic product ion data independent acquisition (DIA). A variable windows calculator (SWATH Variable Window Calculator_V1.0, AB SCIEX) and SWATH acquisition method editor (AB SCIEX) were used to setup the SWATH acquisition. A set of 32 overlapping windows (containing 1 m/z for the window overlap) was constructed, covering the precursor mass range of 400 – 1200 m/z. A 50 ms survey scan was acquired at the beginning of each cycle, and SWATH MS/MS spectra were collected for 96 ms resulting in a cycle time of 3.172 s. Rolling collision energy with a collision energy spread of 15 was used. The spectral alignment and targeted data extraction of DIA samples were performed using PeakView v.2.1 (AB SCIEX; Framingham, US) with the reference spectral library. For data extraction the following parameters were used: six peptides/protein, six transitions/peptide, peptide confidence level of >99%, FDR threshold of 1%, excluded shared peptides, and extracted ion chromatogram (XIC) window of 10 min and width set at 20 ppm. A total of 714 proteins were quantified under these conditions. The full list of quantified proteins can be accessed in supporting information file 4.1, at https://www.dropbox.com/sh/3kemuejjxov0mar/AADZG8V1Bg0tAEeoekCN05_Za?dl=0.

3.8.1.3. Proteomic data analysis

To identify differentially expressed proteins, student's T test analysis was performed using GraphPad Prism6 (GraphPad Software Inc., California, USA). Resulting p-values and fold changes were used to define up- and down- regulated proteins. Differentially expressed proteins were defined as those which showed a fold change greater than 1.5 (up-regulated) or lower than 0.67 (down-regulated) and p-values lower or equal to 0.05. Hierarchical clustering heat map analysis was performed using Perseus software environment [157]. Pathway analysis was performed using Ingenuity Pathway Analysis (IPA, Quiagen, Germany) by up-loading the protein list of interest (only proteins with p-value≤0.05) and the respective fold change. Statistically significant representation of biological functions and canonical pathways was identified based on IPA p-value, displayed as –log(p-value). This probability score is calculated taking into account the total number of proteins known to be associated with a given function or pathway, and their representation in the experimental dataset. Prediction of inhibition and activation of biological functions and canonical pathways was based on IPA z-score, a statistical measure of the match between expected relationship direction and observed protein expression resulting in activation ($z \geq 2$) or inhibition ($z \leq 2$) of the respective pathway.

3.9. Statistical analysis

Statistical analysis and data processing were performed with GraphPad Prism6 and Microsoft Excel 2016 (Microsoft® Office). All data are shown as mean with standard deviation. Data were analysed by One Way ANOVA Tukey test or student t-test (tube formation analysis, cytokine, nuclei counts, ELISA and proteomic results). P-values below 0.05 were considered significant. 2 biological replicates of the bioreactor experiments were performed. For the assays, at least 2 technical replicates of 2 biological replicates were performed.

4. Results and Discussion

4.1. Bioreactor I/R injury in 3D hiPSC-CMs aggregates

4.1.1. Bioreactor I/R injury setup

The two-phased *in vitro* I/R injury setup was developed using hiPSC-CMs aggregates cultured in STBR. The first phase, which aimed to mimic the ischemic period of the injury, had a duration of five hours and combined oxygen and nutrient deprivation with hyperosomosis and acidosis. The following phase, the reperfusion phase, had a period duration of sixteen hours and featured the culturing of hiPSC-CMs in nutrient-rich medium and the reestablishment of normoxic conditions to the myocardial physiological pO_2 of 3% in O_2 [150]. pO_2 and pH profiles were monitored throughout the I/R assay (Figure 4.1).

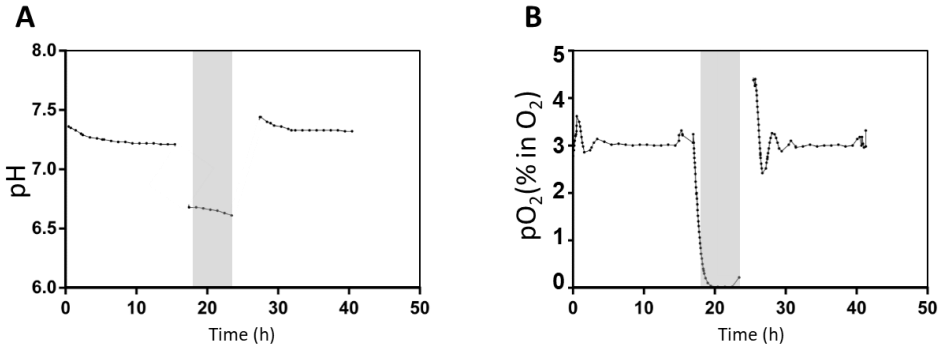

Figure 4.1 pO_2 and pH time-profiles throughout the I/R assay in bioreactors. (B) pH values in the culture medium and (B) pO_2 percentage over time. t=0 corresponds to the time of cell inoculation in the bioreactors. Ischemia phase is depicted in grey.

During the ischemic phase, a drop in pH (~6.7) was achieved by the replacement of the culture medium with IMS (Figure 4.1A). In myocardial ischemia, the extracellular pH has been reported to drop to values lower than 6 [158]. Regarding the oxygen content in the culture, pO_2 was readily dropped to below 0.4% in approximately 1 hour (Figure 4.1B). In the reperfusion phase, the oxygen content was set back to the myocardial physiological pO_2 of 3% in O_2 [150] and the pH values were increased to around 7.4 (Figure 4.1A), which is considered the physiological pH of mammalian arterial blood [159]. These results show that I/R features (drop in pH and O_2) were successfully mimicked using this setup.

4.1.2. Effect of I/R injury on hiPSC-CMs

4.1.2.1. Effect of I/R injury on hiPSC-CMs aggregates' viability

The effect of the I/R injury setup in hiPSC-CMs aggregates viability was accessed by live/dead and caspase-3 staining at several timepoints, namely before insult, post ischemia, 1-hour post reperfusion and 16 hours post reperfusion (Figure 4.2).

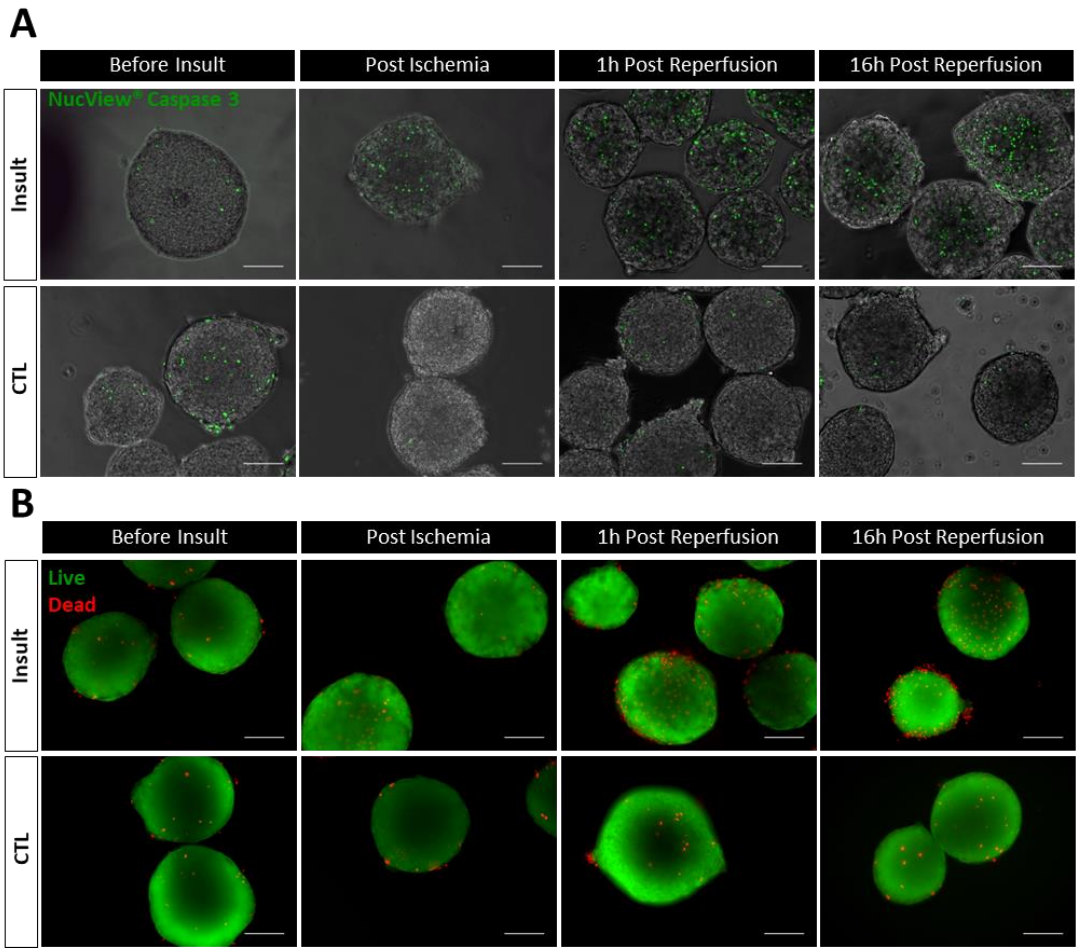

Figure 4.2 Viability of hiPSC-CMs aggregates subjected to the I/R injury. The viability of hiPSC-CM aggregates viability was assessed by NucView Caspase-3 Staining (green) (A) and by double cell staining with FDA (live cells, green) and PI (dead cells, red) (B) at several time points: Before Insult, Post Ischemia, and at 1 hour and 16 hours Post Reperfusion. Scale bars: 200 µm.

A clear decrease in hiPSC-CMs viability was observed when comparing the insult condition with the CTL condition. Throughout the I/R experiment, CTL hiPSC-CMs remained viable with a low number of apoptotic cells (Figure 4.2A) and dead cells (Figure 4.2B). Regarding caspase-3 activity levels, an early marker of apoptosis, hiPSC-CMs showed an increase of apoptotic cells in the insult condition after the ischemia phase when comparing to the CTL condition (Figure 4.2A). However, the abruptly increased caspase-3 activity levels after ischemia, are probably due to the 1-hour caspase-3 immunostaining incubation in fresh medium in reperfusion conditions (3% O_2 in CM001-R). Regarding PI staining, a greater number of dead cells in hiPSC-CMs were present in insult condition when compared to the CTL condition (Figure 4.2B). This increase in CMs death is more noticeable shortly after reperfusion (i.e. 1h post reperfusion) which is consistent with *in vivo* pathophysiology of AMI. In the first minutes of reperfusion, a burst of oxidative stress is induced by several mechanisms, including ROS. Moreover, other mediators also contribute to myocardial injury and CMs death, including intracellular calcium overload and the opening of the mPTP [12].

Other I/R injury studies, using different CMs sources, reported similar results regarding CMs loss of viability. Apoptosis has been also reported to increase significantly in primary cultures of neonatal rat CMs subjected to I/R [160]. In H9c2 cell line subjected to I/R experiments, lower CMs viability and higher expression of apoptosis-related proteins have been detected [161]. The same drop in viability in monocultures of hiPSC-CMs subjected to I/R injury has been reported, also triggered after the first hour of reperfusion [*Sebastião et al.* submitted]. Freshly isolated adult rat CMs also showed a decrease in cell viability regardless different durations of hypoxia and reperfusion when comparing to normoxic conditions [162]. Moreover, previous studies also stated decreased cell viability in hESC-CMs cultures subjected to *in vitro* I/R injury [163].

The average hiPSC-CMs aggregate diameter was accessed before the I/R injury and at the experimental endpoint for the CTL and insult conditions (Figure 4.3).

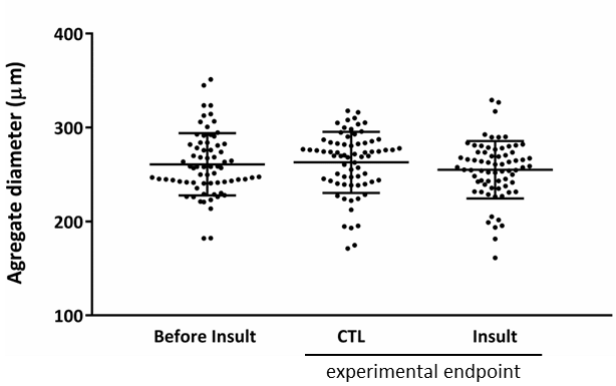

Figure 4.3 hiPSC-CMs aggregate size before and after I/R. Average aggregate diameters (A) were calculated before and after I/R bioreactor setup experiments for both control (CTL) and insult conditions (experimental endpoint, corresponding to 16 h after reperfusion).

Regardless of the advantages of bioreactors (including STBR) (as stated before in section 1.4), cell culture in STBR also presents limitations, including hydrodynamic shear stress, which can be potentially harmful to cell cultures [115]. Comparing the diameters of hiPSC-CMs before the I/R assay (260.8 ± 33.1 µm) with the CTL and insult conditions (262.9 ± 32.6 and 255.0 ± 30.6 µm, respectively), no significant changes were detected in diameter during bioreactor culture, pointing the absence of cell shedding from the hiPSC-CMs aggregates (Figure 4.3). This also indicates that the combination of impeller geometry and positioning inside the STBR, together with the correct agitation rate applied in this *in vitro* I/R model, did not affect hiPSC-CMs integrity.

4.1.2.2. Effect of I/R injury on hiPSC-CMs aggregates' phenotype and ultrastructure

In order to access whether the I/R injury setup affected the phenotype and structure of the hiPSC-CMs, immunocytochemistry tools were used to analyse the expression of CMs specific molecular markers (Figure 4.4).

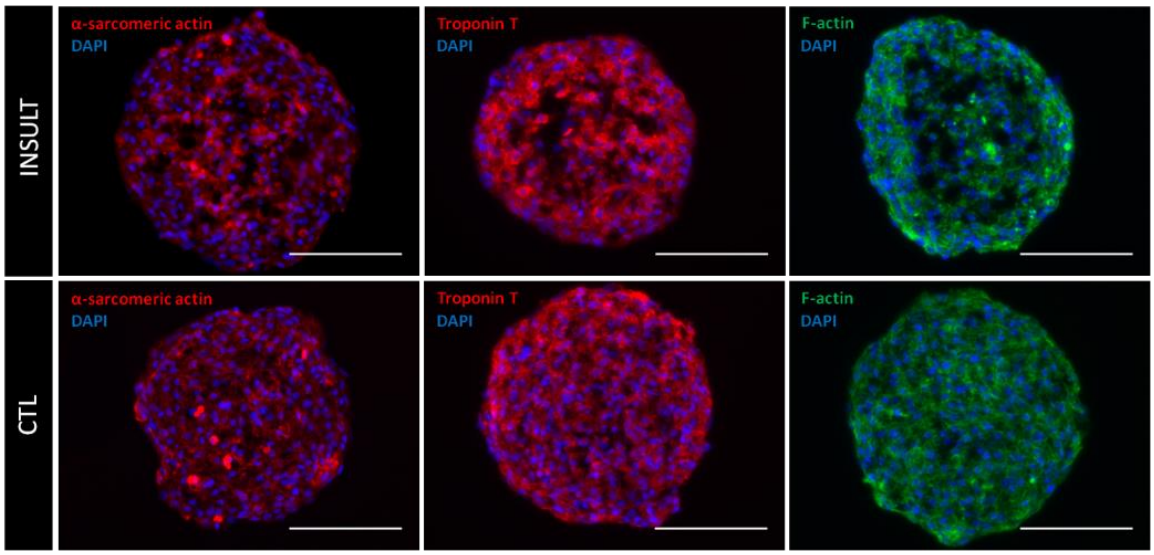

Figure 4.4 Characterization of cryosections of hiPSC-CMs aggregates. Specific molecular markers were accessed at 16 hours post reperfusion (insult) and in control (CTL) conditions. Cardiomyocyte molecular markers (i.e. α-sarcomeric actinin and troponin T) are present in both control (CTL) and insult conditions. hiPSC-CMs aggregates presented hollow lacunae in their core structure upon injury. Scale bars: 100 µm.

hiPSC-CMs aggregates from both CTL and insult conditions stained positive for cardiac-specific molecular markers (α-sarcomeric actinin and troponin T) (Figure 4.4). Interestingly, hiPSC-CMs of the insult condition presented hollow lacunae in the core of the aggregates. These hollow lacunae are likely to be due to the space left behind CMs death. Hollow cores are not present in the CTL hiPSC-CMs, meaning that no necrotic cores due to hypoxia appeared.

It has been previously reported in hESC aggregate cultures, that aggregates with diameters inferior to 300 µm in stirred suspension do not suffer from diffusional mass or gaseous transfer limitations [164]. In fact, the appearance of hollow lacunae in hiPSC-CMs subjected to I/R and their absence in the CTL conditions may be explained by the highly efficient O_2 diffusion in agitation-based systems (such as STBR used in this model) [115].

.

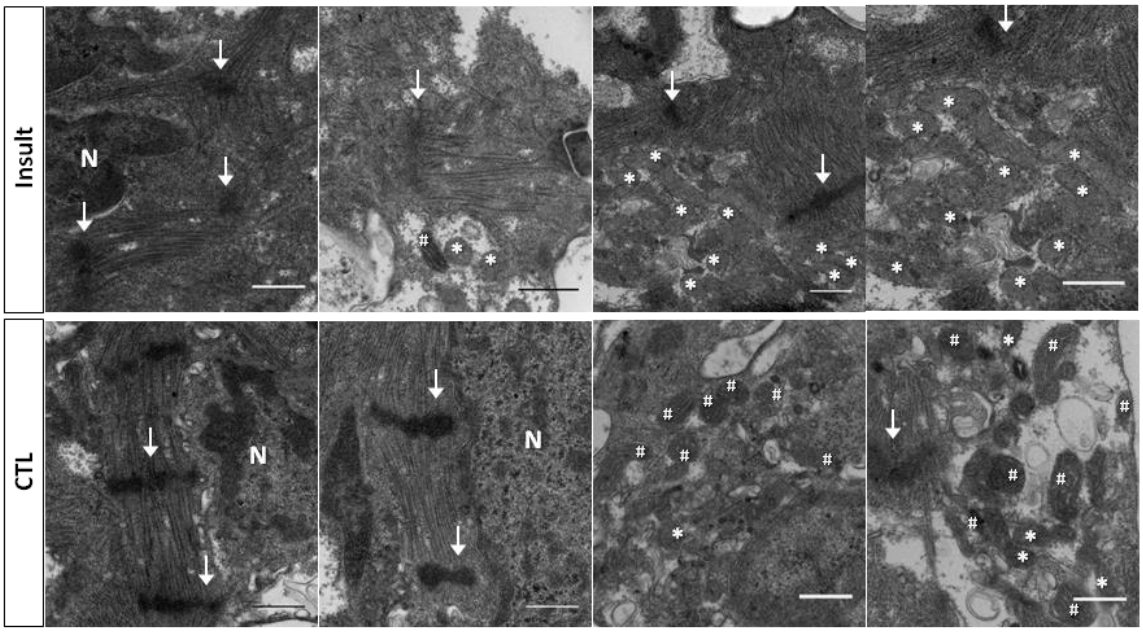

Figure 4.5 Ultrastructural characterization of hiPSC-CM aggregates. Transmission electron microscopy (TEM) images of hiPSC-CMs aggregates in control (CTL) and at 16 hours Post Reperfusion (Insult) conditions. Z-bands (↓), nuclei (N), mitochondria with visible cristae (#) and mitochondria with disorganized cristae structure (*) are highlighted. Scale bars: 500 nm.

To access the ultrastructure and further characterize the impact of the I/R injury setup on hiPSC-CMs, TEM analysis was performed (Figure 4.5). When comparing CTL and insult conditions, typical ultrastructural changes of *in vivo* I/R injury are visible. Cells exposed to the I/R injury revealed: (1) disruption of sarcomeric myofilaments and disorganized Z-bands and; (2) membrane rupture of mitochondria and disorganized cristae (Figure 4.5). Previous studies using cardiac tissue derived from rat models subjected to I/R also reported ultrastructural changes, including changes in mitochondrial morphology, such as extensive loss of cristae and double membrane and mitochondria swelling and loss of cristae. Other changes included the disruption of Z-band architecture and myofilament disruption, absence of sarcomeres and appearance of vacuoles within the cell (autophagy) [165-169].

4.1.2.2. Effect of I/R injury on hiPSC-CMs aggregates' secretome profile

To further evaluate the impact of the I/R injury in bioreactors on hiPSC-CMs, conditioned media was collected after the ischemic and reperfusion phases (of the injury setup) and evaluated in terms of cytokine and growth factors content. The cytokine array was chosen among others, based on which cytokines and growth factors had already been reported to be present in I/R context. Several differentially expressed cytokines were detected between CTL and hiPSC-CMs ischemic conditioned media (Figure 4.6) and between CTL and reperfusion conditioned media (Figure 4.7). Overall, the cytokine and growth factor profile between the ischemic and reperfusion conditioned media is different, with a more acute response during the ischemic period, highlighting the distinct pathophysiology of myocardial I/R injury phases (Figure 4.6 and 4.7).

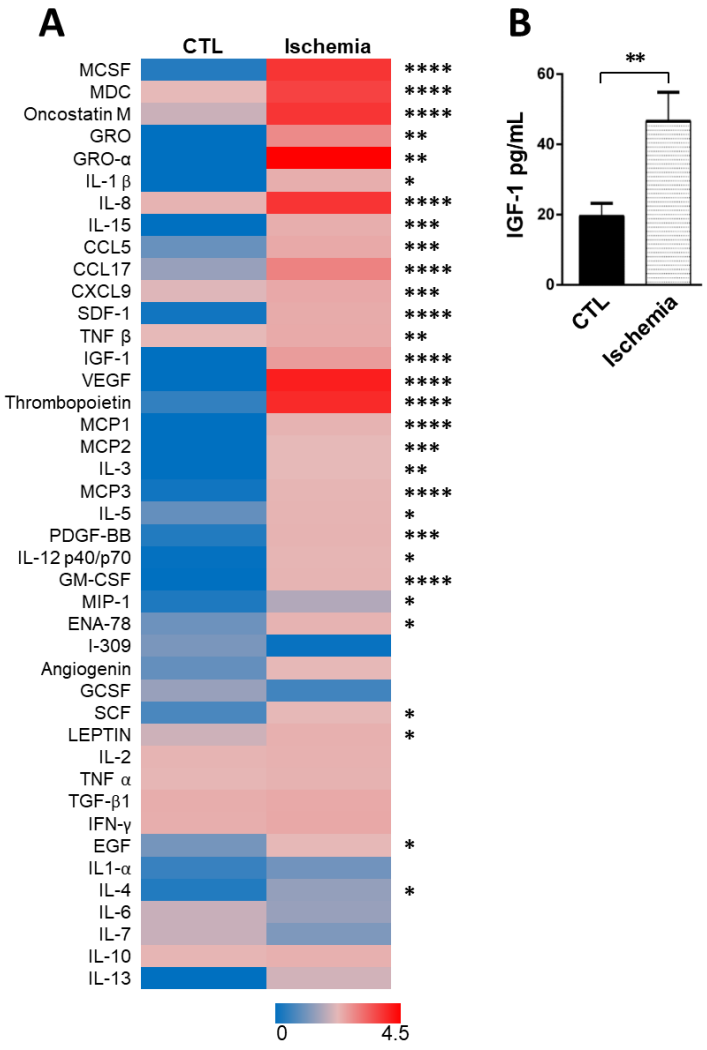

Figure 4.6 Secreted growth factors and cytokines by hiPSC-CMs aggregates during ischemia phase of I/R injury setup. Conditioned media of hiPSC-CMs aggregates from control (CTL) and insult condition of ischemic phase was profiled using a cytokine array. Colour scale from 0 (blue) to 4.5 (red) (arbitrary units in mean normalized spot density) (A). Validation of IGF-1 release was accessed by ELISA assay (B). *P≤0.05; **P≤0.01; ***P≤0.001; ****P≤0.0001 (Student t-test).

During ischemia, hiPSC-CMs aggregates showed significant increased secretion of 30 molecules with key roles in inflammation (MCSF, MDC, Oncostatin-M, GRO, GRO-α, IL-1β, IL-4, IL-5, IL-8, IL-12 p40/p70, IL-15, CCL5, CCL17, CXCL9, TNF-β, VEGF, MCP-1, MCP-2, MCP-3, MIP-1 and ENA-78), migration (GRO, GRO-α, IL-8, SDF-1, IGF-1, VEGF, MCP-1, MCP-2, ENA-78 and SCF) and angiogenesis (Thrombopoietin, PDGF-BB, GM-CSF and ENA-78) (Figure 4.6A).

Several of the detected cytokines have already been reported to be involved in AMI context. IL-1β, IL-8, IL-15 and MCP-1 were detected in AMI-diagnosed human cardiac tissue, where MCP-1 and IL-15 were the most present cytokines in the early onset of ischemia [170]. SCF, GM-CSF, SDF-1, IL-8 and VEGF are cytokines that are involved in migration and mobilization of immune and stem cells (e.g. CSCs and BMSC) upon AMI [171]. Furthermore, IL-8, VEGF, SCF and EGF have also been associated with angiogenesis and pro-survival effects in CMs upon AMI [171,

172]. Thrombopoietin was previously detected as upregulated in AMI patients [173] while ENA-78 and GRO-α have shown to be secreted in cardiac tissues of HF patients and to be involved in migration of c-kit^{+} CSCs [174]. Moreover, ischemia has been shown to induce the expression of MCSF [175] and Oncostatin-M [176] which are associated with inflammation and may contribute to tissue healing after AMI.

In particular, IGF-1 was validated by ELISA quantification (Figure 4.6B), confirming the increased release of this growth factor by hiPSC-CMs aggregates subjected to ischemia when compared to CTL conditions. IGF-1 has been associated with improved cardiac repair after AMI due to its role in the activation of endogenous CSCs [91] and has been previously reported to be released by CMs upon AMI [90, *Sebastião et al.* submitted].

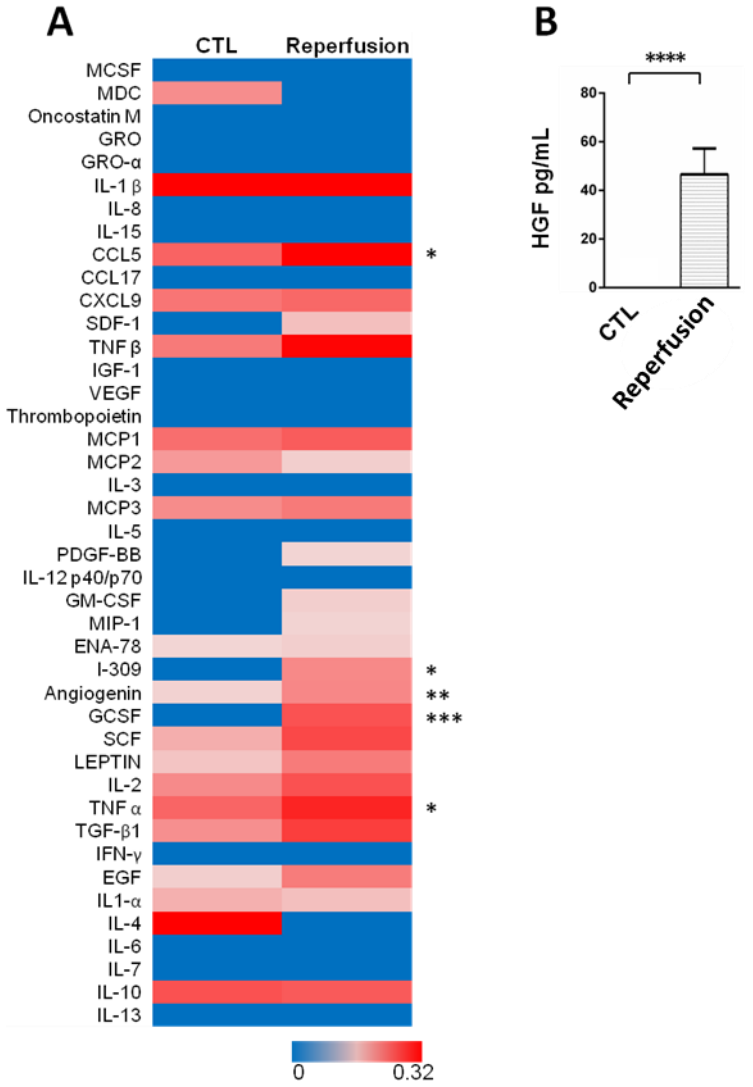

Figure 4.7 Secreted growth factors and cytokines by hiPSC-CMs aggregates during reperfusion phase of I/R injury setup. Conditioned media of hiPSC-CMs aggregates from control (CTL) and insult condition of reperfusion phase was profiled using a cytokine array. Colour scale from 0 (blue) to 0.32 (red) (arbitrary units in mean normalized spot density) (A). HGF concentration was accessed by ELISA assay (B). *P≤0.05; **P≤0.01; ***P≤0.001 (Student t-test).

Throughout the reperfusion phase of I/R injury, hiPSC-CMs also released some pro-inflammatory cytokines which showed increased levels in insult conditions (I-309, CCL5, TNF-α) as well as pro-angiogenic molecules (I-309, Angiogenin and GCSF) (Figure 4.7A).

These molecules have been also previously reported to be relevant in AMI context. I-309, an inflammatory mediator, has been shown to act as a monocyte chemoattractant [177]. In addition to pro-inflammatory functions, I-309 was also described to have a role in the activation of endothelial cell functions and angiogenesis *in vivo* [178]. CCL5 is also related to inflammatory processes, including the activation and recruitment of immune cells [179]. For instance, this chemokine has been shown to play a critical role in neutrophil and macrophage activation during AMI [179]. Similarly, TNF-α is expressed after AMI, being also involved in the following inflammatory response [171].

HGF, although not present in the chosen cytokine array, was also quantified and detected through ELISA only in the reperfusion phase of the I/R assay (Figure 4.7B). HGF has been reported to play a cardioprotective role in I/R rat models by reducing CM death [180]. Moreover, HGF has been shown to promote resident CSC activation, migration and proliferation [181, 182]. GCSF also promotes angiogenesis [183] and can additionally act as a cardioprotective agent by preventing cardiac remodelling after AMI through the promoting of bone marrow stem cell migration to the injured sites [184].

To further validate the angiogenic potential of the hiPSC-CMs conditioned media obtained after the I/R injury, angiogenesis tube formation assay using HUVECs was performed using conditioned media collected after the reperfusion phase (Figure 4.8).

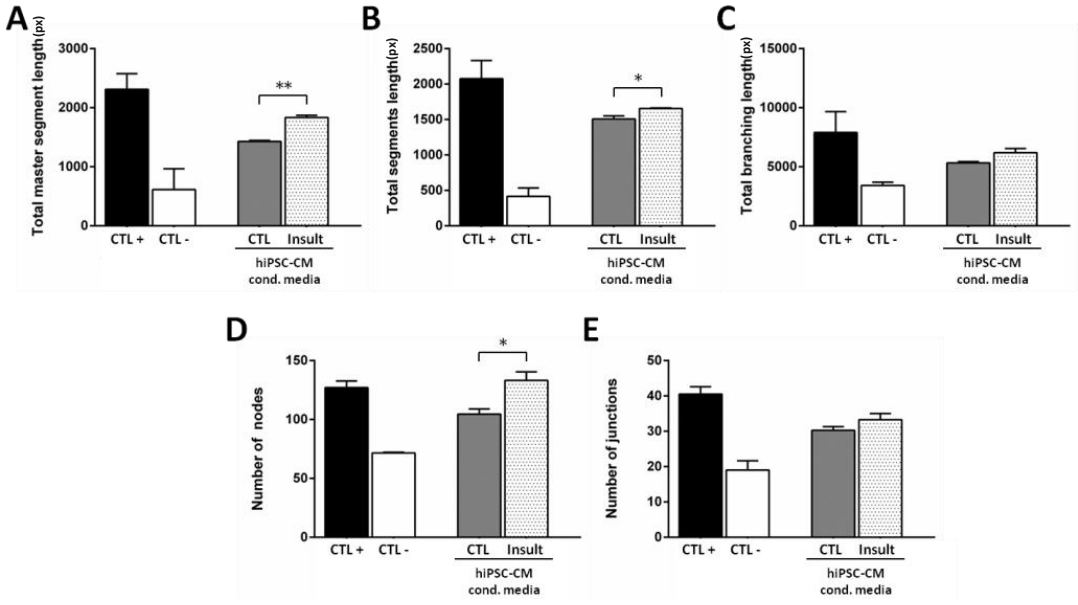

Figure 4.8 Assessment of angiogenic potential of I/R bioreactors conditioned medium. Conditioned media (Cond. Media) of hiPSC-CMs aggregates in control (CTL, grey bars) and at 16 hours Post Reperfusion (Insult, black and white dotted bars) conditions were tested for angiogenic potential by HUVECS tube formation assay. (A) Total master segment length, (B) total segment length, (C) total branching length, (D) number of nodes and (E) number of junctions were quantified by angiogenesis analyser plugin of ImageJ. *P<0.05; **P<0.01 (Student t-test). ECGM2 and DMEM were used as positive (black bars) and negative (white bars) controls for tube formation, respectively.

The results obtained from the incubation of HUVECs in hiPSC-CMs conditioned media, confirmed an increased angiogenic potential of hiPSC-CMs conditioned medium subjected to I/R injury when compared to the CTL (Figure 4.8). This angiogenic potential is unlikely to be solely derived from the release of cytokines and growth factors. Recently, it has been shown that CMs (from H9c2 cell line and primary rat CMs) that were subjected to ischemia, promote heart angiogenesis through the release of miR-containing exosomes [185] and even though equivalent studies in CMs subjected to reperfusion have not been performed, a similar behaviour can be hypothesized.

Overall, several hallmarks regarding CMs response to AMI have been successfully reproduced, including increased cell death, ultrastructural modifications and the release of key molecular factors (i.e. cytokines and growth factors) with pro-inflammatory, -migratory and -angiogenic properties. All these features were mimicked in the novel human I/R injury *in vitro* model established in this work, using 3D culture of hiPSC-CMs aggregates and STBRs.

4.2. Human Cardiac Stem Cells' response to hiPSC-CMs conditioned media

After successfully mimicking myocardial I/R injury using hiPSC-CMs 3D aggregates in STBR, the following step was to study the effect of the hiPSC-CMs secretome in hCSCs, in terms of i) migration, ii) proliferation, iii) factor secretion, iv) angiogenic response and v) protein expression profile.

4.2.1. Effect on hCSCs migration

Firstly, the effect of the hiPSC-CMs conditioned medium (from reperfusion phase) on the migration of hCSCs was accessed by scratch wound healing assay (Figure 4.9).

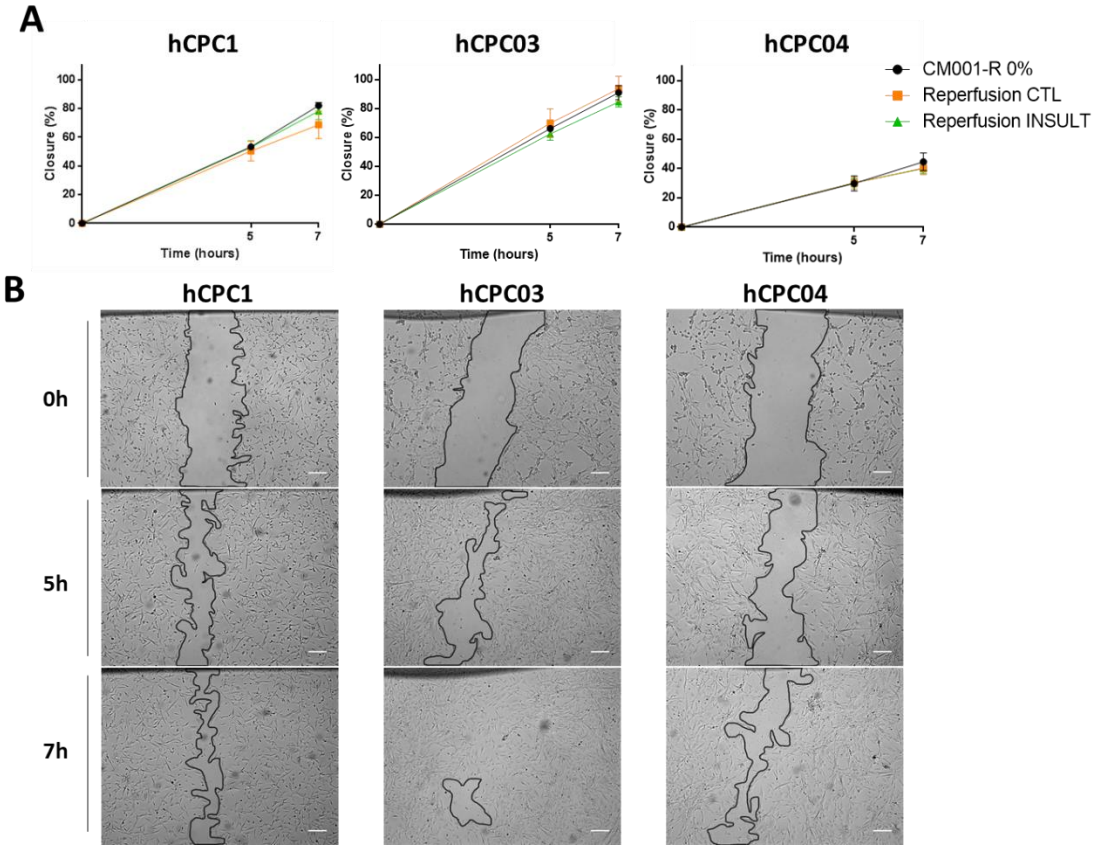

Figure 4.9 hiPSC-CMs conditioned media effect on hCSCs migration. Conditioned media of hiPSC-CMs aggregates in control (Reperfusion CTL) and at 16 hours Post Reperfusion (Reperfusion Insult) was used to incubate hCPC1, hCPC03 and hCPC04 (hCSCs from different donors) to access its effect on cell migration. (A) Rate (%) of wound closure of hCSCs after 7 hours of incubation by quantification of the "wound gap" distance between the front lines of migrating cells. (B) Phase-contrast photographs after wound generation (0h) and after 5 and 7 hours of incubation with basal media (CM001-R 0% FBS). The acquired images and the migration rates were accessed using ImageJ software. Scale bars: 200 µm

The secretion of factors detected on insult hiPSC-CMs conditioned medium (Figure 4.7A) including, SDF-1, SCF and HGF (Figure 4.7B) have been previously reported to be upregulated upon AMI [172]. These cytokines were described to play a role on stem cell migration and homing to injury [186]: SDF-1 and HGF are suggested to be involved in BMSCs migration [187] while SCF can mediate CSCs motility [188]. However, regarding the effect of the secreted factors during I/R by hiPSC-CMs on hCSCs migration, in all donors, no differences were detected when comparing the CTL with the insult conditions (Figure 4.9A). Additionally, no differences were also observed when comparing the migration rate of both conditions with the basal medium (CM001-R without FBS) (Figure 4.9A). This similarity can indicate that, even though the basal media (CM001-R without FBS) had no serum, it was still a nutrient and factor rich medium (e.g. N2 and B27 supplement), potentiating migration by itself. Given this, this method was not appropriate to address the migration potential of this particular media.

Moreover, the scratch wound healing assay showed that different donors have different rates of closure, suggesting that the rate of migration is donor-dependent (Figure 4.9). It has been reported that aged CSCs have impaired functionality due to the accumulation of ROS that induce modifications in guidance protein receptors (i.e. EphA2), ultimately leading to impaired CSC

migration within the heart [189]. The obtained results suggest that other factors other than age are also related to impaired migration capabilities, since HCPC04 (age 17), the younger donor, migrates at a slower rate than the other two older donors (ages 57 and 78). In fact, a more recent study in CDCs subjected to a scratch wound healing assay, suggested that even though CDCs derived from older donors expressed more senescence-associated markers, their migratory abilities were not age-dependent [190].

4.2.2. Effect on hCSCs proliferation

The impact of the reperfusion conditioned media from hiPSC-CMs subjected to I/R on hCSCs proliferation was also studied (Figure 4.10). In terms of total cell number, no differences were observed between the CTL and insult conditions after incubation with hiPSC-CMs conditioned media from reperfusion phase. Low to no proliferation was also observed in FBS-free media (hiPSC-CMs conditioned media and CM001-R 0% FBS). These results might indicate that FBS supplementation in the media is critical and potentiates hCSCs growth, since high proliferation was registered with FBS-containing medium (Figure 4.10).

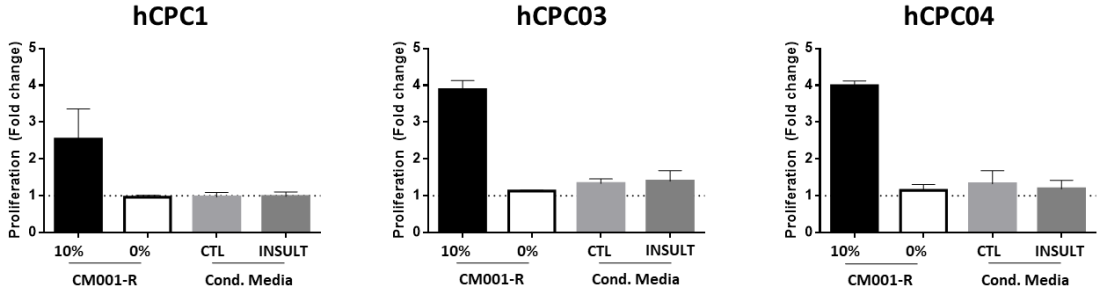

Figure 4.10 Effect of hiPSC-CMs conditioned media in hCSCs proliferation. Three hCSCs from different donors (HCPC1, HCPC03 and HCPC04) were incubated with hiPSC-CMs conditioned media for 3 days. Total cell number was accessed through nuclei counts and fold change was calculated by normalizing proliferation results with cell inoculum. CM001-R 10% and 0% FBS were also tested as quality controls.

It is known that I/R injury is able to promote CSCs proliferation. For instance, it has been reported that inducing I/R in hCSCs in co-culture with hiPSC-CMs induces hCSCs proliferation [*Sebastião et al*. submitted] and that CDCs subjected to hypoxia and reperfusion also respond with an increased proliferation rate [191]. It has also been shown that after AMI, CSCs increase in number both in humans [192] and adult mice [193, 194]. However, no differences in proliferation were obtained after the incubation of hCSCs with hiPSC-CMs conditioned media (Figure 4.10). Besides FBS absence, another hypothesis could be that hCSCs need to be subjected to the I/R injury (including lack of oxygen and nutrients) and that hiPSC-CMs conditioned media itself is not a sufficient stimulus (similar concentration of growth factors after 16h of reperfusion vs CTL - Figure 4.7A) to activate and enhance hCSCs proliferation.

4.2.3. Effect on hCSCs' secretion of IGF-1, HGF and CXCL6

After the end of the incubation of hCSCs with the hiPSC-CMs conditioned media, hCSCs supernatant was collected and further analysed regarding the secretion of three molecules that have known cardiac regenerative properties: IGF-1, HGF and CXCL6 (Figure 4.11).

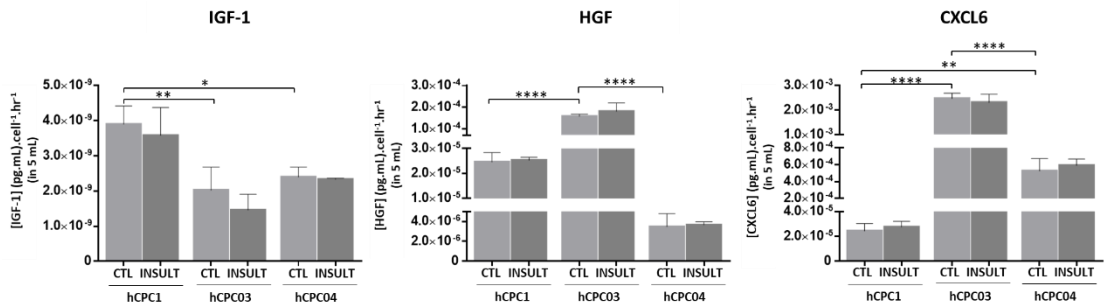

Figure 4.11 Secretion rate of IGF-1, HGF and CXCL6 factors by hCSCs after incubation with hiPSC-CMs conditioned media. Three donors of hCSCs (HCPC1, HCPC03 and HCPC04) were incubated with hiPSC-CMs conditioned media the release of the following factors was accessed through ELISA assay: (A) IGF-1, (B) HGF and (C) CXCL6. Specific growth factor secretion rates were obtained by normalizing growth factor concentration per cell number and incubation time (72 hours). *P<0.05; **P<0.01; ****P≤0.0001 (ANOVA Tukey test).

No differences in the secretion rates in any of the donors of hCSCs for the tested molecules were observed after the incubation with hiPSC-CMs conditioned media of CTL and insult conditions (Figure 14.1). Regarding donor variability in factor secretion, IGF-1 is secreted at higher rates by hCPC1 (Figure 4.11A) (e.g. CTL values for hCPC1 $3.89x10^{-9} \pm 5.22x10^{-10}$, for hCPC03 $2.02x10^{-9} \pm 6.64x10^{-10}$ and for hCPC04 $2.40x10^{-9} \pm 2.81x10^{-10}$) while HCPC03 secreted higher amounts of HGF (e.g. CTL $1.58x10^{-4} \pm 1.10x10^{-5}$), followed by HCPC1 (e.g. CTL $2.46x10^{-5} \pm 3.80x10^{-6}$) and HCPC04 (e.g. CTL $3.48x10^{-6} \pm 1.30x10^{-6}$) (Figure 4.11B). CXCL6 is secreted at a higher rate by HCPC03 (e.g. CTL $2.48x10^{-3} \pm 2.10x10^{-4}$), followed by HCPC04 (e.g. CTL $5.26x10^{-4} \pm 1.47x10^{-4}$), with HCPC1 (e.g. CTL $2.44x10^{-5} \pm 5.95x10^{-6}$), secreting at the lowest rate (Figure 4.11C).

Even though IGF-1 secretion rate is lower for the younger donor (hCPC04) (Figure 4.11A), it is reported that both the expression of IGF-1R (receptor activated by IGF-1) and the synthesis of IGF-1 is attenuated in older CSCs [195]. Further investigation is needed to validate this tendency. Apart from age, other factors, including genetic background and co-morbidities may also contribute to donor variability.

4.2.4. Effect on hCSC's angiogenic potential

hCSC's angiogenic potential was also evaluated in the collected supernatants by HUVECs tube formation assay. Overall, supernatants from HCPC1 and HCPC04 donors showed an increased angiogenic potential after being exposed to hiPSC-CMs conditioned media from the insult condition of the I/R assay (Figure 4.12). This result indicates that these two hCSCs donors produced more pro-angiogenic factors in response to the paracrine factors secreted by hiPSC-

CMs during I/R. While no similar or equivalent assays were found in the literature regarding hCSCs pro-angiogenic potential following incubation with I/R conditioned media, it has been reported that CSCs (in this case, CDCs) characteristically possess high angiogenic potential and tube formation capacity [196], which can be enhanced in an injury context.

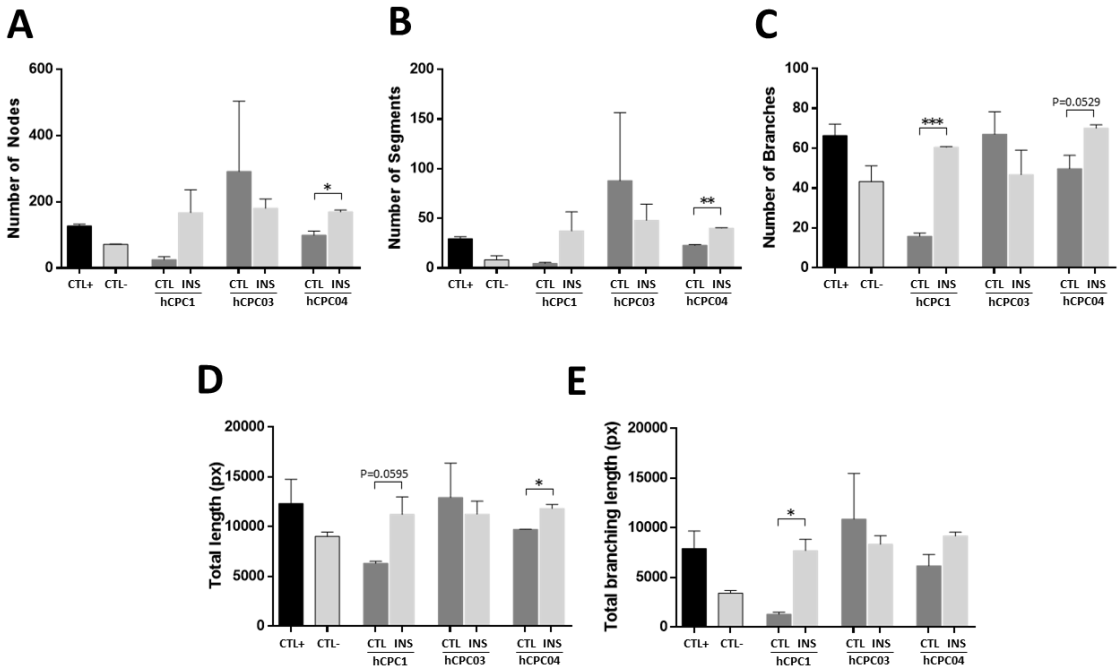

Figure 4.12 Assessment of angiogenic potential of hCSC supernatant after hiPSC-CMs conditioned media incubation. hCSC supernatant of three donors (HCPC1, HCPC03 and HCPC04) was harvested after a 3-day incubation period with hiPSC-CMs conditioned media of control (CTL, dark-grey bars) and at 16 hours Post Reperfusion (Insult, light-grey bars) conditions. Supernatants were tested for angiogenic potential by HUVECS tube formation assay. (A) Number of nodes, (B) number of segments, (C) number of branches, (D) total length and (E) total branching length were quantified by angiogenesis analyser plugin of Image. *P<0.05; **P<0.01; ***P≤0.001 (Student t-test). ECGM2 and DMEM were used as positive (black bars) and negative (outlined bars) controls, respectively.

Regarding donor variability, it has been reported that aged BMSC show reduced pro-angiogenic potential [197], however, such relation for hCSCs is not sustained by the obtained results, as the two older donors (hCPC1 and hCPC03) appear to have similar angiogenic measurements when comparing to the younger one (hCPC04) (Figure 4.12).

Most assays performed on hCSCs for migration, proliferation and key factor secretion showed no differences between the CTL and insult conditions since hiPSC-CMs conditioned media was nutrient rich (thus not allowing to detect possible differences). Due to this, a more sensitive technique was employed to further characterize hCSCs mechanism of action upon incubation with conditioned media from hiPSC-CMs subjected to I/R: SWATH-MS.

4.2.5. SWATH-MS of hCSCs after hiPSC-CM CondM incubation

hCSCs were incubated for 3 days in hiPSC-CMs conditioned media (CTL and insult) and were harvested for further characterization by label-free quantitative proteomics by SWATH-MS.

A total of 714 proteins were quantified in the samples, in which the biological canonical pathways and functions were analysed using IPA software.

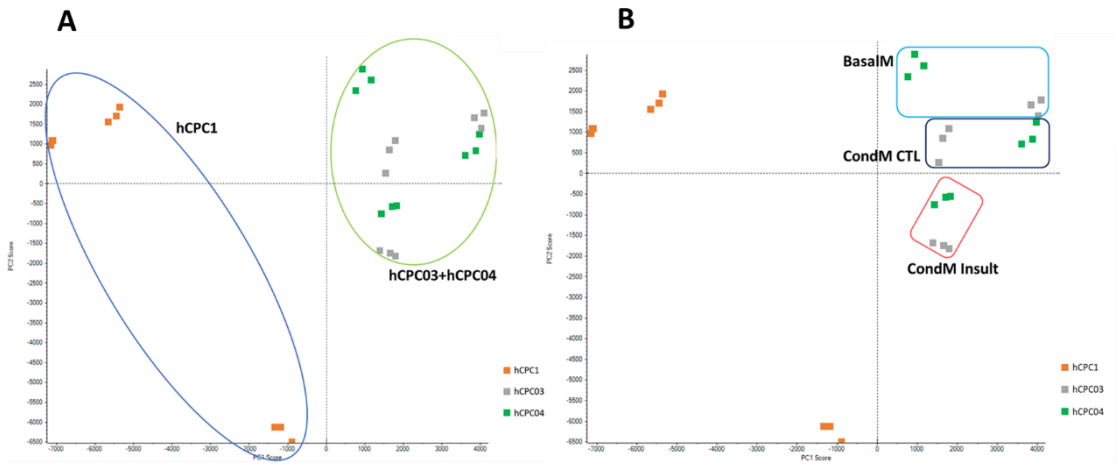

Figure 4.13 Principal Component Analysis (PCA) biplot of hCSC samples, including technical and biological replicates. (PCA settings: Unsupervised; Weighting – None; Scaling – Pareto). Scores for PC1 (39.4%) versus PC2 (18.8%) are displayed. (A) Samples grouped according to donor. Blue: hCPC1 and Light green: hCPC03+hCPC04; (B) Samples grouped according to experimental conditions. Light Blue hCSCs incubated with basal medium (BasalM); Dark Blue: hCSCs incubated with control hiPSC-CMs conditioned medium (CondM CTL); Red: hCSCs incubated with I/R injury hiPSC-CMs conditioned medium, (CondM Insult).

In order to interpret the relationship between the different biological replicates of hCSCs, a Principal Component Analysis (PCA) biplot was used (Figure 4.13). While hCPC03 and hCPC04 donors are relatively close together in the biplot, the hCPC1 donor is completely separated from the other 2 donors (Figure 4.13A). hCPC1 data did not cluster together with the other donors by condition (Figure 4.13B), suggesting that this hCSC donor presented a different protein expression profile. Consequently, hCPC1 was excluded from the subsequent functional proteomic analysis.

4.2.5.1. Proteome profile of hCSCs incubated with hiPSC-CMs control conditioned media

The effect of the hiPSC-CMs CTL secretome in hCSCs was accessed in terms of protein expression profile by comparison with hCSCs incubated with basal media (Figure 4.14). A total of 714 proteins were quantified in which 46 (6.44 %) proteins were found to be differently expressed (Figure 4.14A). Fifteen proteins were found to be up-regulated (fold change≥1.5, p-value≤0.05) while 31 were classified as down-regulated (fold change≤0.67, p-value≤0.05) in hCSCs incubated with hiPSC-CMs CTL conditioned media (Figure 4.14B).

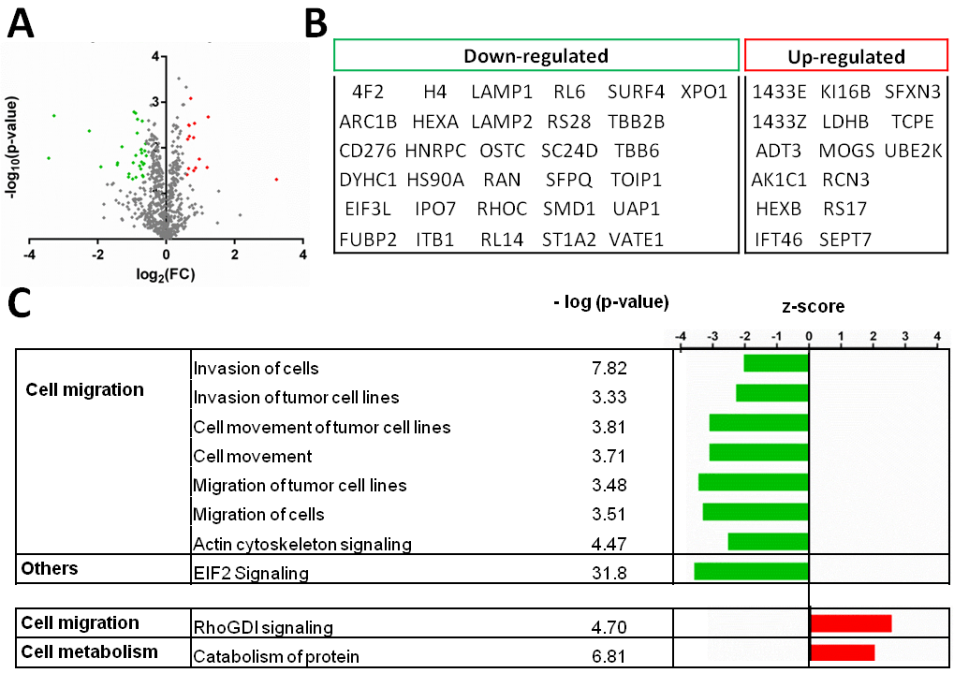

Figure 4.14 Quantitative proteomic analysis and comparison between hCSCs incubated with basal medium and with hiPSC-CMs control conditioned medium. (A) Volcano plot representing the results of differentially expressed proteins quantified by SWATH-MS (Up-regulated:red; Down-regulated:green; No change/non-significant:grey). 714 proteins were identified and quantified, including differentially expressed proteins (p-value≤0.05): 31 down-regulated (log_2(FC)≤-0.58, green) and 15 up-regulated (log_2(FC)≥0.58, red) in hCSCs incubated with hiPSC-CMs CTL conditioned medium. (B) list of down- and up-regulated proteins. (C) Activation (z-score ≥ 2, red) and inhibition (z-score≤ -2, green) scores of canonical pathways and functions. Only pathways and functions with p-value≤0.05 (log p-value ≥1.3) were considered. FC: fold change.

Functional analysis using IPA software (Figure 4.14C) revealed an overall inhibition of canonical pathways and functions involved in cellular migration (only 1 found to be activated) in hCSCs incubated with hiPSC-CMs CTL conditioned media. Other inhibited pathways included EIF2 signalling, an important stress signalling pathway which is associated with endoplasmic reticulum stress response [198]. Regarding cell metabolism, only 1 canonical function associated with protein catabolism was identified as activated. The activation of protein catabolism and inhibition of pathways and functions related to motility may act as a mechanism to preserve hCSCs stemness and quiescence. Adult stem cell migration is important to maintain tissue homeostasis, however, it is only activated under the appropriate stimuli. Factors such as secreted molecules, cell niches (e.g. cell population interaction) [66] and mechanical forces are involved in regulation of stem cell functions, including quiescence, self-renewal, proliferation, differentiation and migration [199]. Since beforehand no differences were expected in the comparison of these controls, the observed differences are likely caused by hiPSC-CMs secreted factors.

In order to address the main focus of this work, a further functional comparison between hCSCs incubated with conditioned media of the CTL and Insult conditions was performed.

4.2.5.2. Proteome profile of hCSCs incubated with hiPSC-CMs I/R injury paracrine factors

To understand if the different hCSCs donors responded similarly to the secretome of the hiPSC-CMs, a hierarchical clustering of the proteomic data was produced (Figure 4.15A). As previously stated, the hierarchical clustering also demonstrated that the 2 hCSCs donors used as biological replicates (hCPC03 and hCPC04) clustered together by condition (i.e. CTL and Insult). This result indicates that the experimental conditions had a greater influence in the hCSC proteome than the biological variability among the 2 donors. In terms of the obtained hCSCs proteome, a total of 714 proteins were identified in which 86 (12.04 %) were found to be differently expressed (Figure 4.15B). Sixty-three were found to be up-regulated (fold change≥1.5, p-value≤0.05) while 23 proteins were classified as down-regulated (fold change≤0.67, p-value≤0.05) in hCSCs incubated with the Insult hiPSC-CMs conditioned media (Figure 4.15C). Almost the double of proteins was differently expressed when comparing to the previous analysis (basal medium vs CTL medium), which points out a greater difference between insult and CTL conditions.

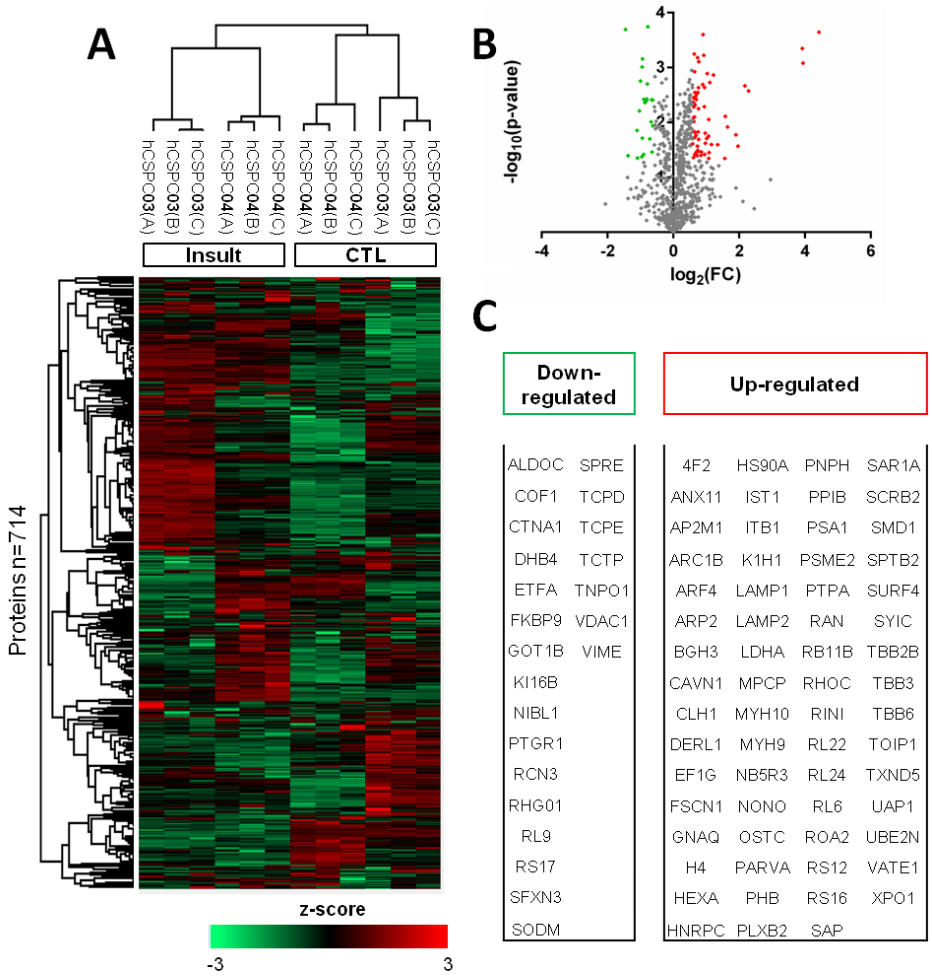

Figure 4.15 Quantitative proteomic analysis between hCSCs incubated with Ischemia/Reperfusion injury (insult) and hiPSC-CMs control (CTL) conditioned media. (A) Heatmap and hierarchical clustering (Eucledian distance) of logarithmized intensities of proteins (n=714) obtained from Perseus. Z-score values were coloured from green to red, representing down-regulation and up-regulation, respectively. Heat map analysis was performed using 2 biological (hCPC03 and hCPC04) and 3 technical (A, B, C) replicates.

Columns represent the technical replicates of the different biological replicates, while each row represents one protein. (B) Volcano plot representing the results of differentially expressed proteins quantified by SWATH-MS (Up-regulated:red; Down-regulated:green; No change/non-significant:grey). 714 proteins were identified and quantified, including differentially expressed proteins (p-value≤0.05) between control and Insult conditions: 23 down-regulated (log_2(FC)≤-0.58, green) and 63 up-regulated (log_2(FC)≥0.58, red). (C) List of down- and up-regulated proteins. FC: fold change.

Further functional analysis was conducted using IPA software, indicating that several canonical pathways and functions associated with cell migration, cell proliferation, paracrine signalling and stress response were activated (z-score≥2) (Table 4.1).

Table 4.1 Activated and inhibited canonical pathway and functions in hCSCs incubated with hiPSC-CMs Insult conditioned medium. Activated (z-score≥2, red) and inhibited z-score≤-2, green) canonical pathways and functions of hCSCs incubated with Ischemia/Reperfusion injury and hiPSC-CMs control conditioned media. Only functions and pathways with -log(p-value)≥1.3 are shown.

		- log (p-value)	z-score -4 -3 -2 -1 0 1 2 3 4
Cell migration	RhoGDI Signaling	5.21	
Cell migration	Actin Cytoskeleton Signaling	6.96	
	Migration of cells	5.66	
	Cell movement of tumor cell lines	5.34	
	Cell movement	6.20	
	Migration of tumor cell lines	4.60	
	Ephrin Receptor Signaling	4.45	
	Rac Signaling	5.13	
	Regulation of Actin-based Motility by Rho	6.53	
	CXCR4 Signaling	1.52	
Cell proliferation	Thrombin Signaling	1.60	
	Cdc42 Signaling	4.12	
	PAK Signaling	2.46	
	p70S6K Signaling	5.50	
Paracrine signaling	Chemokine Signaling	2.45	
	PAK signaling	2.46	
	Neuregulin Signaling	3.55	
	VEGF signaling	2.46	
Stress response	EIF2 Signaling	34.00	
	Apoptosis	7.76	
	NRF2- mediated oxidative stress	4.74	

Regarding cell migration, several functions and pathways were found to be activated in hCSCs incubated with hiPSC-CMs Insult conditioned medium (Table 4.1). CXCR4 signalling was identified as activated, where CXCR4 acts as a protein receptor of SDF-1. SDF-1/CXCR4 pathway is thought to play a role in stem cell migration in ischemia-related tissue repair, such as during AMI, since this pathway can be mediated by HIF-1 (hypoxia-inducible factor-1) signalling [200]. Moreover, 3 proteins (GTR1, HSP90A, and LDHA) associated with HIF-1 signalling were also identified as up-regulated from the subset of the differentially expressed proteins (Figure 4.15C). Regarding the Ephrin Receptor signalling, EphA2, a type of ephrin receptor, was also found to be up-regulated in renal I/R injury [201]. Only 1 pathway, RhoGDI signalling, was classified as inhibited (z-score≤-2). However, RhoGDI signalling has been showed to supress human tumour metastasis and invasion in human cancer (bladder) [202], two processes influenced by cell migration capabilities. Overall, the obtained results suggest that every pathway

and function detected as differentially activated or inhibited might be contributing to an increase in cell migration (Figure 4.16).

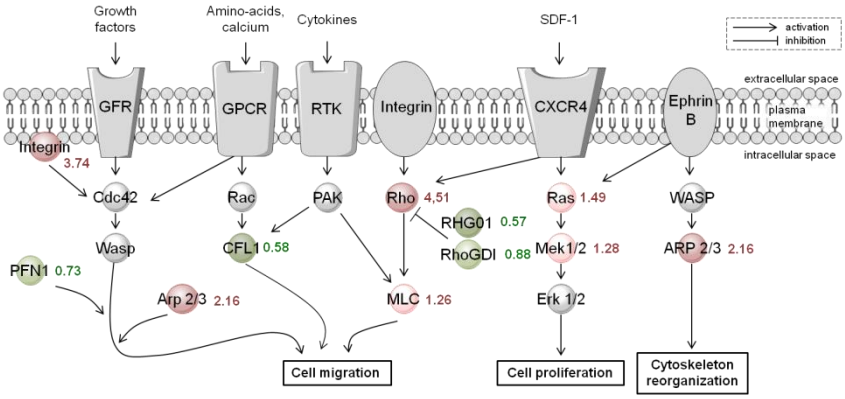

Figure 4.16 hCSCs activate pro-migratory and proliferation associated pathways. Proteomic analysis revealed that Cdc42, Rac, PAK, Rho, CXCR4, and Ephrin Receptor pathways are activated in hCSCs exposed to hiPSC-CM I/R injury conditioned medium, while RhoDGI signalling is inhibited. Proteins are depicted as green (negative fold change), red (positive fold change) and grey (not quantified in our analysis/ p-value≥0.05) circle. Only proteins with p-value≤0.05 were used in the analysis.

In terms of cellular proliferation, 4 pathways (thrombin, Cdc42, p70S6K and PAK signalling) were identified as activated (Table 4.1). For instance, p70S6K has been shown to promote cell growth (and also migration), having an important protective role in intestinal I/R injury in mice [203]. Other pathways including Cdc42 and PAK signalling are also related to increased cell proliferation (in cancer cells) [204, 205].

Paracrine signalling pathways were also found to be activated (Table 4.1). In fact, it is widely accepted that the secretion of paracrine modulators (e.g. cytokines, growth factors and exosomes) induced by cross-talk between cardiac populations are involved in the reported beneficial effects of CSCs in the improvement of cardiac function upon injury [87, 89, 91, 92, 94, *Sebastião et. al*, submitted]. Neuregulin signalling was one of the pathways found to be activated. It has been previously reported that Neuregulin-1 is up-regulated in *in vivo* rat models after AMI and that is able to provide cardioprotection against myocardial I/R by preconditioning [206]. VEGF signalling, also found as activated, is described to improve angiogenesis of hCSCs and to play a protective role in CMs upon AMI [171, 172]. Additionally, several proteins associated with clathrin-mediated endocytosis were also identified as upregulated (Figure 4.15C), which may indicate that hCSCs use this pathway to internalize paracrine signals when exposed to I/R injury milieu (Figure 4.17).

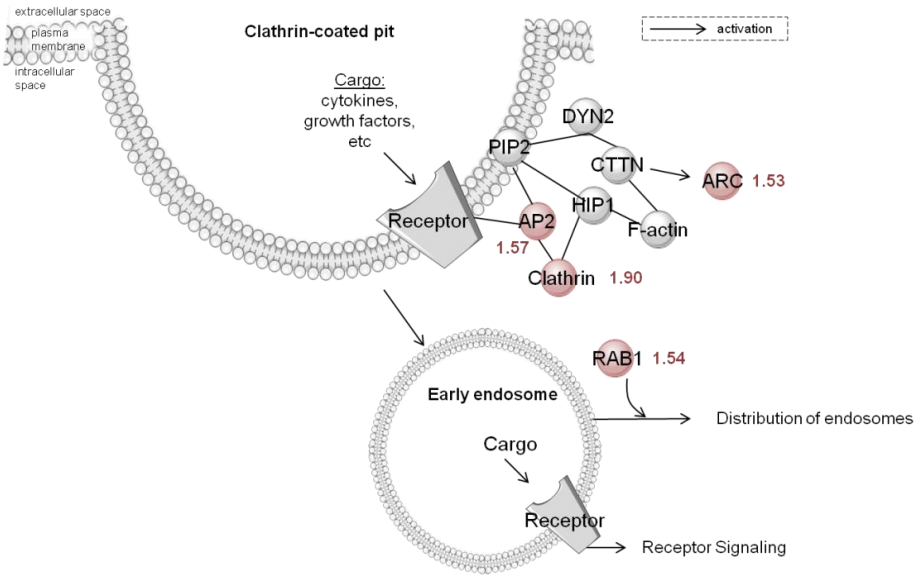

Figure 4.17 hCSCs secrete factors that activate clathrin-mediated endocytosis mechanisms. Proteins are depicted as red (positive fold change) and grey (not quantified in our analysis/p-value≥0.05) circles. Only proteins with p-value≤0.05 were used in the analysis.

Regarding stress signalling (Figure 4.18), 3 pathways and functions were identified as activated, including the EIF2 Signalling pathway (Table 4.1). An increase of EIF2 and EIF2B (involved in eukaryotic translation) phosphorylation has been previously suggested to control mRNA translation thus determining protein expression following myocardial I/R injury [207]. Since EIF2 phosphorylation is associated with stress response, the paracrine factors in the hiPSC-CMs secretome may be hypothesized to promote alterations in gene expression in hCSCs related to stress coping mechanisms at the translation level. NRF-2-mediated oxidative stress was also activated, which could be due to the presence of ROS in the hiPSC-CMs conditioned media from the reperfusion phase. Moreover, HSP90, a heat shock protein related to stress-response that acts as a regulator of HIF-1 signalling (activated in stem cells in response to hypoxia [200]) was also found to be upregulated (Figure 4.15C).

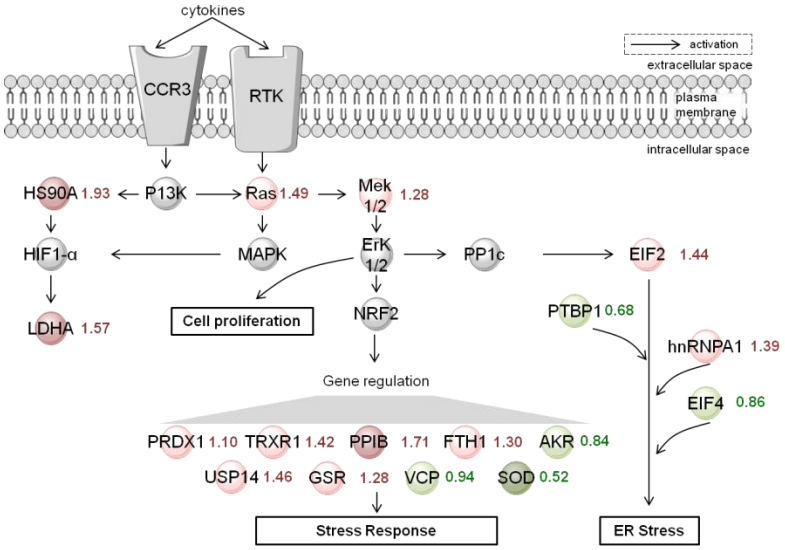

Figure 4.18 hCSCs activate stress response and proliferation-associated pathways. Proteomic analysis revealed that HIF1-α, EIF2 and NFR2 pathways are activated in hCSCs incubated with hiPSC-CMs I/R injury conditioned media. Proteins are depicted as green (negative fold change), red (positive fold change) and grey (not quantified in our analysis/p-value≥0.05) circles. Only proteins with p-value≤0.05 were used in the analysis.

Overall, when hCSCs were exposed to hiPSC-CMs CTL conditioned media, stress-related pathways (i.e. EIF2 signalling) and several migratory-related pathways and functions were inhibited, suggesting that hCSCs were not activated, thus being kept under quiescence to maintain cell stemness and homeostasis. In contrast, when hCSCs were incubated with insult hiPSC-CMs conditioned media, proliferation, migration and stress response mechanisms were activated, suggesting that hiPSC-CMs secretome activates these cellular functions through paracrine signalling.

5. Conclusion

In this work, a novel human cell-based *in vitro* myocardial I/R injury model was developed. The combination of 3D cell culture of hiPSC-CMs with bioreactor technology allowed a more accurate definition of the extracellular cues and physicochemical parameters of both phases of the I/R injury. In this setup, both phases of I/R were correctly mimicked in terms of nutrients, oxygen content and pH. Additionally, sampling during I/R did not compromise the culture conditions in any of the I/R phases, not disturbing the injury model. Moreover, the model was able to successfully recapitulate several CM AMI hallmarks, including increased CMs death, ultrastructural modifications of mitochondria and sarcomeres, and the secretion of key molecules (i.e. cytokines and growth factors) with pro-inflammatory, migratory and angiogenic properties.

Furthermore, the response of hCSCs to the secretome of hiPSC-CMs was evaluated. In terms of functional assays, migration, proliferation and factor secretion (IGF-1, HGF and CXCL6), hCSCs presented no differences between incubation with CTL or I/R injury hiPSC-CMs conditioned media. Regarding tube formation assay, the supernatant derived from hCSCs incubated with I/R hiPSC-CMs conditioned media held greater angiogenic potential when compared to CTL hiPSC-CMs. Furthermore, quantitative whole-proteomic analysis of hCSCs by SWATH-MS was employed as a more sensitive approach to study the response of hCSCs to hiPSC-CMs secretome. A total of 714 quantified proteins, 86 were differentially expressed, including 63 upregulated and 23 downregulated proteins in hCSCs exposed to I/R hiPSC-CMs conditioned medium vs CTL hiPSC-CMs conditioned medium. The obtained results indicated an upregulation of several proteins associated with pathways and functions involved in proliferation, migration and endocytosis in hCSCs, which is concordant with the literature regarding hCSCs response to AMI. An opposite trend was observed when comparing CTL hiPSC-CMs conditioned medium vs hCSCs incubated with basal medium. An inhibition of functions related with migration and pathways related with stress, together with the increase activation of protein catabolism suggested that CMs released factors to maintain hCSCs quiescence and stemness.

As future work, a more complex *in vitro* model could be achieved by the introduction of different cell populations of the myocardium, including cardiac fibroblasts, smooth muscle cells, endothelial cells and/or immune system cells. The secretome could be further characterized in terms of other paracrine cues such as exosomes or microvesicles. Regarding hCSCs response, a validation of the several activated pathways could be performed to confirm the SWATH-MS results. Since the tested hCSCs donors presented different characteristics, further in-depth studies should also be performed to study donor variability.

Expectantly, this new developed *in vitro* myocardial I/R model, together with the knowledge obtained on how CSCs act upon an AMI context, will aid in the development and research of novel therapies focused on the endogenous heart regeneration capacity. This work also demonstrates that more sensitive and robust tools are needed to characterize cells and their mechanisms of action.

6. References

[1] E. J. Benjamin *et al.*, *Heart Disease and Stroke Statistics'2017 Update: A Report from the American Heart Association*, vol. 135, no. 10. 2017.

[2] N. D. Wong, "Epidemiological studies of CHD and the evolution of preventive cardiology," *Nat. Rev. Cardiol.*, vol. 11, no. 5, pp. 276–289, 2014.

[3] K. Bhagat, "Endothelium function and myocardial infarction," *Cardiovasc. Res.*, vol. 39, no. 2, p. 312, 1998.

[4] P. Anversa and E. H. Sonnenblick, "Ischemic cardiomyopathy: Pathophysiologic mechanisms," *Prog. Cardiovasc. Dis.*, vol. 33, no. 1, pp. 49–70, 1990.

[5] E. Antman *et al.*, "Myocardial infarction redefined - A consensus document of The Joint European Society of Cardiology/American College of Cardiology Committee for the redefinition of myocardial infarction," *J. Am. Coll. Cardiol.*, vol. 36, no. 3, pp. 959–969, 2000.

[6] A. H. Kashou and H. E. Kashou, *Rhythm, ST Segment*. StatPearls Publishing, 2018.

[7] K. J. Overbaugh, "Acute Coronary Syndrome," *Am. J. Nurs.*, vol. 109, no. 5, pp. 42–52, 2009.

[8] J. L. Anderson and D. A. Morrow, "Acute Myocardial Infarction," *N. Engl. J. Med.*, vol. 376, no. 21, pp. 2053–2064, 2017.

[9] R. B. Jennings, H. M. Sommers, G. A. Smyth, H. A. Flack, and H. Linn, "Myocardial necrosis induced by temporary occlusion of a coronary artery in the dog," *Arch. Pathol.*, vol. 70, pp. 68–78, Jul. 1960.

[10] M. Neri, I. Riezzo, N. Pascale, C. Pomara, and E. Turillazzi, "Ischemia/Reperfusion Injury following Acute Myocardial Infarction: A Critical Issue for Clinicians and Forensic Pathologists," vol. 2017, 2017.

[11] L. M. Buja, "Myocardial ischemia and reperfusion injury," *Cardiovasc. Pathol.*, vol. 14, no. 4, pp. 170–175, 2005.

[12] D. Hausenloy and D. Yellon, "Myocardial ischemia-reperfusion injury: a neglected therapeutic target," *J Clin Invest*, vol. 123, no. 1, pp. 92–100, 2013.

[13] T. Kalogeris, C. P. Baines, M. Krenz, and R. J. Korthuis, "Cell Biology of Ischemia/Reperfusion Injury," *Int. Rev. Cell Mol. Biol.*, vol. 298, pp. 229–317, 2012.

[14] S. Homer-Vanniasinkam, J. N. Crinnion, and M. J. Gough, "Post-ischaemic Organ Dysfunction: A Review," *Eur J Vasc Endovasc Surg*, vol. 14, pp. 195–203, 1997.

[15] E. Braunwald and R. A. Kloner, "Myocardial reperfusion: a double-edged sword?," *J. Clin. Invest.*, vol. 76, no. 5, pp. 1713–9, Nov. 1985.

[16] J. Navarro-Yepes *et al.*, "Oxidative Stress, Redox Signaling, and Autophagy: Cell Death *Versus* Survival," *Antioxid. Redox Signal.*, vol. 21, no. 1, pp. 66–85, Jul. 2014.

[17] H. Wiseman and B. Halliwell, "Damage to DNA by reactive oxygen and nitrogen species: role in inflammatory disease and progression to cancer.," *Biochem. J.*, vol. 313 (Pt 1, no. 2, pp. 17–29, 1996.

[18] J. Zweier and M. Talukder, "The role of oxidants and free radicals in reperfusion injury," *Cardiovasc. Res.*, vol. 70, no. 2, pp. 181–190, May 2006.

[19] G. Kroemer, B. Dallaporta, and M. Resche-Rigon, "The mitochondrial death/life regulator in apoptosis and necrosis," *Annu. Rev. Physiol.*, vol. 60, no. 1, pp. 619–642, Oct. 1998.

[20] A. Halestrap, S. J. Clarke, and S. A. Javadov, “Mitochondrial permeability transition pore opening during myocardial reperfusion—a target for cardioprotection,” *Cardiovasc. Res.*, vol. 61, no. 3, pp. 372–385, Feb. 2004.

[21] A. P. Halestrap, “Calcium-dependent opening of a non-specific pore in the mitochondrial inner membrane is inhibited at pH values below 7. Implications for the protective effect of low pH against chemical and hypoxic cell damage.,” *Biochem. J.*, vol. 278 (Pt 3), pp. 715–9, Sep. 1991.

[22] M. Ruiz-Meana, A. Abellán, E. Miró-Casas, and D. Garcia-Dorado, “Opening of mitochondrial permeability transition pore induces hypercontracture in Ca2+ overloaded cardiac myocytes,” *Basic Res. Cardiol.*, vol. 102, no. 6, pp. 542–552, Nov. 2007.

[23] J. J. Lemasters *et al.*, “The mitochondrial permeability transition in cell death: a common mechanism in necrosis, apoptosis and autophagy.,” *Biochim. Biophys. Acta*, vol. 1366, no. 1–2, pp. 177–196, 1998.

[24] D. M. Y. D.J. Hausenloy, “The mitochondrial permeability transition pore: its fundamental role in mediating cell death during ischaemia and reperfusion,” *J. Mol. Cell. Cardiol.*, vol. 4, no. 35, pp. 339–341, 2003.

[25] C. Giorgi, A. Romagnoli, P. Pinton, and R. Rizzuto, “Ca2+ signaling, mitochondria and cell death.,” *Curr. Mol. Med.*, vol. 8, no. 2, pp. 119–30, Mar. 2008.

[26] Z. V. Schofield *et al.*, “Neutrophils – a key component of ischemia reperfusion injury,” *Shock*, vol. 40, no. 6, pp. 463–470, 2013.

[27] J. Vinten-Johansen, “Involvement of neutrophils in the pathogenesis of lethal myocardial reperfusion injury,” *Cardiovasc. Res.*, vol. 61, no. 3, pp. 481–497, Feb. 2004.

[28] S.-B. Ong *et al.*, “Inflammation following acute myocardial infarction: Multiple players, dynamic roles, and novel therapeutic opportunities,” *Pharmacol. Ther.*, Jan. 2018.

[29] S. D. Francis Stuart, N. M. De Jesus, M. L. Lindsey, and C. M. Ripplinger, “The crossroads of inflammation, fibrosis, and arrhythmia following myocardial infarction.,” *J. Mol. Cell. Cardiol.*, vol. 91, pp. 114–22, Feb. 2016.

[30] T. A. Wynn, “Cellular and molecular mechanisms of fibrosis.,” *J. Pathol.*, vol. 214, no. 2, pp. 199–210, Jan. 2008.

[31] V. Talman and H. Ruskoaho, “Cardiac fibrosis in myocardial infarction-from repair and remodeling to regeneration.,” *Cell Tissue Res.*, vol. 365, no. 3, pp. 563–81, 2016.

[32] A. Piek, R. A. de Boer, and H. H. W. Silljé, “The fibrosis-cell death axis in heart failure,” *Heart Fail. Rev.*, vol. 21, no. 2, pp. 199–211, Mar. 2016.

[33] A. M. Segura, O. H. Frazier, and L. M. Buja, “Fibrosis and heart failure,” *Heart Fail. Rev.*, vol. 19, no. 2, pp. 173–185, Mar. 2014.

[34] L. H. Lund *et al.*, “The registry of the international society for heart and lung transplantation: Thirty-first official adult heart transplant report - 2014; Focus theme: Retransplantation,” *J. Hear. Lung Transplant.*, vol. 33, no. 10, pp. 996–1008, 2014.

[35] P. G. Steg *et al.*, “ESC Guidelines for the management of acute myocardial infarction in patients presenting with ST-segment elevation,” *Eur. Heart J.*, vol. 33, no. 20, pp. 2569–2619, 2012.

[36] E. A. Amsterdam *et al.*, *2014 AHA/ACC guideline for the management of patients with non-st-elevation acute coronary syndromes: A report of the American college of cardiology/American heart association task force on practice guidelines*, vol. 130, no. 25. 2014.

[37] Z.-Q. Zhao *et al.*, “Inhibition of myocardial injury by ischemic postconditioning during reperfusion: comparison with ischemic preconditioning,” *Am. J. Physiol. Circ. Physiol.*, vol. 285, no. 2, pp. H579–H588, Aug. 2003.

[38] H. Sato, J. E. Jordan, Z.-Q. Zhao, S. S. Sarvotham, and J. Vinten-Johansen, “Gradual Reperfusion Reduces Infarct Size and Endothelial Injury but Augments Neutrophil Accumulation,” *Ann Thorac Surg*, vol. 64, pp. 1099–107, 1997.

[39] G. Heusch, “Postconditioning: Old wine in a new bottle?,” *J. Am. Coll. Cardiol.*, vol. 44, no. 5, pp. 1111–1112, 2004.

[40] R. A. Kloner and S. H. Rezkalla, “Preconditioning, postconditioning and their application to clinical cardiology,” *Cardiovasc. Res.*, vol. 70, no. 2, pp. 297–307, 2006.

[41] K. Przyklenk, B. Bauer, M. Ovize, R. A. Kloner, and P. Whittaker, “Regional ischemic ‘preconditioning’ protects remote virgin myocardium from subsequent sustained coronary occlusion,” *Circulation*, vol. 87, no. 3, pp. 893–899, 1993.

[42] D. J. Hausenloy and D. M. Yellon, “Remote ischaemic preconditioning: Underlying mechanisms and clinical application,” *Cardiovasc. Res.*, vol. 79, no. 3, pp. 377–386, 2008.

[43] D. J. Duncker, C. L. Klassen, Y. Ishibashi, S. H. Herrlinger, T. J. Pavek, and R. J. Bache, “Effect of temperature on myocardial infarction in swine,” *Am. J. Physiol. Circ. Physiol.*, vol. 270, no. 4, pp. H1189–H1199, Apr. 1996.

[44] W. W. O’Neill *et al.*, “Acute Myocardial Infarction With Hyperoxemic Therapy (AMIHOT),” *J. Am. Coll. Cardiol.*, vol. 50, no. 5, pp. 397–405, Jul. 2007.

[45] D. M. Yellon and D. Hausenloy, “Myocardial reperfusion injury.,” *N. Engl. J. Med.*, vol. 357, pp. 1121–35, 2007.

[46] X. Rossello and D. M. Yellon, “The RISK pathway and beyond,” *Basic Res. Cardiol.*, vol. 113, no. 1, p. 2, 2018.

[47] D. J. Hausenloy *et al.*, “Translating novel strategies for cardioprotection: the Hatter Workshop Recommendations,” *Basic Res. Cardiol.*, vol. 105, no. 6, pp. 677–686, Nov. 2010.

[48] M. I. Schaun *et al.*, “Cell Therapy in Ischemic Heart Disease: Interventions That Modulate Cardiac Regeneration,” *Stem Cells Int.*, vol. 2016, 2016.

[49] I. L. Weissman, “Stem cells: units of development, units of regeneration, and units in evolution,” *Cell*, vol. 100, no. 1, pp. 157–168, 2000.

[50] M. Shoukhrat and D. Wolf, “Totipotency, Pluripotency and Nuclear Reprogramming,” *Adv. Biochem. Eng. Biotechnol.*, no. 114, pp. 185–199, 2009.

[51] S. Arbatlı, G. S. Aslan, and F. Kocabas, “Stem Cells in Regenerative Cardiology,” in *Cell Biology and Translational Medicine. Advances in Experimental Medicine and Biology*, Boston, MA: Springer, Cham, 2017, pp. 37–53.

[52] D. A. Taylor *et al.*, “Regenerating functional myocardium: improved performance after skeletal myoblast transplantation.,” *Nat. Med.*, vol. 4, no. 8, pp. 929–33, Aug. 1998.

[53] P. Menasché *et al.*, “Myoblast transplantation for heart failure,” *Lancet*, vol. 357, no. 9252, pp. 279–280, Jan. 2001.

[54] R. Madonna, P. Ferdinandy, R. De Caterina, J. T. Willerson, and A. J. Marian, “Recent Developments in Cardiovascular Stem Cells,” *Circ. Res.*, vol. 115, no. 12, pp. e71–e78, Dec. 2014.

[55] V. Bellamy *et al.*, “Long-term functional benefits of human embryonic stem cell-derived cardiac progenitors embedded into a fibrin scaffold.,” *J. Heart Lung Transplant.*, vol. 34, no. 9, pp. 1198–207, Sep. 2015.

[56] R. Madonna *et al.*, “Position Paper of the European Society of Cardiology Working Group Cellular Biology of the Heart: cell-based therapies for myocardial repair and regeneration in ischemic heart disease and heart failure,” *Eur. Heart J.*, vol. 37, no. 23, pp. 1789–1798, Jun. 2016.

[57] A. P. Beltrami *et al.*, “Adult Cardiac Stem Cells Are Multipotent and Support Myocardial Regeneration,” vol. 114, pp. 763–776, 2003.

[58] E. Messina *et al.*, “Isolation and Expansion of Adult Cardiac Stem Cells From Human and Murine Heart,” *Circ. Res.*, vol. 95, pp. 911–921, 2004.

[59] R. R. Smith, “Cardiospheres,” in *Manual of Research Techniques in Cardiovascular Medicine*, Oxford, UK: John Wiley & Sons, Ltd, 2013, pp. 95–103.

[60] C. Report, L. Bin, Z. Jian, and C. Lz, “Cardiac Stem Cells and their Regenerative Role on Myocardial Infarction,” vol. 8, no. 4, 2014.

[61] B. Dawn *et al.*, “Cardiac stem cells delivered intravascularly traverse the vessel barrier, regenerate infarcted myocardium, and improve cardiac function,” *Proc. Natl. Acad. Sci.*, vol. 102, no. 10, pp. 3766–3771, Mar. 2005.

[62] P. V. Johnston *et al.*, “Engraftment, Differentiation, and Functional Benefits of Autologous Cardiosphere-Derived Cells in Porcine Ischemic Cardiomyopathy,” *Circulation*, vol. 120, no. 12, pp. 1075–1083, Sep. 2009.

[63] L. Bin, Z. Jian, Shaheen, and L. Cheng, “Cardiac Stem Cells and their Regenerative Role on Myocardial Infarction,” *J. Mol. Genet. Med.*, vol. 8, no. 4, 2014.

[64] A. Hasan *et al.*, “Engineered Biomaterials to Enhance Stem Cell-Based Cardiac Tissue Engineering and Therapy.,” *Macromol. Biosci.*, vol. 16, no. 7, pp. 958–77, 2016.

[65] B. Nadal-Ginard, G. M. Ellison, and D. Torella, “The cardiac stem cell compartment is indispensable for myocardial cell homeostasis, repair and regeneration in the adult,” *Stem Cell Res.*, vol. 13, no. 3, pp. 615–630, Nov. 2014.

[66] A. Leri, M. Rota, T. Hosoda, P. Goichberg, and P. Anversa, “Cardiac stem cell niches,” *Stem Cell Res.*, vol. 13, no. 3, pp. 631–646, 2014.

[67] P. Anversa, J. Kajstura, A. Leri, and R. Bolli, “Life and death of cardiac stem cells: A paradigm shift in cardiac biology,” *Circulation*, vol. 113, no. 11, pp. 1451–1463, 2006.

[68] M. P. Santini, E. Forte, R. P. Harvey, and J. C. Kovacic, “Developmental origin and lineage plasticity of endogenous cardiac stem cells,” *Development*, vol. 143, no. 8, pp. 1242–1258, 2016.

[69] H. Reinecke, E. Minami, W. Z. Zhu, and M. A. Laflamme, “Cardiogenic differentiation and transdifferentiation of progenitor cells,” *Circ. Res.*, vol. 103, no. 10, pp. 1058–1071, 2008.

[70] H. Oh *et al.*, “Cardiac progenitor cells from adult myocardium: Homing, differentiation, and fusion after infarction,” *Proc. Natl. Acad. Sci.*, vol. 100, no. 21, pp. 12313–12318, 2003.

[71] K. L. Laugwitz *et al.*, “Postnatal isl1+cardioblasts enter fully differentiated cardiomyocyte lineages,” *Nature*, vol. 433, no. 7026, pp. 647–653, 2005.

[72] L. Barile, M. Gherghiceanu, L. M. Popescu, T. Moccetti, and G. Vassalli, “Human cardiospheres as a source of multipotent stem and progenitor cells,” *Stem Cells Int.*, vol. 2013, 2013.

[73] I. L. Lei, L. Bu, and Z. Wang, “Derivation of cardiac progenitor cells from embryonic stem cells.,” *J. Vis. Exp.*, no. 95, p. 52047, Jan. 2015.

[74] L. Drowley *et al.*, “Human Induced Pluripotent Stem Cell-Derived Cardiac Progenitor Cells in Phenotypic Screening: A Transforming Growth Factor-β Type 1 Receptor Kinase Inhibitor Induces Efficient Cardiac Differentiation,” *Stem Cells Transl. Med.*, vol. 5, no. 2, pp. 164–174, Feb. 2016.

[75] B. Nadal-Ginard, G. M. Ellison, and D. Torella, “The cardiac stem cell compartment is indispensable for myocardial cell homeostasis, repair and regeneration in the adult,” *Stem Cell Res.*, vol. 13, no. 3, pp. 615–630, Nov. 2014.

[76] K. Urbanek *et al.*, “Myocardial regeneration by activation of multipotent cardiac stem cells in ischemic heart failure.,” *Proc. Natl. Acad. Sci. U. S. A.*, vol. 102, no. 24, pp. 8692–7, Jun. 2005.

[77] G. M. Ellison, D. Torella, I. Karakikes, and B. Nadal-Ginard, “Myocyte death and renewal: modern concepts of cardiac cellular homeostasis,” *Nat. Clin. Pract. Cardiovasc. Med.*, vol. 4, no. S1, pp. S52–S59, Feb. 2007.

[78] C. D. Waring *et al.*, “The adult heart responds to increased workload with physiologic hypertrophy, cardiac stem cell activation, and new myocyte formation,” *Eur. Heart J.*, vol. 35, no. 39, pp. 2722–2731, Oct. 2014.

[79] G. M. Ellison, C. D. Waring, C. Vicinanza, and D. Torella, “Physiological cardiac remodelling in response to endurance exercise training: cellular and molecular mechanisms,” *Heart*, vol. 98, no. 1, pp. 5–10, Jan. 2012.

[80] D. Orlic *et al.*, “Bone marrow cells regenerate infarcted myocardium,” *Nature*, vol. 410, no. 6829, pp. 701–705, Apr. 2001.

[81] C. E. Murry *et al.*, “Haematopoietic stem cells do not transdifferentiate into cardiac myocytes in myocardial infarcts,” *Nature*, vol. 428, no. 6983, pp. 664–668, Apr. 2004.

[82] S. A. Jesty *et al.*, “c-kit+ precursors support postinfarction myogenesis in the neonatal, but not adult, heart.,” *Proc. Natl. Acad. Sci. U. S. A.*, vol. 109, no. 33, pp. 13380–5, Aug. 2012.

[83] G. M. Ellison *et al.*, “Adult c-kitpos Cardiac Stem Cells Are Necessary and Sufficient for Functional Cardiac Regeneration and Repair,” *Cell*, vol. 154, no. 4, pp. 827–842, Aug. 2013.

[84] M. Wu and F. Meng, “Has the cardiac stem cell controversy settled down?,” *Sci. China Life Sci.*, vol. 57, no. 9, pp. 949–950, Sep. 2014.

[85] J. H. van Berlo *et al.*, “c-kit+ cells minimally contribute cardiomyocytes to the heart,” *Nature*, vol. 509, no. 7500, pp. 337–341, May 2014.

[86] C. F. Leite, T. R. Almeida, C. S. Lopes, and V. J. Dias da Silva, “Multipotent stem cells of the heart-do they have therapeutic promise?,” *Front. Physiol.*, vol. 6, pp. 1–17, 2015.

[87] C.-Y. Park *et al.*, “Cardiac Stem Cell Secretome Protects Cardiomyocytes from Hypoxic Injury Partly via Monocyte Chemotactic Protein-1-Dependent Mechanism.,” *Int. J. Mol. Sci.*, vol. 17, no. 6, May 2016.

[88] R. M. Strieter *et al.*, “The functional role of the ELR motif in CXC chemokine-mediated angiogenesis.,” *J. Biol. Chem.*, vol. 270, no. 45, pp. 27348–57, Nov. 1995.

[89] G. M. Ellison *et al.*, “Endogenous Cardiac Stem Cell Activation by Insulin-Like Growth Factor-1/Hepatocyte Growth Factor Intracoronary Injection Fosters Survival and Regeneration of the Infarcted Pig Heart,” *J. Am. Coll. Cardiol.*, vol. 58, no. 9, pp. 977–986, Aug. 2011.

[90] K. Reiss, L. G. Meggs, P. Li, G. Olivetti, J. M. Capasso, and P. Anversa, “Upregulation of IGF1, IGF1-receptor, and late growth related genes in ventricular myocytes acutely after infarction in rats,” *J. Cell. Physiol.*, vol. 158, no. 1, pp. 160–168, Jan. 1994.

[91] S. Koudstaal *et al.*, “Sustained delivery of insulin-like growth factor-1/hepatocyte growth factor stimulates endogenous cardiac repair in the chronic infarcted pig heart.,” *J. Cardiovasc. Transl. Res.*, vol. 7, no. 2, pp. 232–41, Mar. 2014.

[92] A. G.-E. Ibrahim, K. Cheng, and E. Marbán, “Exosomes as critical agents of cardiac regeneration triggered by cell therapy.,” *Stem cell reports*, vol. 2, no. 5, pp. 606–19, May 2014.

[93] R. Wu, X. Hu, and J. Wang, “Concise Review: Optimized Strategies for Stem Cell-based Therapy in Myocardial Repair: Clinical Translatability and Potential Limitation,” *Stem Cells*, 2018.

[94] R. Gallet *et al.*, “Exosomes secreted by cardiosphere-derived cells reduce scarring, attenuate adverse remodelling, and improve function in acute and chronic porcine myocardial infarction,” *Eur. Heart J.*, vol. 38, no. 3, p. ehw240, Sep. 2016.

[95] A. M. Abarbanell *et al.*, “Animal Models of Myocardial and Vascular Injury,” *J. Surg. Res.*, vol. 162, no. 2, pp. 239–249, Aug. 2010.

[96] G. J. Gross, “Models of Cardiac Ischemia-Reperfusion Injury in Dogs and Rats,” in *Current Protocols in Pharmacology*, Hoboken, NJ, USA: John Wiley & Sons, Inc., 2002.

[97] A. Akhtar, “The flaws and human harms of animal experimentation.,” *Camb. Q. Healthc. Ethics*, vol. 24, no. 4, pp. 407–19, Oct. 2015.

[98] H. B. van der Worp *et al.*, “Can Animal Models of Disease Reliably Inform Human Studies?,” *PLoS Med.*, vol. 7, no. 3, p. e1000245, Mar. 2010.

[99] K. H. Benam *et al.*, “Engineered In Vitro Disease Models,” *Annu. Rev. Pathol. Mech. Dis.*, vol. 10, no. 1, pp. 195–262, Jan. 2015.

[100] A. Hidalgo *et al.*, “Modelling ischemia-reperfusion injury (IRI) *in vitro* using metabolically matured induced pluripotent stem cell-derived cardiomyocytes,” *APL Bioeng.*, vol. 2, no. 2, p. 026102, Jun. 2018.

[101] C. Denning *et al.*, “Cardiomyocytes from human pluripotent stem cells: From laboratory curiosity to industrial biomedical platform.,” *Biochim. Biophys. Acta*, vol. 1863, no. 7 Pt B, pp. 1728–48, Jul. 2016.

[102] Y. Li *et al.*, “Sulforaphane prevents rat cardiomyocytes from hypoxia/reoxygenation injury in vitro via activating SIRT1 and subsequently inhibiting ER stress.,” *Acta Pharmacol. Sin.*, vol. 37, no. 3, pp. 344–53, Mar. 2016.

[103] P. M. Kang, A. Haunstetter, H. Aoki, A. Usheva, and S. Izumo, “Morphological and molecular characterization of adult cardiomyocyte apoptosis during hypoxia and reoxygenation.,” *Circ. Res.*, vol. 87, no. 2, pp. 118–25, Jul. 2000.

[104] T. Zhu, Q. Yao, X. Hu, C. Chen, H. Yao, and J. Chao, “The Role of MCPIP1 in Ischemia/Reperfusion Injury-Induced HUVEC Migration and Apoptosis.,” *Cell. Physiol. Biochem.*, vol. 37, no. 2, pp. 577–91, 2015.

[105] E. Robin *et al.*, “Oxidant stress during simulated ischemia primes cardiomyocytes for cell death during reperfusion.,” *J. Biol. Chem.*, vol. 282, no. 26, pp. 19133–43, Jun. 2007.

[106] Y. Xu *et al.*, “Substance P Attenuates Hypoxia/Reoxygenation-Induced Apoptosis Via the Akt Signalling Pathway and the NK1-Receptor in H9C2Cells,” *Hear. Lung Circ.*, Oct. 2017.

[107] X. Li *et al.*, “Quantitative profiling of the rat heart myoblast secretome reveals differential responses to hypoxia and re-oxygenation stress,” *J. Proteomics*, vol. 98, pp. 138–149, Feb. 2014.

[108] M. Zhao *et al.*, “Acetylcholine Mediates AMPK-Dependent Autophagic Cytoprotection in H9c2 Cells During Hypoxia/Reoxygenation Injury,” *Cell. Physiol. Biochem.*, vol. 32, no. 3, pp. 601–613, 2013.

[109] J. Li, C. Wang, and B. Z. B. Tang, “7, 8, 3’-Trihydroxyflavone protects H/R-induced apoptosis and induces in vivo growth of human embryonic stem cell-derived cardiomyocytes,” *J. Cell. Biochem.*, May 2017.

[110] K. Duval *et al.*, “Modeling Physiological Events in 2D vs. 3D Cell Culture,” *Physiology*, vol. 32, no. 4, pp. 266–277, Jul. 2017.

[111] M. W. Tibbitt and K. S. Anseth, “Hydrogels as extracellular matrix mimics for 3D cell culture,” *Biotechnol. Bioeng.*, vol. 103, no. 4, pp. 655–663, Jul. 2009.

[112] F. Pampaloni, E. G. Reynaud, and E. H. K. Stelzer, “The third dimension bridges the gap between cell culture and live tissue,” *Nat. Rev. Mol. Cell Biol.*, vol. 8, no. 10, pp. 839–845, Oct. 2007.

[113] H. K. Kleinman, D. Philp, and M. P. Hoffman, “Role of the extracellular matrix in morphogenesis.,” *Curr. Opin. Biotechnol.*, vol. 14, no. 5, pp. 526–32, Oct. 2003.

[114] A. Birgersdotter, R. Sandberg, and I. Ernberg, “Gene expression perturbation in vitro—A growing case for three-dimensional (3D) culture systems,” *Semin. Cancer Biol.*, vol. 15, no. 5, pp. 405–412, Oct. 2005.

[115] M. Serra, C. Brito, C. Correia, and P. M. Alves, “Process engineering of human pluripotent stem cells for clinical application,” *Trends Biotechnol.*, vol. 30, no. 6, pp. 350–359, Jun. 2012.

[116] L. Polonchuk *et al.*, “Cardiac spheroids as promising in vitro models to study the human heart microenvironment,” *Sci. Rep.*, vol. 7, no. 1, p. 7005, Dec. 2017.

[117] G. A. Figtree, K. J. Bubb, O. Tang, E. Kizana, and C. Gentile, “Vascularized Cardiac Spheroids as Novel 3D in vitro Models to Study Cardiac Fibrosis,” *Cells Tissues Organs*, vol. 204, no. 3–4, pp. 191–198, 2017.

[118] B. Mosadegh *et al.*, “Three-Dimensional Paper-Based Model for Cardiac Ischemia,” *Adv. Healthc. Mater.*, vol. 3, no. 7, pp. 1036–1043, Jul. 2014.

[119] R. G. Katare, M. Ando, Y. Kakinuma, and T. Sato, “Engineered Heart Tissue: A Novel Tool to Study the Ischemic Changes of the Heart In Vitro.”, PLoS One, vol. 5, no. 2, 2010

[120] M. Serra, C. Brito, E. M. Costa, M. F. Sousa, and P. M. Alves, “Integrating human stem cell expansion and neuronal differentiation in bioreactors,” *BMC Biotechnol.*, vol. 9, no. 1, p. 82, Sep. 2009.

[121] J. Hansmann, F. Groeber, A. Kahlig, C. Kleinhans, and H. Walles, “Bioreactors in tissue engineering-principles, applications and commercial constraints,” *Biotechnol. J.*, vol. 8, no. 3, pp. 298–307, Mar. 2013.

[122] I. Martin, D. Wendt, and M. Heberer, “The role of bioreactors in tissue engineering,” *Trends Biotechnol.*, vol. 22, no. 2, pp. 80–86, Feb. 2004.

[123] D. Wang, W. Liu, B. Han, and R. Xu, “The Bioreactor: A Powerful Tool for Large-Scale Culture of Animal Cells,” *Curr. Pharm. Biotechnol.*, vol. 6, no. 5, pp. 397–403, Oct. 2005.

[124] D. Antoni, H. Burckel, E. Josset, and G. Noel, “Three-dimensional cell culture: a breakthrough in vivo.,” *Int. J. Mol. Sci.*, vol. 16, no. 3, pp. 5517–27, Mar. 2015.

[125] G. J. M. Cabrita, B. S. Ferreira, C. L. da Silva, R. Gonçalves, G. Almeida-Porada, and J. M. S. Cabral, “Hematopoietic stem cells: from the bone to the bioreactor,” *Trends Biotechnol.*, vol. 21, no. 5, pp. 233–240, May 2003.

[126] A. Kumar and B. Starly, “Large scale industrialized cell expansion: producing the critical raw material for biofabrication processes,” *Biofabrication*, vol. 7, no. 4, p. 044103, Nov. 2015.

[127] J. W. Allen and S. N. Bhatia, “Formation of steady-state oxygen gradients in vitro:Application to liver zonation,” *Biotechnol. Bioeng.*, vol. 82, no. 3, pp. 253–262, May 2003.

[128] S. Sá Santos, U. Sonnewald, M. J. T. Carrondo, and P. M. Alves, “The role of glia in neuronal recovery following anoxia: In vitro evidence of neuronal adaptation,” *Neurochem. Int.*, vol. 58, no. 6, pp. 665–675, May 2011.

[129] C. Correia *et al.*, “Combining Hypoxia and Bioreactor Hydrodynamics Boosts Induced Pluripotent Stem Cell Differentiation Towards Cardiomyocytes,” *Stem Cell Rev. Reports*, vol. 10, no. 6, pp. 786–801, Dec. 2014.

[130] M. Stastna, M. R. Abraham, and J. E. Van Eyk, “Cardiac stem/progenitor cells, secreted proteins, and proteomics.,” *FEBS Lett.*, vol. 583, no. 11, pp. 1800–7, Jun. 2009.

[131] N. L. Anderson and N. G. Anderson, “Proteome and proteomics: New technologies, new concepts, and new words,” *Electrophoresis*, vol. 19, no. 11, pp. 1853–1861, Aug. 1998.

[132] P. R. Graves and T. A. J. Haystead, “Molecular Biologist’s Guide to Proteomics,” *Microbiol. Mol. Biol. Rev.*, vol. 66, no. 1, p. 39, 2002.

[133] K. Chandramouli and P.-Y. Qian, “Proteomics: challenges, techniques and possibilities to overcome biological sample complexity.,” *Hum. Genomics Proteomics*, vol. 2009, Dec. 2009.

[134] F. X. R. Sutandy, J. Qian, C.-S. Chen, and H. Zhu, “Overview of protein microarrays.,” *Curr. Protoc. protein Sci.*, vol. Chapter 27, p. Unit 27.1, Apr. 2013.

[135] R. Aebersold and M. Mann, “Mass spectrometry-based proteomics,” *Nature*, vol. 422, no. 6928, pp. 198–207, Mar. 2003.

[136] X. Han, A. Aslanian, and J. R. Yates, “Mass spectrometry for proteomics,” *Curr. Opin. Chem. Biol.*, vol. 12, no. 5, pp. 483–490, Oct. 2008.

[137] T. Shi *et al.*, “Advances in targeted proteomics and applications to biomedical research.,” *Proteomics*, vol. 16, no. 15–16, pp. 2160–82, Aug. 2016.

[138] L. C. Gillet *et al.*, “Targeted Data Extraction of the MS/MS Spectra Generated by Data-independent Acquisition: A New Concept for Consistent and Accurate Proteome Analysis,” *Mol. Cell. Proteomics*, vol. 11, no. 6, p. O111.016717, Jun. 2012.

[139] M. Nikolov, C. Schmidt, and H. Urlaub, “Quantitative Mass Spectrometry-Based Proteomics: An Overview,” in *Quantitative Methods in Proteomics. Methods in Molecular Biology (Methods and Protocols)*, vol. 893, Humana Press, Totowa, NJ, 2012, pp. 85–100.

[140] J. Vowinckel, F. Capuano, K. Campbell, M. J. Deery, K. S. Lilley, and M. Ralser, “The beauty of being (label)-free: sample preparation methods for SWATH-MS and next-generation targeted proteomics,” *F1000Research*, vol. 2, p. 272, Apr. 2014.

[141] L. Tuli and H. W. Ressom, “LC-MS Based Detection of Differential Protein Expression.,” *J. Proteomics Bioinform.*, vol. 2, pp. 416–438, Oct. 2009.

[142] S. Cappadona, P. R. Baker, P. R. Cutillas, A. J. R. Heck, and B. van Breukelen, “Current challenges in software solutions for mass spectrometry-based quantitative proteomics,” *Amino Acids*, vol. 43, no. 3, pp. 1087–1108, Sep. 2012.

[143] P. Gomes-Alves *et al.*, “Exploring analytical proteomics platforms toward the definition of human cardiac stem cells receptome,” *Proteomics*, vol. 15, no. 7, pp. 1332–1337, 2015.

[144] P. Gomes-Alves *et al.*, “In vitro expansion of human cardiac progenitor cells: Exploring ’omics tools for characterization of cell-based allogeneic products,” *Transl. Res.*, vol. 171, pp. 96–110, 2016.

[145] S. Doll *et al.*, “Region and cell-type resolved quantitative proteomic map of the human heart,” *Nat. Commun.*, vol. 8, no. 1, p. 1469, Dec. 2017.

[146] C. Correia *et al.*, “Effective Hypothermic Storage of Human Pluripotent Stem Cell-Derived Cardiomyocytes Compatible With Global Distribution of Cells for Clinical Applications and Toxicology Testing,” *Stem Cells Transl. Med.*, vol. 5, no. 5, pp. 658–669, May 2016.

[147] D. C. Nguyen *et al.*, “Microscale generation of cardiospheres promotes robust enrichment of cardiomyocytes derived from human pluripotent stem cells,” *Stem Cell Reports*, vol. 3, no. 2, pp. 260–268, 2014.

[148] C. Correia *et al.*, “3D aggregate culture improves metabolic maturation of human pluripotent stem cell derived cardiomyocytes.,” *Biotechnol. Bioeng.*, vol. 115, no. 3, pp. 630–644, Mar. 2018.

[149] M. C. Ribeiro *et al.*, “Functional maturation of human pluripotent stem cell derived cardiomyocytes in vitro – Correlation between contraction force and electrophysiology,” *Biomaterials*, vol. 51, pp. 138–150, 2015.

[150] M. Khan, S. Meduru, M. Mostafa, S. Khan, K. Hideg, and P. Kuppusamy, “Trimetazidine, administered at the onset of reperfusion, ameliorates myocardial dysfunction and injury by activation of p38 mitogen-activated protein kinase and Akt signaling.,” *J. Pharmacol. Exp. Ther.*, vol. 333, no. 2, pp. 421–9, May 2010.

[151] L. Lauden *et al.*, “Allogenicity of Human Cardiac Stem/Progenitor Cells Orchestrated by Programmed Death Ligand 1Novelty and Significance,” *Circ. Res.*, vol. 112, no. 3, pp. 451–464, Feb. 2013.

[152] D. C. S. Pedroso *et al.*, “Improved Survival, Vascular Differentiation and Wound Healing Potential of Stem Cells Co-Cultured with Endothelial Cells,” *PLoS One*, vol. 6, no. 1, p. e16114, Jan. 2011.

[153] G. Carpentier, “ImageJ contribution: Angiogenesis Analyzer,” *ImageJ News*, Oct-2012. .

[154] D. D. Ross *et al.*, “Estimation of Cell Survival by Flow Cytometric Quantification of Fluorescein Diacetate/Propidium Iodide Viable Cell Number,” Cacer Res., Jul. 1989.

[155] B. Abecasis *et al.*, “Expansion of 3D human induced pluripotent stem cell aggregates in bioreactors: bioprocess intensification and scaling-up approaches,” *J. Biotechnol.*, pp. 1–13, 2017.

[156] H. R. Soares *et al.*, “Tetraspanins displayed in retrovirus-derived virus-like particles and their immunogenicity,” *Vaccine*, vol. 34, no. 13, pp. 1634–1641, Mar. 2016.

[157] S. Tyanova *et al.*, “The Perseus computational platform for comprehensive analysis of (prote)omics data,” *Nat. Methods*, vol. 13, no. 9, pp. 731–740, Sep. 2016.

[158] H. Hirche, “Myocardial extracellular K+ and H+ increase and noradrenaline release as possible cause of early arrhythmias following acute coronary artery occlusion in pigs,” *J. Mol. Cell. Cardiol.*, vol. 12, no. 6, pp. 579–593, Jun. 1980.

[159] W. Aoi and Y. Marunaka, “Importance of pH homeostasis in metabolic health and diseases: crucial role of membrane proton transport.,” *Biomed Res. Int.*, vol. 2014, p. 598986, Sep. 2014.

[160] H. Li *et al.*, “Effect of Dopamine Receptor 1 on Apoptosis of Cultured Neonatal Rat Cardiomyocytes in Simulated Ischaemia/Reperfusion,” *Basic Clin. Pharmacol. Toxicol.*, vol. 102, no. 3, pp. 329–336, Mar. 2008.

[161] Y.-Y. Li *et al.*, “Thioredoxin-2 protects against oxygen-glucose deprivation/reperfusion injury by inhibiting autophagy and apoptosis in H9c2 cardiomyocytes.,” *Am. J. Transl. Res.*, vol. 9, no. 3, pp. 1471–1482, 2017.

[162] L. Portal *et al.*, “A Model of Hypoxia-Reoxygenation on Isolated Adult Mouse Cardiomyocytes,” *J. Cardiovasc. Pharmacol. Ther.*, vol. 18, no. 4, pp. 367–375, Jul. 2013.

[163] J. Pálóczi *et al.*, “Exogenous Nitric Oxide Protects Human Embryonic Stem Cell-Derived Cardiomyocytes against Ischemia/Reperfusion Injury,” *Oxid. Med. Cell. Longev.*, vol. 2016, pp. 1–9, Jun. 2016.

[164] J. Wu, M. R. Rostami, D. P. Cadavid Olaya, and E. S. Tzanakakis, “Oxygen Transport and Stem Cell Aggregation in Stirred-Suspension Bioreactor Cultures,” *PLoS One*, vol. 9, no. 7, p. e102486, Jul. 2014.

[165] M. Hao, S. Zhu, L. Hu, H. Zhu, X. Wu, and Q. Li, “Myocardial Ischemic Postconditioning Promotes Autophagy against Ischemia Reperfusion Injury via the Activation of the nNOS/AMPK/mTOR Pathway.,” *Int. J. Mol. Sci.*, vol. 18, no. 3, Mar. 2017.

[166] M. S. T. Sheik Uduman, R. B. Reddy, P. Punuru, G. Chakka, and G. Karunakaran, “Protective Role of Ramipril and Candesartan against Myocardial Ischemic Reperfusion Injury: A Biochemical and Transmission Electron Microscopical Study.,” *Adv. Pharmacol. Sci.*, vol. 2016, p. 4608979, 2016.

[167] S. Cao *et al.*, “Ischemic postconditioning influences electron transport chain protein turnover in Langendorff-perfused rat hearts,” *PeerJ*, vol. 4, p. e1706, Feb. 2016.

[168] M. R. Hollander *et al.*, “Dissecting the Effects of Ischemia and Reperfusion on the Coronary Microcirculation in a Rat Model of Acute Myocardial Infarction,” *PLoS One*, vol. 11, no. 7, p. e0157233, Jul. 2016.

[169] J. Zhang *et al.*, “Sevoflurane Postconditioning Protects Rat Hearts against Ischemia-Reperfusion Injury via the Activation of PI3K/AKT/mTOR Signaling,” *Sci. Rep.*, vol. 4, no. 1, p. 7317, May 2015.

[170] E. Turillazzi, M. Di Paolo, M. Neri, I. Riezzo, and V. Fineschi, “A theoretical timeline for myocardial infarction: immunohistochemical evaluation and western blot quantification for Interleukin-15 and Monocyte chemotactic protein-1 as very early markers,” *J. Transl. Med.*, vol. 12, no. 1, p. 188, Jul. 2014.

[171] S. Vandervelde, M. J. A. van Luyn, R. A. Tio, and M. C. Harmsen, “Signaling factors in stem cell-mediated repair of infarcted myocardium.,” *J. Mol. Cell. Cardiol.*, vol. 39, no. 2, pp. 363–76, Aug. 2005.

[172] S.-G. Ong *et al.*, “Microfluidic Single-Cell Analysis of Transplanted Human Induced Pluripotent Stem Cell–Derived Cardiomyocytes After Acute Myocardial Infarction,” *Circulation*, vol. 132, no. 8, pp. 762–771, Aug. 2015.

[173] H. Senaran *et al.*, “Thrombopoietin and mean platelet volume in coronary artery disease.,” *Clin. Cardiol.*, vol. 24, no. 5, pp. 405–8, May 2001.

[174] R. J. Boucek *et al.*, “Ex vivo paracrine properties of cardiac tissue: Effects of chronic heart failure,” *J. Hear. Lung Transplant.*, vol. 34, no. 6, pp. 839–848, Jun. 2015.

[175] N. G. Frangogiannis *et al.*, “MCSF expression is induced in healing myocardial infarcts and may regulate monocyte and endothelial cell phenotype,” *Am. J. Physiol. Circ. Physiol.*, vol. 285, no. 2, pp. H483–H492, Aug. 2003.

[176] M. Gwechenberger, D. Moertl, R. Pacher, and M. Huelsmann, “Oncostatin-M in myocardial ischemia/reperfusion injury may regulate tissue repair.,” *Croat. Med. J.*, vol. 45, no. 2, pp. 149–57, Apr. 2004.

[177] M. D. Miller and M. S. Krangel, “The human cytokine I-309 is a monocyte chemoattractant.,” *Proc. Natl. Acad. Sci. U. S. A.*, vol. 89, no. 7, pp. 2950–4, Apr. 1992.

[178] G. Bernardini *et al.*, “I-309 binds to and activates endothelial cell functions and acts as an angiogenic molecule in vivo.,” *Blood*, vol. 96, no. 13, pp. 4039–45, Dec. 2000.

[179] F. Montecucco *et al.*, “CC chemokine CCL5 plays a central role impacting infarct size and post-infarction heart failure in mice,” *Eur. Heart J.*, vol. 33, no. 15, pp. 1964–1974, Aug. 2012.

[180] T. Nakamura, S. Mizuno, K. Matsumoto, Y. Sawa, H. Matsuda, and T. Nakamura, “Myocardial protection from ischemia/reperfusion injury by endogenous and exogenous HGF,” *J. Clin. Invest.*, vol. 106, no. 12, pp. 1511–1519, Dec. 2000.

[181] K. Urbanek, “Cardiac Stem Cells Possess Growth Factor-Receptor Systems That After Activation Regenerate the Infarcted Myocardium, Improving Ventricular Function and Long-Term Survival,” *Circ. Res.*, vol. 97, no. 7, pp. 663–673, Sep. 2005.

[182] K. G. Aghila Rani and C. C. Kartha, “Effects of epidermal growth factor on proliferation and migration of cardiosphere-derived cells expanded from adult human heart.,” *Growth Factors*, vol. 28, no. 3, pp. 157–65, Jun. 2010.

[183] T. Natori, M. Sata, M. Washida, Y. Hirata, R. Nagai, and M. Makuuchi, “G-CSF stimulates angiogenesis and promotes tumor growth: potential contribution of bone marrow-derived endothelial progenitor cells.,” *Biochem. Biophys. Res. Commun.*, vol. 297, no. 4, pp. 1058–61, Oct. 2002.

[184] M. Harada *et al.*, “G-CSF prevents cardiac remodeling after myocardial infarction by activating the Jak-Stat pathway in cardiomyocytes,” *Nat. Med.*, vol. 11, no. 3, pp. 305–311, Mar. 2005.

[185] T. M. Ribeiro-Rodrigues *et al.*, “Exosomes secreted by cardiomyocytes subjected to ischaemia promote cardiac angiogenesis,” *Cardiovasc. Res.*, vol. 113, no. 11, pp. 1338–1350, Sep. 2017.

[186] S. X. Liang and W. D. Phillips, “Migration of Resident Cardiac Stem Cells in Myocardial Infarction,” *Anat. Rec.*, vol. 296, no. 2, pp. 184–191, 2013.

[187] B.-R. Son *et al.*, “Migration of Bone Marrow and Cord Blood Mesenchymal Stem Cells In Vitro Is Regulated by Stromal-Derived Factor-1-CXCR4 and Hepatocyte Growth Factor-c-met Axes and Involves Matrix Metalloproteinases,” *Stem Cells*, vol. 24, no. 5, pp. 1254–1264, May 2006.

[188] D. Kuang *et al.*, “Stem cell factor/c-kit signaling mediated cardiac stem cell migration via activation of p38 MAPK,” *Basic Res. Cardiol.*, vol. 103, no. 3, pp. 265–273, May 2008.

[189] P. Goichberg *et al.*, “Age-Associated Defects in EphA2 Signaling Impair the Migration of Human Cardiac Progenitor CellsClinical Perspective,” *Circulation*, vol. 128, no. 20, pp. 2211–2223, Nov. 2013.

[190] T. Nakamura *et al.*, “Influence of aging on the quantity and quality of human cardiac stem cells,” *Sci. Rep.*, vol. 6, no. 1, p. 22781, Sep. 2016.

[191] D. S. RajendranNair, J. Karunakaran, and R. R. Nair, “Differential response of human cardiac stem cells and bone marrow mesenchymal stem cells to hypoxia–reoxygenation injury,” *Mol. Cell. Biochem.*, vol. 425, no. 1–2, pp. 139–153, Jan. 2017.

[192] K. Urbanek *et al.*, “Myocardial regeneration by activation of multipotent cardiac stem cells in ischemic heart failure.,” *Proc. Natl. Acad. Sci. U. S. A.*, vol. 102, no. 24, pp. 8692–7, Jun. 2005.

[193] I. Valiente-Alandi, C. Albo-Castellanos, D. Herrero, I. Sanchez, and A. Bernad, “Bmi1 (+) cardiac progenitor cells contribute to myocardial repair following acute injury.,” *Stem Cell Res. Ther.*, vol. 7, no. 1, p. 100, Jul. 2016.

[194] G. M. Ellison *et al.*, “Adult c-kit(pos) cardiac stem cells are necessary and sufficient for functional cardiac regeneration and repair.,” *Cell*, vol. 154, no. 4, pp. 827–42, Aug. 2013.

[195] D. D’Amario *et al.*, “Insulin-like growth factor-1 receptor identifies a pool of human cardiac stem cells with superior therapeutic potential for myocardial regeneration.,” *Circ. Res.*, vol. 108, no. 12, pp. 1467–81, Jun. 2011.

[196] T.-S. Li *et al.*, “Direct Comparison of Different Stem Cell Types and Subpopulations Reveals Superior Paracrine Potency and Myocardial Repair Efficacy With Cardiosphere-Derived Cells,” *J. Am. Coll. Cardiol.*, vol. 59, no. 10, pp. 942–953, Mar. 2012.

[197] T.-S. Li, M. Kubo, K. Ueda, M. Murakami, A. Mikamo, and K. Hamano, “Impaired angiogenic potency of bone marrow cells from patients with advanced age, anemia, and renal failure,” *J. Thorac. Cardiovasc. Surg.*, vol. 139, no. 2, pp. 459–465, Feb. 2010.

[198] N. Shrestha, W. Bahnan, D. J. Wiley, G. Barber, K. A. Fields, and K. Schesser, “Eukaryotic initiation factor 2 (eIF2) signaling regulates proinflammatory cytokine expression and bacterial invasion.,” *J. Biol. Chem.*, vol. 287, no. 34, pp. 28738–44, Aug. 2012.

[199] B. de Lucas, L. M. Pérez, and B. G. Gálvez, “Importance and regulation of adult stem cell migration.,” *J. Cell. Mol. Med.*, vol. 22, no. 2, pp. 746–754, Feb. 2018.

[200] D. J. Ceradini *et al.*, “Progenitor cell trafficking is regulated by hypoxic gradients through HIF-1 induction of SDF-1,” *Nat. Med.*, vol. 10, no. 8, pp. 858–864, Aug. 2004.

[201] C. Baldwin *et al.*, “Upregulation of EphA2 during in vivo and in vitro renal ischemia-reperfusion injury: role of Src kinases,” *Am. J. Physiol. Physiol.*, vol. 291, no. 5, pp. F960–F971, Nov. 2006.

[202] J. J. Gildea *et al.*, “RhoGDI2 is an invasion and metastasis suppressor gene in human cancer.,” *Cancer Res.*, vol. 62, no. 22, pp. 6418–23, Nov. 2002.

[203] K. Ban and R. A. Kozar, “Protective role of p70S6K in intestinal ischemia/reperfusion injury in mice.,” *PLoS One*, vol. 7, no. 7, p. e41584, 2012.

[204] D.-S. DU *et al.*, “Effects of CDC42 on the proliferation and invasion of gastric cancer cells,” *Mol. Med. Rep.*, vol. 13, no. 1, pp. 550–554, Jan. 2016.

[205] M. Radu, G. Semenova, R. Kosoff, and J. Chernoff, “PAK signalling during the development and progression of cancer.,” *Nat. Rev. Cancer*, vol. 14, no. 1, pp. 13–25, Jan. 2014.

[206] S.-J. Fang *et al.*, “Neuregulin-1 preconditioning protects the heart against ischemia/reperfusion injury through a PI3K/Akt-dependent mechanism.,” *Chin. Med. J. (Engl).*, vol. 123, no. 24, pp. 3597–604, Dec. 2010.

[207] S. J. Crozier, X. Zhang, J. Wang, J. Cheung, S. R. Kimball, and L. S. Jefferson, “Activation of signaling pathways and regulatory mechanisms of mRNA translation following myocardial ischemia-reperfusion.,” *J. Appl. Physiol.*, vol. 101, no. 2, pp. 576–82, Aug. 2006.